ENGINEERING
EDGE

Accelerate Innovation with CFD & Thermal Characterization

mentor.com/mechanical

Mentor®
A Siemens Business

Perspective

Greetings readers! I have been thinking recently about the 'Democratization of CFD', not least because our Mechanical Analysis Division mission statement over the last three years since I became General Manager recognizes it:

"To democratize the use of thermal simulation & test solutions to multiply the productivity of any engineer, anywhere in the world, at any time."

To democratize any engineering simulation software is not an easy thing; it requires clever engineering approximations, innovative numerical methodologies, lots of automation, plus tremendous attention to user experience and ease of use. Nevertheless, I believe we have been pivotal in our sector in achieving unique workflows, integrated simulation & test solutions, and 1D-3D workflows that yield large user productivity gains through a fixation on democratization without compromising accuracy and engineering usefulness. Read more on page 6.

The customer stories in this edition of Engineering Edge lead with Team Velarde's attempt at winning the Red Bull Air Race World Championship with an aerodynamic study of their plane using FloEFD. Huawei in China use our thermal simulation & test tools, FloTHERM and T3Ster, to optimize the thermal performance of their communication devices – a great cutting edge application. There are great interviews and articles from two French leaders in Automotive Lighting, Paul-Henri Matha at Renault and Jean-Paul Savier at ELS. Bose Automotive Systems in America are also in the spotlight as they use FloTHERM and our unique subtractive design methodology to optimize their heatsink's size and weight for almost the same thermal performance: a significant cost saving. Several great applications of FloEFD are reported including Irkut in Russia (high lift wing flaps), E-Cooling GmbH in Germany (room-level power electronics thermal), Dr. Schneider in Germany (optimizing automotive HVAC ducts), and race car brake cooling design by a student at the Halmstad University in Sweden.

With regard to product news, FloTHERM XT 3.0 has recently hit the market with some cool fan modeling capabilities, plus a standalone MicReD DynTIM S Dynamic Thermal Interface Material (TIM) Tester with an integrated T3Ster unit. FloMASTER recently celebrated 25 years since the commercial company was founded (Flowmaster Ltd), and a technical feature article on its new capability, Waste Heat Recovery, is outlined herein. Finally, Jurgen Sprengle in Australia reports using FloMASTER to simulate a cool municipal domestic water supply network – probably one of the biggest ever in the code's history – and a thing of beauty to look at.

Roland Feldhinkel, General Manager,
Mechanical Analysis Division, Mentor Graphics

12

News

Engineering Edge

Contents

24

36

56

Regular Features

27

The Democratization of CFD – a Personal Journey

By Roland Feldhinkel, General Manager, Mechanical Analysis Division, Mentor Graphics

I have been thinking about a phrase that has been dear to my heart for many years now, but has only recently become one of the latest buzzwords to hit our Industry: 'the democratization of CFD". When I think of my career in CFD, I would say that it has all been about democratizing CFD. Ever since I set up Nika GmbH [1] in 1999 with the goal of producing CAD-embedded CFD software, I have had the dream of moving CFD down the 'pyramid of users' to the designers and engineers in the world who can benefit from it. These are the men and women who want to dip in and out of CFD rather than the full-time analysts and CFD experts who have been the main exponents and advocates of CFD over the years. I recall talking about democratizing CFD back in 2004 during an interview for a German CAD/CAM engineering magazine [2].

I am therefore pleased to see that for the upcoming NAFEMS World Congress in Sweden this June that my colleagues, Keith Hanna and Ivo Weinhold, have dug deeply into this subject in writing their paper "The
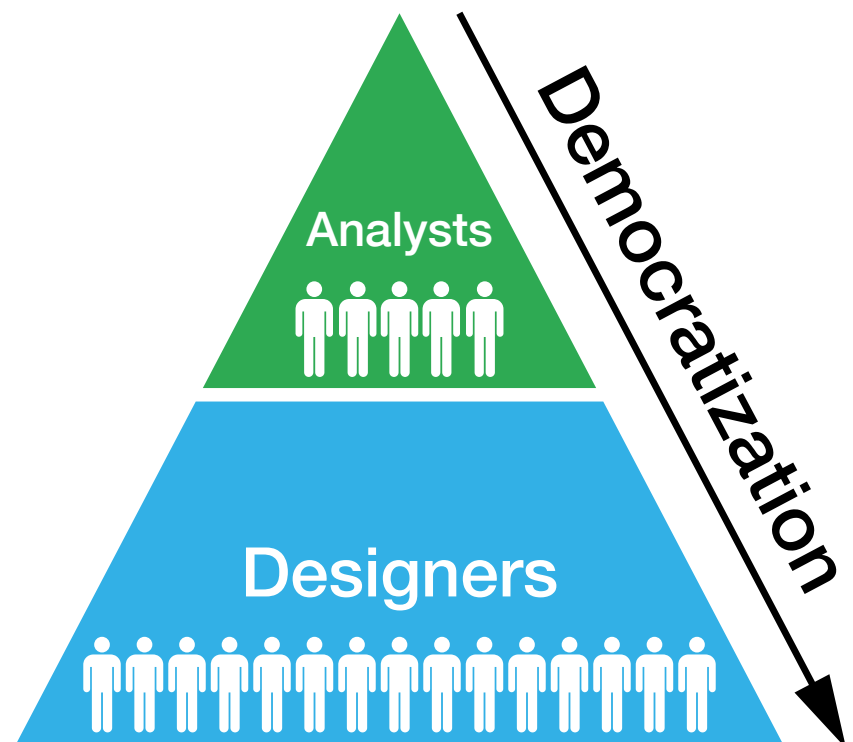
Figure 1: CFD User Pyramid

Democratization of CFD – is it Possible?" [3] because I, like them, believe that there are many strands to solving the democratization challenge and no one single factor is delivering a solution to this problem today. A democratization deficit is plaguing the larger CAE and MCAD markets too. One could argue that the creation of Onshape a few years ago by Jon Hirschtick is an attempt to democratize MCAD in the cloud. With CFD we are inherently trying to solve very complex second order non-linear differential equations through empirical models that approximate the physics and chemistry of a given industrial application. There is always therefore a risk for ill-posed CFD simulations of getting the wrong answer as much as the right answer. Unless a code is robust, its meshing has to capture the relevant phenomena, and the right boundary conditions and material properties are known (or chosen), not to mention the underlying quality of the CFD solver. Even after 40 years of commercial CFD, the market is still barely 10% penetrated; that is, the number of actual users divided by the total possible number of users of CFD, is quite small. And that number has only doubled in the last five years despite significant improvements in computer hardware speed and available CPU RAM. There are pros and cons to several solutions being offered by the CFD Industry today to bridge this 'democratization' gap:

- "Appification";
- High Performance Computing (HPC) and faster solvers;
- Multivariable design optimization;
- Cloud-deployed solutions;
- Open Source CFD;
- User Experience and ease-of-use enhancements;
- CAD-embedding; and
- 1D fluid system modeling / 2D CFD.

The table in figure 2 summarizes our conclusions on each of these democratization factors in terms of their impact on how many extra CFD users could be expected to come from the democratization factor, and how much the productivity of existing and new CFD users will be improved significantly by the factor.

I believe that most engineers live in a CAD-centric, PLM-enabled universe, and CFD software implementations have to deal with customer workflows to make engineers as productive as possible with the least amount of physics and CFD-specific knowledge possible. Users want realistic simulations in real-time, or as close to it as possible. 'Democratization of CFD' is indeed possible, but to get from 5-10% market penetration to 80-90% in the next 30-40 years will require more thinking out of the current box and probably radical rethinking of CFD code structures, automation and user experience,

along with more fundamental research. The biggest impact on democratization will come from PLM-enabled CAD-embedded CFD and cloud deployment. Moreover, user experience needs to be front and center. Some 'CFD Apps' in key industries will have a place in the democratization thrust, but the very challenge of CFD democratization itself will be an agent for change in our industry. It is entirely conceivable that one day our grandchildren will laugh at us when we say we spent two-thirds of our time in creating geometry and meshes when we did fluid flow simulation with CFD!

References:

[1] Engineering Edge Magazine, Mentor Graphics, Vol 3, Edition 1, May 2014, p5

[2] "Strömender Erfolg", CAD-CAM Magazine, March 2004, pp18-20

[3] Hanna, R.K. and Weinhold, I.W., "The Democratization of CFD – is it Possible?", NAFEMS World Congress, June 2017, Stockholm, Sweden.

CFD MARKET PENETRATION
2017 = 10%

NON PENETRATED = 90%
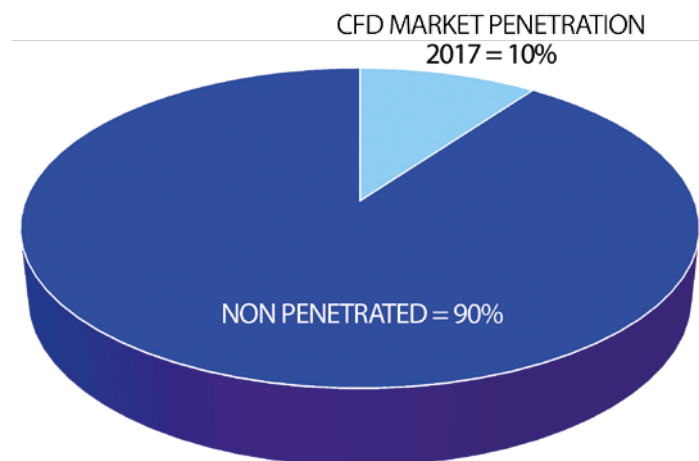
Democratization Factor	# Extra CFD Users	Productivity of CFD Users
1. Appification	●●○○○	●●●○○
2. HPC	●○○○○	●●●○○
3. Multivariable Design Optimization	●○○○○	●●○○○
4. Cloud Deployment	●●●●●	●●●○○
5. Open Source CFD	●●○○○	●○○○○
6. User Experience & Ease of Use	●●●○○	●●●●○
7. CAD-Embedding & PLM Enablement	●●●●○	●●●●○
8. 1D/2D/3D CFD	●●○○○	●●●○○

Impact of Democratization Factors on CFD Penetration in Future

Figure 2: Impact of Democratization Factors on CFD Penetration in Future

New Release:
DynTIM S & T3Ster Booster (240A/11V)

Early in 2017 the MicReD team, answering market demand, released the DynTIM S, combining the power of T3Ster with the unique capabilities of the DynTIM into one standalone unit. This brings a more cost effective TIM measurement system to the market since there is no requirement to purchase a separate T3Ster system.

This new release is used for measuring bulk thermal conductivity of thermal interface materials by varying thickness. The DynTIM S includes mechanics for thickness control, a diode for heating and sensing control electronics, and heating and sensing circuits. The in-built technology from T3Ster enables measurement by heating up the thermal structure, switching off the power and then measuring the thermal transient (temp. vs. time). The unchanged measurement control and results processing tool allows quick and simple test setup and a clear and intuitive interface to review and process the data or prepare it for reporting. This standalone system offers exactly the same

TIM measurement capability as the combined systems with an identical User Interface. The MicReD team also updated and released the T3Ster Booster (240A/11V) which is available to order now. It enables easier measurement of IGBT half-bridges, both the gate drivers and the heating current sources are floating, not grounded. The new 240A booster can heat MOSFET on open channel and measure on body diode. This new booster can be rack mounted to become part of the measurement set-up easily.

New Release:
FloTHERM® XT 3.0

At the beginning of 2017, the FloTHERM XT product line released V3, and the latest version offers new functionalities developed from customer feedback. This leading Electronics Cooling Simulation tool simulates thermal effects of complex geometries. Key capabilities include :

- Simulation of spinning parts;
- Temperature-dependent power simulation;
- Enhanced "Design of Experiments" parametric studies functionality to determine best design coverage; and
- Thermal Territory Simulation to enhance accuracy with heat transfer from components.

These features are important for electronics devices used in the transportation, aerospace, defense, and consumer electronics markets.

Based on the electronics cooling DNA of Mentor Graphics market-leading FloTHERM technology and the FloEFD® CAD-centric philosophy, the award-winning FloTHERM XT product is the industry's first integrated mechanical design automation (MDA) and electronic design automation (EDA) electronics

cooling solution. The FloTHERM XT product can be used at all stages of the electronic design process, from design concept through manufacturing. Its CAD-centric technology and robust mesher simulates complex geometries with ease, speed, and accuracy for improved product quality and reliability.

Key Features in the FloTHERM XT Release:

- **Explicit Models for Spinning Parts:** The new sliding mesh capability easily meshes the rotation region to accurately simulate the effects of spinning parts such as fans and rotors used in electronics devices such as fansinks and drones.
- **Temperature-Dependent Power Simulation:** When attached to an object or planar source, the FloTHERM XT software will use the object's own average temperature goal to adjust the applied power, enabling users to capture the leakage current effects in dies. This feature was developed from customer feedback.
- **Thermal Territory Simulation:** This new feature is critical for detailed copper "under the component" designs, used to draw heat away from that component - providing an accurate simulation methodology.

- **Enhanced Parametric Study Functionality:** The addition of a "Design of Experiments" scenario table allows users to set up a number of studies to ensure the best coverage of the design field. These scenarios can also be sent to remote machines with more capacity. The addition of this key enhancement was based on customer feedback.
- **Improved User Interface:** Enhancements to the user interface makes it easier to set model parameters and find mesh controls for improved thermal design predictability.
- **Design Tool Integration:** Two approaches are available for tool interoperability in this release: Files can be directly imported through the FloEDA Bridge module with ease-of-use features such as undo/redo, access to power displayed in tree, and the graphical representation of component types. The second approach uses a neutral file format allowing the user to interact with the setup of a model outside of the standard interface.

FloTHERM XT is available now. For more information, visit the product website: www. mentor.com/products/mechanical/flotherm/ flotherm-xt/

Training the Next Generation of Engineers

By Dr. Ivo Weinhold, University and Technology Partnerships Manager, Mechanical Analysis Division

Mentor Graphics' Mechanical Analysis Division has launched a new 'University and Technology Partnerships Program', offering the division's leading software tools for Computational Fluid Dynamics, Electronics Thermal Design, and Fluid Systems Simulation for engineering education and academic research.

Engineering trends like Industry 4.0, Internet of Things, integrated digital product development processes, massive product customization, and the revolution in manufacturing and factory automation, create new career paths for the next generation of engineers. Research and development departments of large industrial companies, design teams of small and medium enterprises, and innovative start-up entrepreneurs alike are demanding comprehensive engineering education for their innovators of tomorrow. Simulation of physical product functionality, seamlessly integrated within virtual product development processes, will be an integral part of future engineering career paths, requiring sound expertise in using the latest simulation technology. Engineering schools across the globe are embracing this demand, striving to best prepare their students for a successful professional career. Mentor Graphics' Mechanical Analysis Division is committed to support engineering education at all stages by providing easy access to its advanced engineering tools for physical simulation and test, allowing students to gain hands-on, real-world, industry-level experience for tomorrow's simulation-driven virtual product design workflows.

Higher Education Program

Mentor Graphics Corporation founded the Higher Education Program (HEP) to further the development of skilled engineers within the industry. The program provides universities, colleges, and schools with leading edge design tools for classroom instruction and academic research to help ensure that engineering graduates enter into industry, proficient with state-of-the-art tools and techniques. Through HEP, Mentor strives to develop long term relationships with engineering schools and universities around the world. To date, Mentor is proud to have partnered with more than 1,600 academic institutions worldwide.

Program Benefits

The program helps engineering students by providing simulation software, technical support, training, and resources during school and post-graduation and is open to all educational institutions. The software is donated and levies a nominal annual support charge based on the design package(s) used, irrespective of the number of licenses. HEP members have access to:

- As many copies of the software as needed;
- The same customer support services as corporate customers;
- Mentor's advertised public training classes on a space-available basis, and on-demand training (for nominated faculty staff members); and
- Online product demonstrations and tutorials.

HEP Mechanical Analysis Design Package

The HEP Mechanical Analysis design package ensures that engineering students have access to the latest Computational Fluid Dynamics, Electronics Thermal Design, and Fluid Systems Simulation software used in industry. From high school programs through to higher degree university research, Mentor's physical simulation software provides both the ease-of-use and technical depth needed for all educational needs. The design package contains only full capability software versions without reduced feature sets or artificial limitations. Currently, the HEP Mechanical Analysis Package contains the following simulation tools:

- FloEFD;
- FloEFD for Siemens NX, FloEFD for Solid Edge;
- FloMASTER;
- FloTHERM XT;
- FloTHERM, FloTHERM PCB; and
- FloVENT.

For more information and a HEP membership online application form visit www.mentor.com/company/higher_ed/ or contact Ivo Weinhold: ivo_weinhold@mentor.com

Dr. Ivo Weinhold is University and Technology Partnerships Manager for the Mechanical Analysis Division of Mentor Graphics. In this role he promotes Mechanical Analysis' simulation software and thermal test solutions for engineering education, helping the next generation of engineers to become familiar with cutting-edge technology for physical simulation and test.

Prior to Mentor Graphics, Ivo worked for Flomerics, NIKA, Fluent and Fluid Dynamics International, starting his career in the CFD industry in 1993. His engineering, sales and management roles through the years have included technical support, sales and marketing of electronics cooling CFD software, and over 13 years Product Management for the FloEFD line of CFD products at NIKA, Flomerics, and Mentor Graphics.

Mentor Learning Center

Interview with Lane Giles, Director of Education Services, Mentor Graphics

Q. What is a Mentor On-Demand Training library?
A. Mentor On-Demand training libraries provide customers with a full featured library of content that covers material delivered in Instructor led training. Students watch live topical videos by Mentor experts, practice in secure licensed online labs, and assess their proficiency with knowledge checks and assessments. Each learner's activity is tracked and progress completion certificates can be printed from their profile.

Q. How long can I access the videos and labs in the library?
A. On-Demand training is provided to individual users on a 12 month subscription. Although a learner could go through the materials for their unique role in roughly a week, they can refresh knowledge and practice design work in the virtual labs during the annual subscription.

Q. What are the benefits of the library subscription?
A. Learners benefit from the annual subscription in several ways. They can:

1. View Mentor experts demonstrate concepts and features in the live software;
2. Practice in fully licensed virtual lab environments without using a license of their installed software;
3. Search for answers to technical questions at their "moment of need";
4. Discover new features as the library content is updated in real-time;
5. Learn about new software release features without needing to purchase another training course or subscription;
6. Demonstrate Mentor proficiency with completion certificates; and
7. Use the library as a reference to keep their knowledge fresh and current.

Q. Why should an enterprize consider Mentor On-Demand training?
A. Enterprizes with 10's or 100's of design engineers rarely have the budget, time, or capability to schedule these individuals into traditional training classes in a timely manner. Furthermore, if they were able to schedule and send engineers to classes, as soon as that class ends, they begin forgetting what they learned. The industry estimates that students forget around 70% of what they learn in a class, depending on how quickly that can apply the learning. Mentor On-Demand training enables enterprises to send everyone to "class" on the same day at the same time. For example, if you have 400 engineers scattered across divisions and locations, access to the library is simultaneous.

Q. How old is the Mentor Learning Center and how has it been accepted?
A. The MLC initially launched with the first library in late 2015. Thanks to Mentor's unique development methodology, and seasoned subject matter experts, the MLC now has a very robust and active publishing cycle. The content that is added during an annual subscription keeps users engaged in the learning process and has helped 1000's of users across 55 countries become more efficient and productive with Mentor tools. People are saving hours of development time due to proper use of the tool and its functionality.
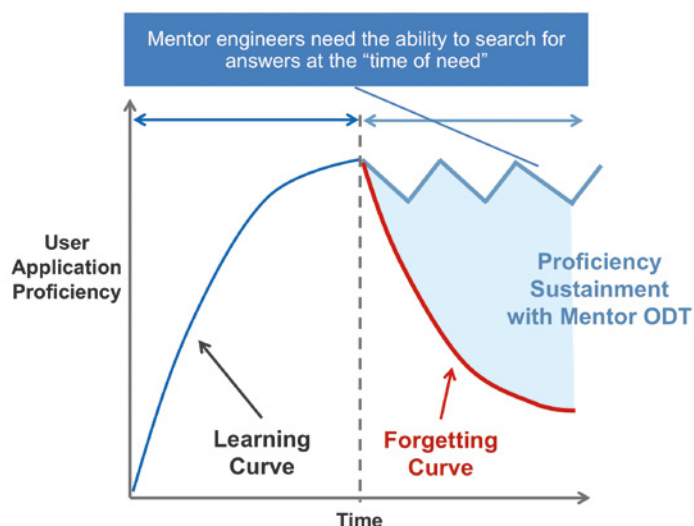
Seven years considered minimum experience needed
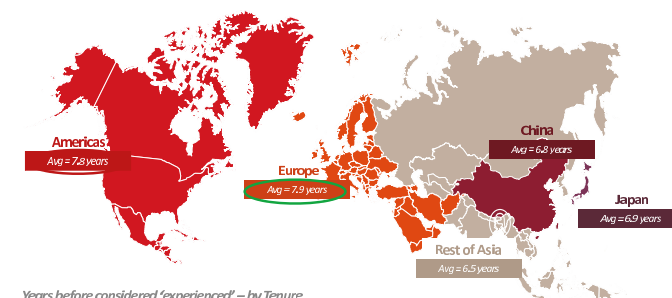
Years before considered 'experienced' – by Tenure

Total	Just Starting	Prime Timers	Tenured
7.2 years	5.5 years	6.3 years	8.1 years

Green indicates significant difference between groups at 95% confidence level

8. How many years do you feel it takes for engineers to be considered 'experienced'?

n = 3273

Unique 'Embedded Lighting Systems' Masters Course in Paris

The world's first Advanced Masters degree in Embedded Lighting Systems (ELS) at the prestigious Institute d'Optique in Paris, at ESTACA Ecole d'Ingénieurs and at the State School of Design in Paris is now entering its third year. With a select annual intake of twenty engineers and scientists from across the world, and led by ELS Chair Jean-Paul Ravier, it seeks to cater for the rapidly expanding market for car lighting design and engineering which is growing at 7.5% annually.

It is estimated that there are around 50,000 R&D engineers involved in automotive lighting systems catering for over 1,000 car models around the world today. Historically, automotive lighting evolved slowly over its first 100 years, but in the last decade it has seen an explosion in interest with the advent of Light Emitting Diodes (LEDs) and more recently laser lighting. Increasingly, function and styling are becoming intertwined in automotive lighting design as head and tail lights become aesthetic signatures for both car brands and individual models in ever more complex design situations.

Mr Ravier brings tremendous practical
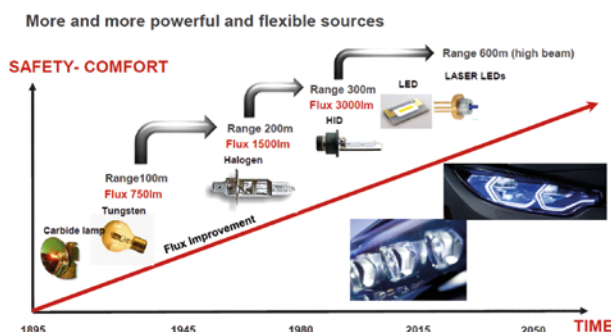
Jean-Paul Ravier, ELS Chair

knowhow to his new academic role with over forty years of experience in the lighting sector, thirty of those at Valeo S.A. And having secured sponsorship from Renault, Valeo, PSA and Automotive Lighting GmbH, ELS selected Mentor Graphics and its FloEFD product line to help students understand how an advanced CAD-embedded 3D CFD tool can be used to thermally optimize the design of lighting assemblies.

Commenting on the automotive lighting revolution, Mr Ravier notes that "Modern automotive lighting is developing dramatically. Headlights are seen as the eyes of the car. Their design is somewhere between an art

and a science. We have designers who are having to do engineering to see if their ideas are feasible; and we have engineers who are appreciating the aesthetics of good design to apply their technical knowledge to it. You have to be multidisciplinary to operate in this new paradigm."

ELS aims to stay ahead of technology trends such as ever more complex lighting systems, embedded sensors in head and taillights, lighting for autonomous cars, the advent of OLEDs (Organic LEDS), and Adaptive Driving Beam (ADB) systems. For more information on the ELS course, visit www.embedded–lighting.com

Mentor Graphics Team Receives the Harvey Rosten Award for Thermal Heatsink Optimization Methodology

SEMI-THERM 2017, announced that Dr. Robin Bornoff, Dr. John Parry and John Wilson, a team from Mentor Graphics Mechanical Analysis Division, received the Harvey Rosten Award for Excellence in thermal modeling and analysis of electronics. The team received the award for their paper, Subtractive Design: A Novel Approach to Heatsink Improvement, at the 33rd annual IEEE Thermal Measurement, Modeling and Management Symposium (SEMI-THERM) in San Jose, California.

The Mentor Graphics team created a unique methodology to sequentially remove

underperforming portions of a heatsink to save weight and cost without compromising overall thermal performance. This method using Mentor Graphics® FloTHERM® technology provides a variety of automated optimization approaches to gain deeper insights into thermal characterizations to determine the best thermal design solution.

"We are extremely proud of our team for their commitment and dedication in discovering ways in which heatsinks may be optimized," stated Roland Feldhinkel, General Manager of Mentor Graphics Mechanical Analysis Division. "To be recognized by the selection committee consisting of highly esteemed

thermal experts is a tremendous honor, and particularly personal since this award is named after the co-founder of Flomerics, which Mentor Graphics acquired in 2008."

Aces High for Team Velarde

FloEFD® explores external aerodynamics for Team Velarde in the Red Bull Air Race World Championship

By Matt Milne, Application Engineer, Mentor Graphics

I don't know about you but I'm partial to a bit of Iron Maiden now and then. And if there's a more fitting, more intense, higher energy soundtrack than "Aces High" to accompany the Red Bull Air Races then I want to know about it! Established in 2003, the Red Bull Air Race World Championship sees pilots from around the world compete against the clock as they navigate their aircraft through a challenging obstacle course in a breath-taking combination of high-speed low-level flying.

2017 sees Team Velarde begin their third year in the championship. Pilot Juan Velarde is looking to build upon his impressive 2016 record where he took the top spot in qualifying in one round and proved he could be competitive against the other more experienced pilots.
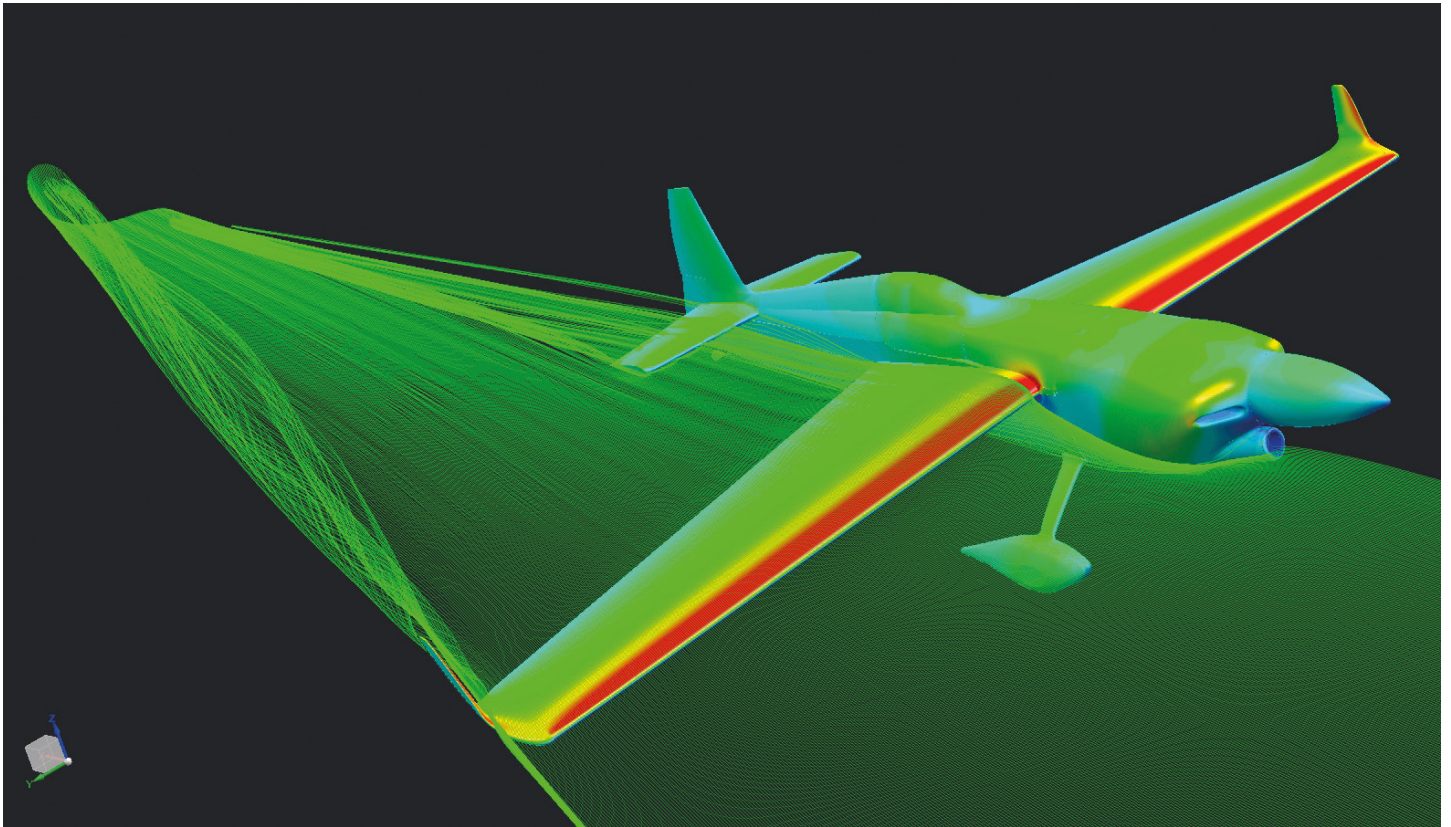
It is often said in racing that to stand still is to go backwards. With this in mind, Team Velarde continued working hard through the off-season to make their goal a reality. "Regarding the race plane, we are

aiming to have a new set of winglets and a few other aerodynamic improvements ready by the second race of the season," explained Velarde. "We are working with a team of engineers to optimize the performance of the plane," he added.

Team Velarde approached Mentor Graphics for help investigating the aerodynamics of the race plane. Specifically they wanted to use CFD to investigate the performance benefits of the new winglets. Working with CAEsoft in Madrid, Team Velarde used 3D scanning technology to create a 3D CAD model of the aircraft which was then provided to Mentor Graphics for CFD analysis.

While modern 3D scanning techniques are without question impressive, it turns out that the technology does a rather better job than some might desire for CFD analysis. Close inspection of the CAD model revealed a number of excrescences and other lumps and bumps. For traditional CFD, such features might be the cause of considerable pain, requiring time and effort to modify the CAD geometry to a state where it is suitable for meshing. However, with FloEFD these features are simply not a problem.

During my time in aerospace research, a lot of effort was spent working on the CAD geometry to get it into a suitable state for meshing - the process was well developed
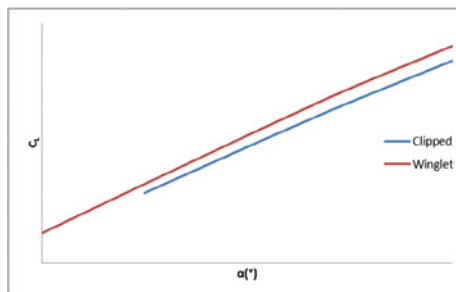
Figure 1. C_L vs. α (Full span model)

but it still had to be done manually. And then came meshing. For conceptual models with a relatively clean shape some degree of automation was possible, but for more complex models meshing had to be completed manually. I remember clearly some cases where meshing alone took more than a month.

This is all in stark contrast to the situation today with FloEFD. Put simply, the SmartCell™ meshing technology employed by FloEFD addresses meshing challenges with minimal user effort. Regardless of whether the geometry is a clean conceptual model, or dirty with lumps, bumps and excrescences, FloEFD can mesh it. With less time spent on geometry preparation and meshing, the user has more time to think about the results, what they mean and how to improve performance.
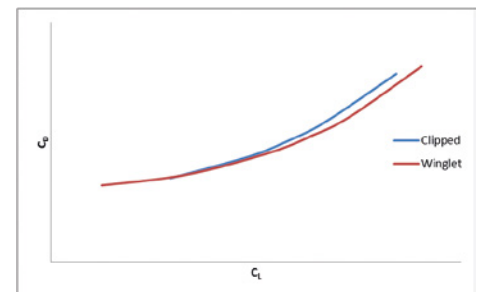
Figure 2. C_D vs. C_L (Full span model)

A new simulation was set up using the CAD geometry supplied by Team Velarde. The time taken to prepare the model, generate the mesh and begin the first flow calculation was less than one hour. Furthermore, our previous work on a wide range of well-known external aerodynamics test-cases meant we could follow a set of well documented best practices for this class of simulation and be confident of obtaining consistent and reliable results.

Initial calculations were run at low-medium angle of attack (AoA) at M=0.25, comparing the original clipped wing and revised "winglet" designs. These calculations were run using the complete aircraft span (i.e. port and starboard sides) but omitting the propeller blades. It was assumed that the propeller wash has only an incremental effect on the overall wing performance and

that since the wing leading edge is unswept any interaction between the propeller and wingtip flows is negligible. Each calculation used approximately 1.9 million cells and took around two hours to run using 12 cores (Intel Xeon E5-2643 v3).

It can be seen from Figure 1 that the "Winglet" design yields a slight increase in lift curve slope ($dC_L/d\alpha$). Figure 2 shows that there is also a reduction in drag. These predictions are expected from basic aerodynamic theory, since both designs effectively increase wing aspect ratio.

Further simulations were run to quantify performance of the "Winglet" design at medium-high AoA at M=0.25. It is noted that this area of the flight envelope (i.e. accurate prediction of onset and development of flow separation and associated effects) continues to be a challenge for all CFD methods today. While validation against well-established aerospace test-cases has shown FloEFD to perform acceptably in this regard, caution is nevertheless advised when interpreting computed predictions in this part of the flight envelope - the ability to obtain plausible looking solutions is no guarantee of accuracy.

To increase computational efficiency, only the starboard half of the aircraft was simulated. The effects of asymmetry in the model were assumed to be negligible and the propeller blades were again omitted. Appropriate revisions were made to the aircraft reference
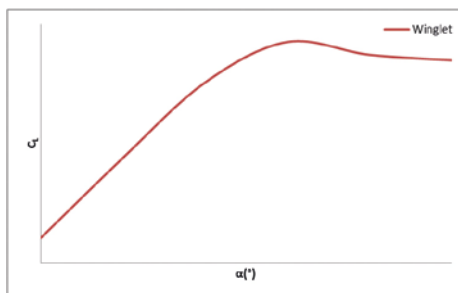

Figure 4. C_L vs. α (Half span model)

dimensions used to non-dimensionalize the integrated forces and moments. Each calculation used approximately 5.6 million cells and took around seven hours to run using 12 cores (Intel Xeon E5-2643 v3).

Predictions of integrated forces are shown in Figures 4 and 5. As expected the lift curve slope remains linear at low-medium AoA before becoming non-linear as flow separations develop. A thorough investigation of the predictions obtained using FloEFD is ongoing. This will give more insight into the development of the flow topology, and hence ways in which the "Winglet" design might be optimized to improve performance.

The improvement from the original clipped wing to the "Winglet" design is expected and indeed is predicted by basic aerodynamic theory. Performance of the "Winglet" design has been quantified for a wider range of AoA. Further improvement of the "Winglet" design may be possible through the use of
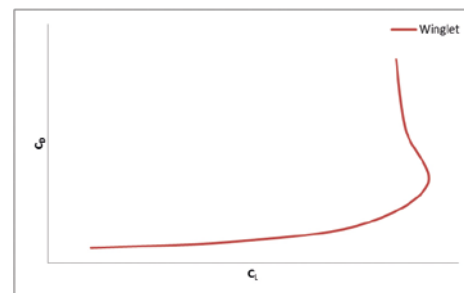
Figure 5. C_D vs. C_L (Half span model)

optimization and further work in this regard is recommended for the future. Based on these findings, the team are currently working on modifications to the race plane.

The first race of the 2017 Red Bull Air Race World Championship took place in Abu Dhabi on 10-11 February. After setting an impressive fifth fastest time in qualifying, Team Velarde took a sensational second place finish in the race, a best ever result for the team. The second race takes place in San Diego on 15-16 April. With luck, FloEFD will prove to be the ace in Team Velarde's hand and help them on their way to success in the 2017 Red Bull Air Race World Championship.

More information:
www.juanvelarde26.es
www.redbullairrace.com

Huawei Delivers
Outstandingly
Accurate Models

By Yake Fang, Senior Engineer, Huawei Technologies Co., Ltd.

Packaging high-performance multi-core IC devices used in communication applications is a key challenge for both manufacturers and system integrators. Traditionally a System-in-Package (SiP) has been taken, with chips mounted side-by-side, allowing differing semiconductor technologies to be mixed. More recently stacking silicon die has become more commonly used, as volumes have increased, making the System-on-Chip (SoC) design approach, which has much higher upfront non-recoverable expenditure, the cheapest option overall. These multi-heat source devices require very careful thermal design frontloaded in the design process, due to the very high cost of changes during detailed design.

The increased functionality and power dissipation has made the thermal design of communication device applications crucial in today's increasingly high computing power communication device industry. These products present a very challenging thermal environment for our SoC packages, with the need to design to very tight thermal tolerances to meet size, weight and form factor goals.

Huawei always pays attention to thermal challenges in product design and uses thermal analysis throughout the whole product R&D phase. We have the ambitious program to develop an internal thermal design flow for multi-core SoC and SiP devices that would enable us to use the highest possible quality thermal data and models to facilitate our own design efforts.

We have used FloTHERM™ for almost 15 years, so we have a rich depth of experience and so are able to create detailed thermal models of our SoC and SiP products. However, we needed a way to test that these packages achieved the 'as-designed' thermal performance, and to test packages from other
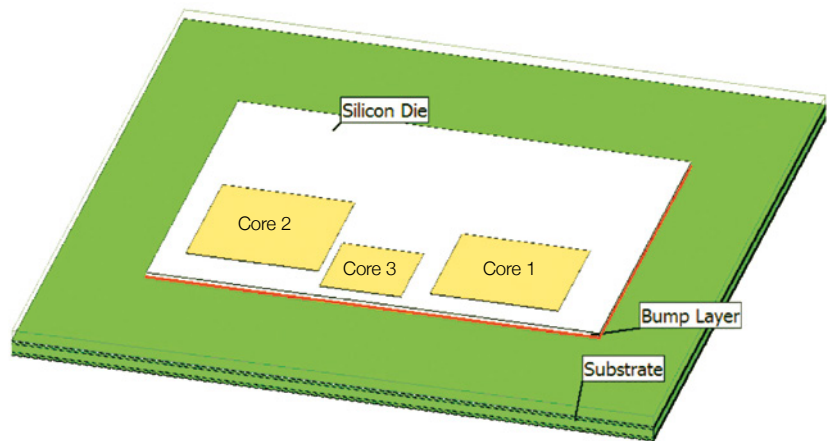

Figure 1. Overview of SoC device construction

suppliers rather than rely on their thermal data, which is often not sufficiently accurate or suitable for design. As it is based on the thermal transient measurement principle, giving the highest available fidelity, we turned to Mentor Graphics' T3Ster® hardware to perform a series of thermal tests so our thermal engineers could better understand the thermal impedance characteristics of these high-performance products, and reduce time and resources needed to achieve a good design.

As a test vehicle for this new design workflow we chose to investigate a 3-core SoC device typical of those now used in communication device applications and assembled in a Package-on-Package (PoP) format that allows package stacking. The FloTHERM model is shown in figure 1.

As soon as the first working packages were produced, they were measured using Mentor Graphics T3Ster hardware, which records the temperature response of the part to a power step from just a few microseconds until steady-state is reached, with an accuracy of ±0.01°C.

Having creating the detailed numerical model of the package in FloTHERM we performed a

transient simulation to get a baseline result for this, as yet, uncalibrated model, which we built using the best available information during the design. The temperature vs. time graphs we got from FloTHERM and T3Ster seemed to match quite well.

Using a model of the package in the same thermal environment in FloTHERM allows the temperature vs. time response from the FloTHERM simulation to also be converted into a Structure Function, and then the two Structure Functions compared. This is a plot of the cumulative thermal capacitance vs. the cumulative thermal resistance that the heat experiences as it leaves the package. If the model exactly matches reality for the package, then the two Structure Function curves should match perfectly, as the heat flow paths from the die junction out to the environment should be identical.

We then post-processed this temperature vs. time data to create a Structure Function graph for the T3Ster and FloTHERM results, and compared these. We were not expecting an exact match, as there are always uncertainties surrounding material thermal properties. The thickness and uniformity of bond lines,

"To design successful communication devices, Huawei first performs thermal simulations in FloTHERM, and then calibrates the detailed thermal model based on accurate thermal measurement data obtained from T3Ster. In parallel with this Huawei optimizes the design through different material selection to decrease thermal resistance, confirmed using T3Ster's transient thermal measurement. This process is much faster and requires fewer resources than we needed before, and provides Huawei with a highly-accurate thermal model to use in our system-level modeling, helping us get products to market faster than our competitors."

Fang Yake, Senior Engineer, Huawei Technologies Co. Ltd.

and contact resistances within the structure where one material is not in perfect thermal contact with its neighbor materials. However, we were somewhat surprised at how big the differences were when we compared Structure Functions, as shown in figure 2. The Structure Function comparison is a very powerful tool for showing up differences between the model and the experimental result, and where those differences are in the heat flow path.

Figure 2 shows the Structure Functions for the initial FloTHERM simulation (black) vs. the T3Ster measurement data (blue), shown here when Core 1 is powered. The two Structure Functions are clearly quite different. At the far right of the plot the thermal capacitance becomes infinite, as heat reaches the environment. For the FloTHERM model this occurs at a lower thermal resistance than found in practice, so the model is underestimating the temperature rise. Some of this difference may be due to deficiencies in the way the cold plate is modeled. However, the differences seen on the left of the graph are within the package model itself, and close to the heat source. Simulation vs. test results, when cores two and three are powered, both showed similar discrepancies.

To modify the model manually to bring it in line with the experimental results would be very time consuming and error prone as it would be a guess-and-correct process that is impractical to undertake a fast-paced design environment like ours. However, part of our reason for choosing T3Ster is that its results can be read into FloTHERM's Command Center tool, which allows automatic calibration of multiple user-selected parameters to adjust the model to match the measurement data. This calibration gives a very good fit, something that would be extremely difficult and time consuming to do manually, and so results in a model that has very high accuracy for us to use in system design.

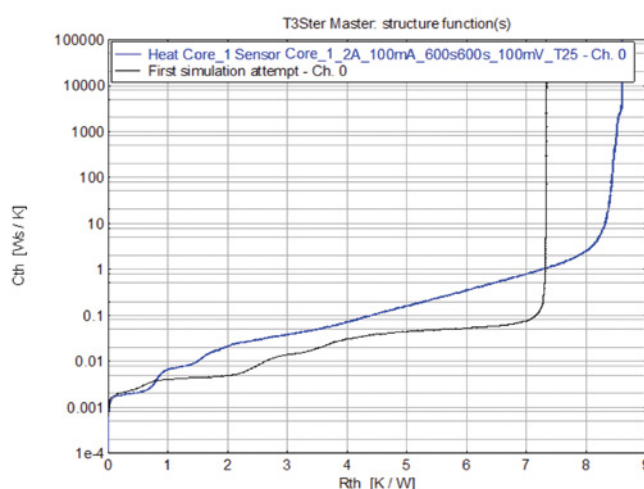To do this automatic calibration, we selected the time range corresponding to heating

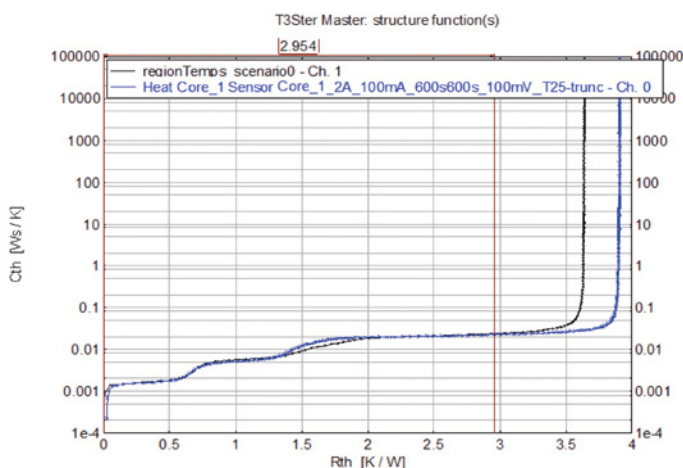**Figure 2.** Initial simulated curve (black) vs.curve measured with T3Ster (blue)

Figure 3. Final Calibration Result Showing Excellent Match

within the package, ignoring the part of the curve that represents heating of the board and the cold plate, so truncating the transient calculation to 0.15 s. The optimization requires a list of parameters, the exact values of which are uncertain, and a possible range for their thermal conductivity values. The parameters selected were the C4 bumps, with a conductivity ranging from 40 W/mK to 70 W/mK; the underfill (0.2 W/mK to 0.7 W/mK; the package substrate (10 W/mK to 20 W/mK); and the solder mask (0.5 W/mK to 3 W/mK).

The result, shown in figure 3, gives an excellent match within the thermal resistance range up to the junction-to-board thermal resistance (RthJB). This has proved to us the effectiveness of FloTHERM's auto calibration technology coupled with T3Ster, and the calibrated model can be used for board-level and system-level thermal analysis with a very high degree of confidence in the fidelity of the results.

E-Cooling: Cooling Power Electronics at Room Level

By John Wilson, Technical Marketing Engineer, Mentor Graphics

The conversion of electrical power with power electronics has become a key technology that enables many of today's innovations for electric vehicles as well as electricity production. Though the applications vary greatly there are two features they have in common: the electric components generate a significant amount of heat, and are trusted to operate reliably. A key factor in the reliability of electronics is the operating temperature. To maintain the operating temperature within specifications with a high heat dissipation, a proper thermal design must be developed.

Challenges

The market of inverter solutions for photovoltaic is growing. The Middle East, Africa and India are expected to massively invert in photovoltaic. In these regions, an average summer's day temperature of 50°C is usual. The customers require reliable inverters integrated in enclosures or containers without air conditioning. As the cooling air takes away the electrical losses, its temperature usually exceeds the environment temperature. Dust or sand entering the electric enclosures must also be avoided. Therefore, filters are necessary, despite large pressure losses.

E-Cooling, an engineering consultancy firm based in Germany, has expertise in the thermal design of Power Electronics, Transformers and Chokes at the component level or at room level where the computational domain enhances a complete enclosure, container or room. At room level, it must be ensured that the cooling path provides adequate airflow to all critical components.

Solution

E-Cooling performs thermal and airflow design with FloEFD® from Mentor Graphics. One of their recent designs involved the overall cooling of a 2.2 MW frequency converter enclosure. Such a frequency converter could be used for a wind power station to provide the grid with the correct frequency or for an electrical drive in order
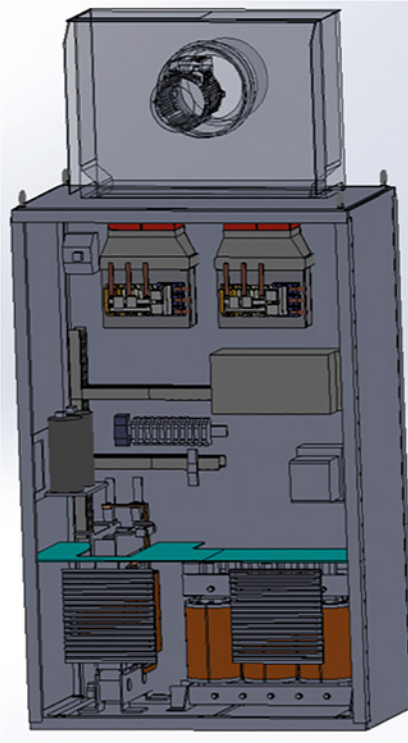

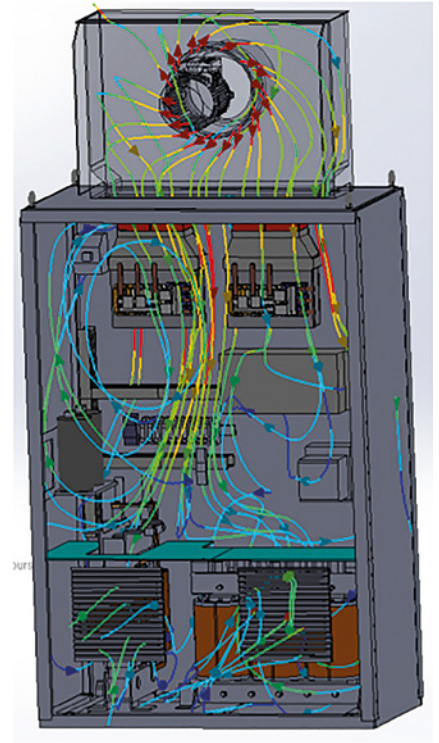**Figure 2.** The enclosure with its electric components and fan

Figure 3. Streamlines starting from fan colored with the velocity
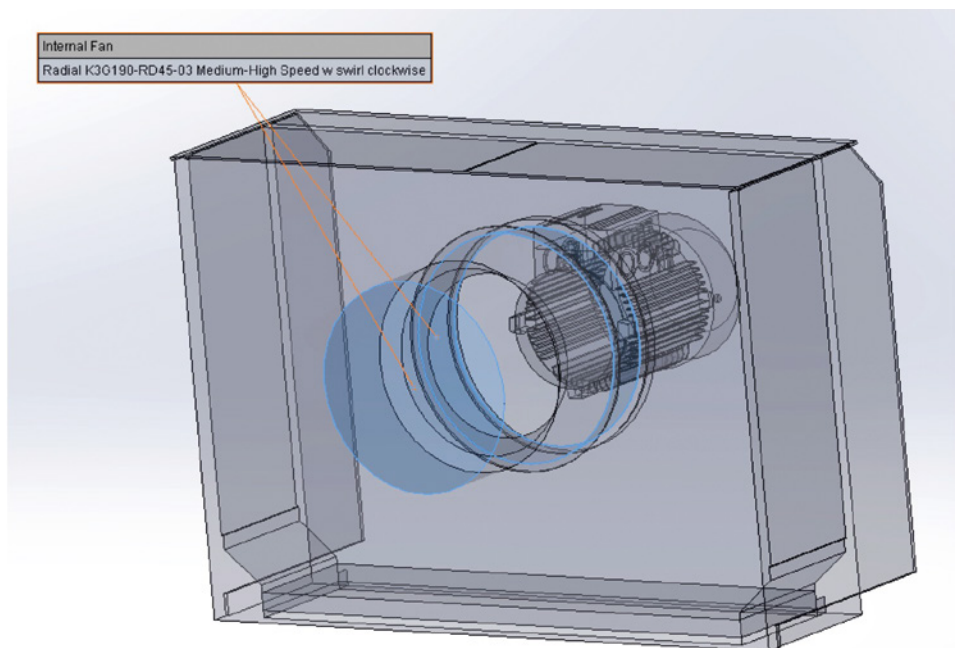

Figure 4. Frequency Converter Fans

to control the rotation speed. This power is reached by two frequency converter boards, each has three IGBT power modules and two dedicated axial fans. Each board dissipates 1,350 Watts.

When integrating electronic systems into an enclosure, it is important to determine if there is enough airflow through all critical components. This requires the accurate representation of all the significant flow obstructions as well as the fans. Here each fan as well as the dust filter were modeled with characteristic performance curves (pressure vs. volume flow) provided by the manufacturers. With the analysis, E-Cooling is able to determine the flow distribution within the enclosure and make any design modifications to allow the neccesary airflow for each component, including the use of alternative fans.

In the lower portion of the enclosure the model detail was not compromised. A detailed representation of the choke and auxiliary transformer was included as well as the flow diaphragm flow upwards and the exhaust grid flow downwards. A critical aspect of the design is to ensure that a large amount of the flow is going through the tiny passages between the windings. This can only be realized by obstructing the flow with a diaphragm or inner walls.

Benefits

Designing airflow and cooling solutions at the room level for power electronics is essential for providing reliable products to the market. During a development project the electrical requirements and losses usually change and components are likely to be replaced. With FloEFD embedded in the MCAD program, the automatic Cartesian meshing, and the possibility to start a calculation with an initial field, E-Cooling can update the thermal and flow model very quickly to meet project datelines.

"The most viable method of airflow design prior to testing is with CFD simulation based design software such as FloEFD. FloEFD allows E-Cooling to quickly build and assess the viability of an airflow and thermal design." Karim Segond, Consulting Engineer, E-Cooling.

E-Cooling in Berlin is an engineering consultancy founded by Karim Segond. Their expertize lies in providing 3D thermal and flow analysis, enhancement and development supporting electronics, electric engines, and power electronics.
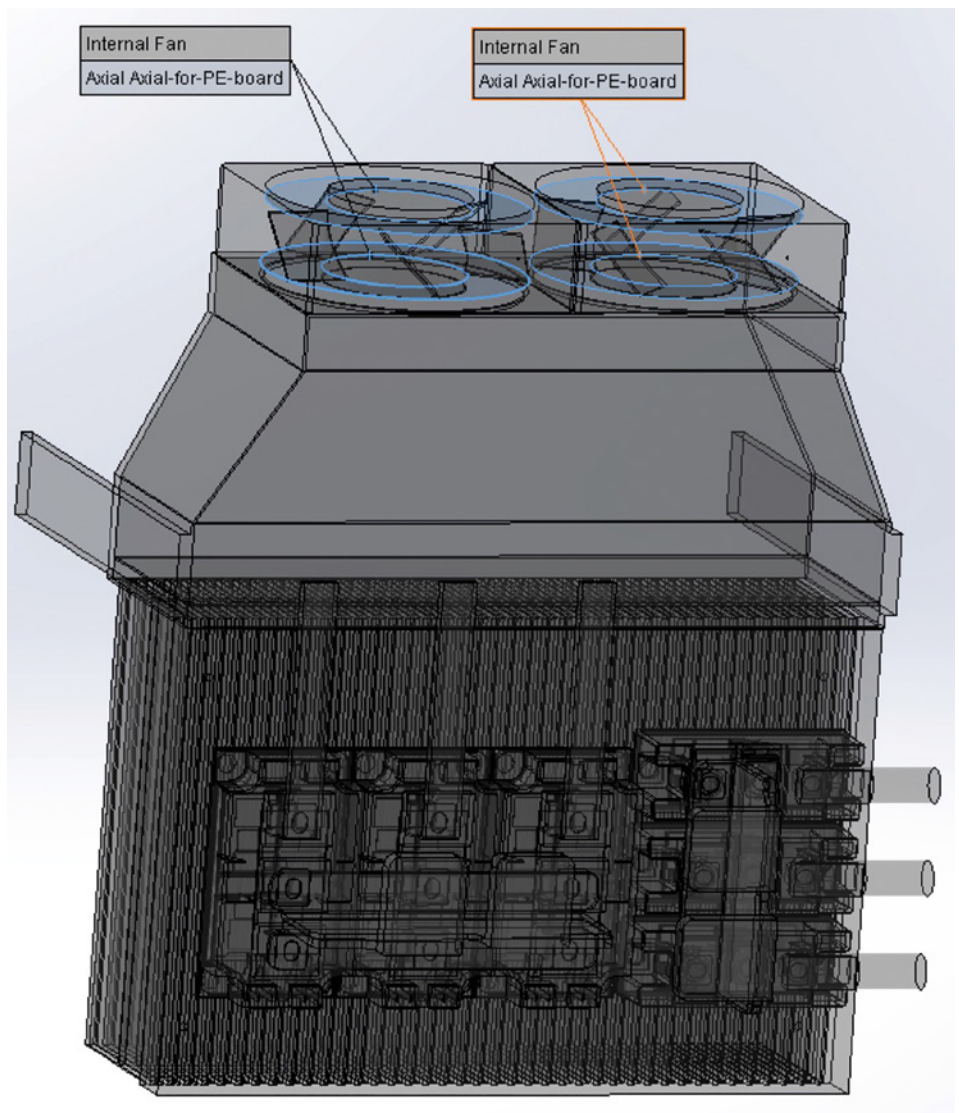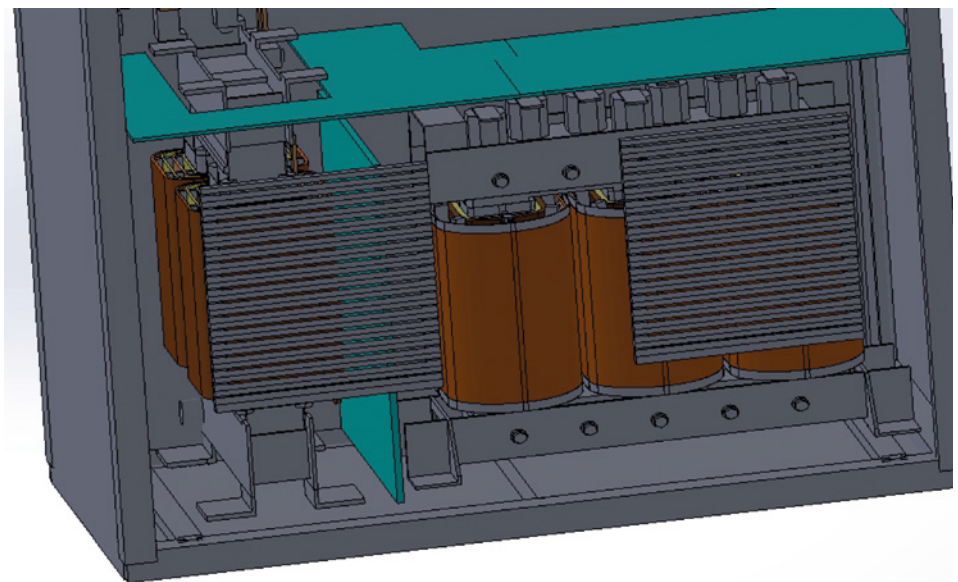

Figure 5. Enclosure Fan

Figure 6. Lower portion of the enclosure

Ask The GSS Expert

Excel export function

By Kate Boyd, Application Engineer, Mentor Graphics

The ability to run FloMASTER via a third party application, such as Excel, has long been recognized by users as an invaluable productivity aid. It streamlines the post-processing effort and opens up the power of the FloMASTER solver engine to engineers without previous experience of the software or who use FloMASTER infrequently. An experienced user of FloMASTER can make and set up a model, then create an Excel spreadsheet front end through which other users can access the model and run simulations in a familiar interface.

In V8.0, accessing this facility has been considerably streamlined: a simple export button in conjunction with the use of the existing variable parameters tool automatically creates spreadsheets which can be used to run and post-process FloMASTER simulations.

The export functionality is accessed from the experiments tab of the Network View window. (Figure 1)

The result is a spreadsheet which will run the variable parameter study outside of the FloMASTER GUI. The spreadsheet can be run directly with a FloMASTER solver licence, thus freeing up a GUI license for other users to increase productivity.

For example, take a simple ECS system containing a Compressor, Heat Exchanger and Turbine as shown in figure 2. The aim of the model is to examine a range of input conditions and see how the established system reacts, like a virtual test bench.

The system shows a simple arrangement of a turbine and compressor powered by the same shaft (modeled using controller components) and a heat exchanger using RAM air as a coolant.

The input variables to be controlled are the Hot Air Inlet Temperature, Shaft Speed, RAM Air Mass Flow Rate, and Hot Air Inlet Pressure. The variables to be measured are the Outlet Temperature, the Power Output, and the Heat Duty of the heat exchanger. Creating the input parameters can be done on
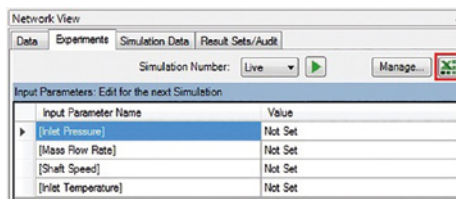

Figure 1. Input Variable Parameters
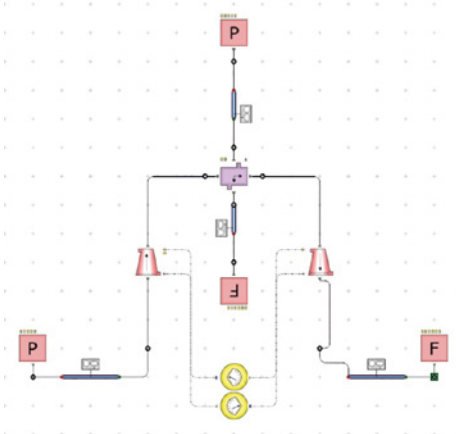
Figure 2. ECS System

Figure 3. Output Variable Parameters
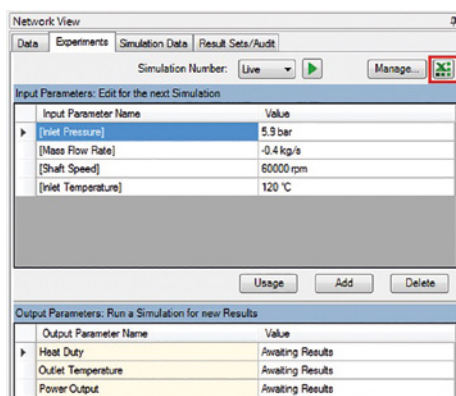
Figure 4. Export to Excel from the Experiments tab

Figure 5. Excel GUI Automation spreadsheet

Figure 6. Excel Options

Figure 7. Excel Add-ins

the Experiments tab or by simply typing the value in square brackets into the input field of the component.

Input parameters are not limited to just simple real values; they can also be set for:
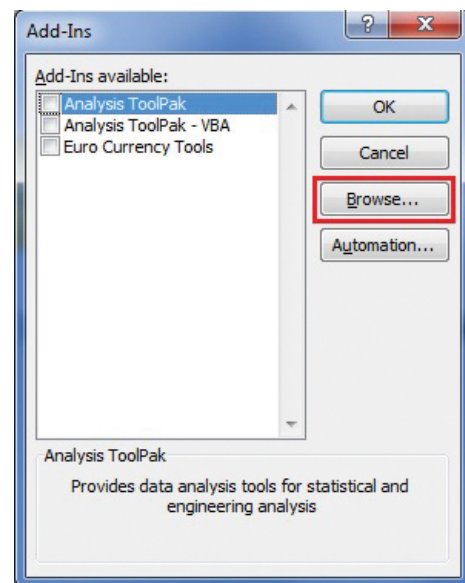
- Curves and surfaces,
- Scripts,
- Convergence and tolerance criteria,
- Materials, and
- General Data.

Figure 8. A successful run of experiments

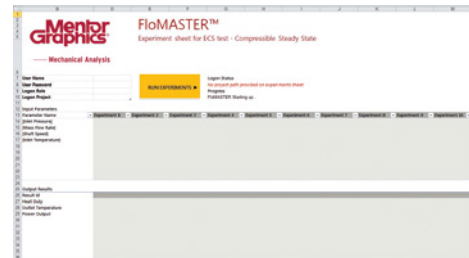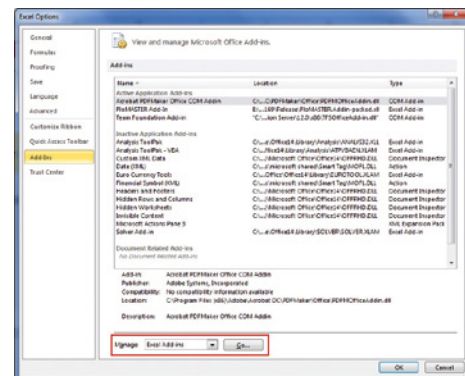|	FloMASTER Excel Export	Traditional Excel COM
Running simple experiments and post processing results in excel	•	
Steady state parameter investigations	•	
Modelling What if Scenarios	•	
Transient parameter effects		•
Large numbers of parameters and results		•

Table 1. Strengths of the FloMASTER Excel Export and Traditional Excel COM

Figure 9. Login details

Figure 10. An unsuccessful run of experiments

Creating output parameters is best done by highlighting the result in question and right-clicking to bring up the create output parameter menu. However, output parameters can be created on the Experiments tab as well.

After all of the input and output parameters have been created and the model has been validated, it can then be exported to Excel by clicking the button in the upper right corner of the Experiments tab.

An Excel window will appear with all of the input and output parameters already filled in. By default, it is in a read-only state; it is recommended to save it on one's local machine at this point.

Since this is the first time running the automation, it may be best at this point to create a folder which automatically allows macros. More information on this can be found in the user guide. This is not always required; however it is invaluable for the convenience of the users.

Next the FloMASTER Add-in for Excel must be activated. First, click the File tab, then go to Options and click the 'Add-ins' category. In the Manage drop-down, select Excel Add-ins and click Go.

The Add-Ins dialog will appear.

Click Browse… and browse to the location of the FloMASTER application (product of Mentor Graphics) directory. Select 'FloMASTER.Addin-packed.xll' and make sure that the checkbox is checked for the Add-In. Click OK. Once this is set up, the spreadsheet is ready to run.

In order for the simulation to run, much like in the GUI version of FloMASTER, login information must be given. Fill in the login information into the appropriate boxes. Make sure the correct User Name, User Password, and Logon Project are entered.

Next the values for Input Parameters must be entered. The units of the inputs and outputs in the Excel sheet are the same as the selected unit set for the Logon Project in the FloMASTER GUI.

Once the input parameters have been entered for all the desired experiments, the simulations can run in batch mode by clicking the yellow "Run Experiments" button.

The results of the simulation(s) will be displayed in the lower half of the Excel spreadsheet in the results output window.

It should be noted that the new Excel export is not intended to replace the current functionality already in place in the FloMASTER API. Both of the methods of linking to Excel have their own set of benefits.

The main difference between traditional COM and the Excel export is the flexibility of traditional COM scripting. Any component input or result can be added with a few lines of code in a COM script, whereas in the export function, the user would have to create the parameter in the Experiments tab in FloMASTER and then export the model again.

There are a few common trouble shooting issues which can easily be resolved:

Q: I received the error message: "Create failed with exception: Could not load file or assembly 'Flowmaster.Interfaces, Version=9.4.1.0, Culture=neutral, PublicKeyToken=a622c4c62ff70785' or one of its dependencies. The located assembly's manifest definition does not match the assembly reference. (Exception from HRESULT: 0x80131040)".
A: The Excel.exe.config file is not at the right version. The correct Excel config file will need to be copied from the FloMASTER V8 folder into the Office folder.

Q: I received the error message: "No project Path Provided on Experiment Sheet".
A: The field 'Logon Project' value cannot be blank. The Logon Project is the name of the folder in FloMASTER which will be logged in to (typically called FloMASTER).

Q: I have entered correct values for my input parameters, but I can only see 'Result IDs' and not 'Output Result' values.
A: The simulation failed for the network. This can be caused by a number of reasons. Contact FloMASTER support for assistance.

Q: Can I run the Experiment if some of the input parameters values are not set?
A: It is mandatory to add values for all of the Input Parameters. The current experiment will not generate results if any input parameters are missing.

Q: Can I run more than ten experiments?
A: Yes. By default ten experiments are shown in Excel, however further experiments can be added by selecting the Input Parameters and Output Parameters columns, then dragging Excel's fill handle to create as many experiments as required. The number of Input Parameters and Output Parameters columns should be equal for all simulations to complete.

Effective Vehicle Thermal Management

Improving Vehicle Thermal Management Simulation with MotorSolve and FloMASTER

By Doug Kolak, Technical Marketing Engineer, Mentor Graphics

When looking at system simulation in the automotive industry there are many areas where computer aided engineering (CAE) can be deployed effectively. One of the most valuable systems on the vehicle to analyze is the thermal management system. Traditionally this importance has been derived from the requirement to keep the internal combustion engine at a reasonable operating temperature. By doing so it would ensure not only that the vehicle was operating as efficiently as possible with minimal pollution, but critically that it would not overheat and experience significant thermal damage.

Today, as automotive manufacturers continue to shift towards additional electrification of the vehicle, both in the powertrain with hybrid and plug-in electric vehicles and in the controls and displays, the need for thermal management increases. FloMASTER™ is often used for this type of analysis because at a system level, it is able to account for all of the different components in the various systems such as the engine, thermostat, pumps, heat exchangers, fans, batteries, and power electronics. With all of these systems interacting through the flow of under-hood air, FloMASTER is able to simulate how the different systems will potentially affect another's thermal performance. One of the newer components of these EVs and HEVs, that now need to be included in the overall thermal management of the system, are the electric motors. As with other components in a system level model, it is the thermal performance of these components that can sometimes be challenging to find.

One of the most popular ways of obtaining this type of information, especially early on in the design process, is to characterize performance virtually. In this case a finite element tool called MotorSolve produced by Infolytica Corporation. MotorSolve simulates machine performance using equivalent circuit
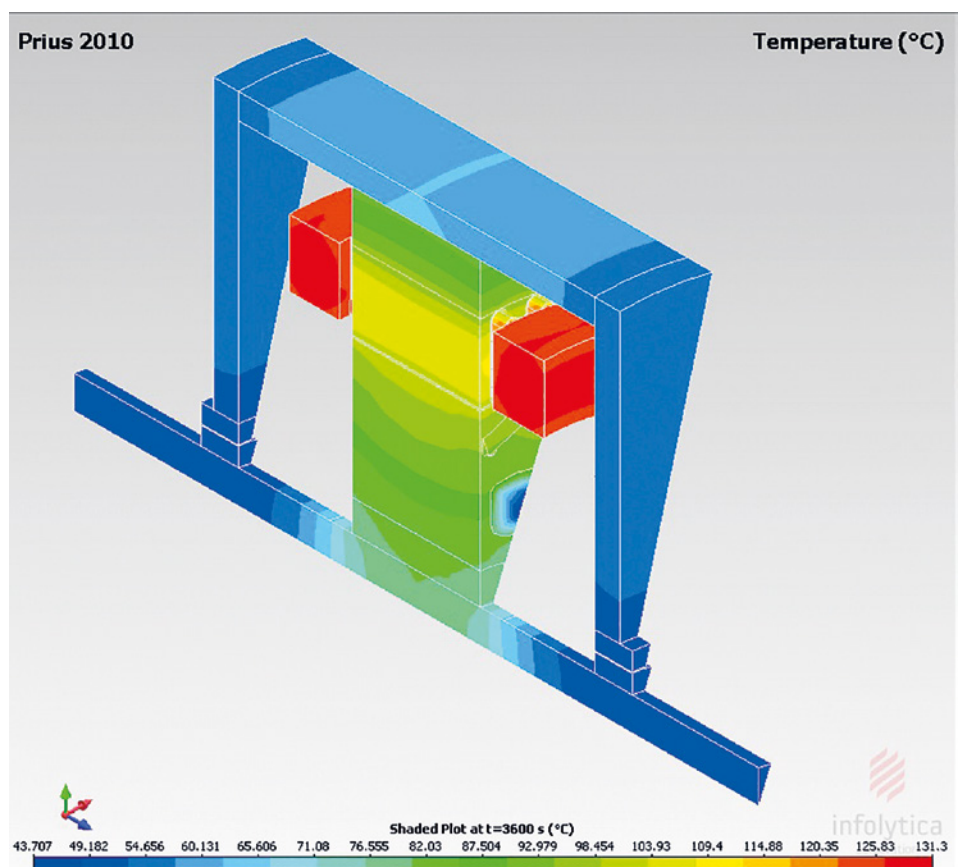

Figure 1. 3D Motor Temperature Result

calculations and a unique finite element analysis engine, allowing designers to quickly prototype motors and generators virtually. The purpose of this study was to incorporate the motor and the thermal load that it generates into a full system level hybrid-electric vehicle thermal management model.

Motor Model

For the study, the 2010 Toyota Prius was selected since it had full data available for which to build and calibrate the model. When configuring the geometry of the model in MotorSolve, the rotor geometry was imported using a dxf file and the stator lamination was already part of the built-in library so the process was very quick. The next step was

to configure the cooling setup for the motor. The 2010 Prius uses a partially submerged cooling system that removes the heat through the outside enclosure. In MotorSolve, the cooling was set up as a submerged spray type cooling with the number of jets calibrated to match the data available. This resulted in 32 nozzles each with a diameter of 2.5 mm and an oil velocity of 0.745 m/s. The engine oil that entering the cooling system was assumed to be at 25°C.

For the characterization, two analyses need to be run, first of which being a 3D thermal analysis. Since a motor is symmetrical, only one section of the model needed to be considered as shown in figure 1. The analysis
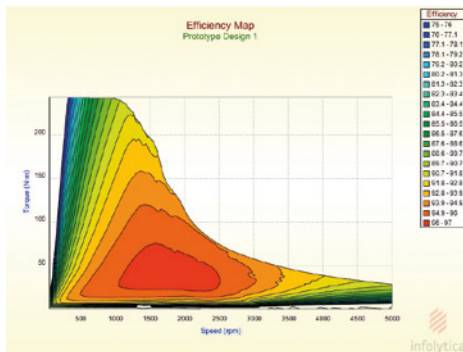
Figure 2. Motor Efficiency Map

Figure 3. Motor Cooling Loop in FloMASTER

Figure 4. Full FloMASTER Vehicle Thermal Management Model

is very fast, taking only a few minutes, but providing several key factors for use in FloMASTER. First it calculated the overall thermal resistance which is used to calculate the heat transfer coefficient. Second it calculated the total thermal capacity of the motor and housing. Because there is a combination of parts in a motor made of different types of metals, this total thermal capacity is converted for use in FloMASTER by calculating an equivalent mass of steel.

The second analysis run was to create efficiency maps for the motor. There are several factors that can affect the efficiency of a motor but for this study three were considered: motor temperature, speed, and torque. To populate data for the characterization, the temperature was limited to two data points, one at the cold ambient and one at the pseudo steady-state temperature from the thermal analysis. For speed, a range of values from 0-5000 rpm was used, and for torque values from 0-250 Nm. The analysis accounts for all losses of the motor including friction, windage, Joule heating, eddy current, and iron and stray. It produces a surface map of efficiency versus speed and torque at each temperature. (Figure 2)

System Model
When looking at cooling the motor from the system perspective, the first thing to consider is how to represent the oil circuit that is dissipating the heat from the motor. One way to do this is by constructing a closed loop circuit comprised of a reservoir for the fluid, a heat exchanger, a pump, and a component to represent the motor. For this study the motor is represented by a collection of components (figure 3):

- Thermal bridge to calculate the amount of heat transferred from the motor to the cooling oil,
- Point mass to represent the thermal inertia of the motor,
- Heat source to apply a thermal load to the

Figure 5. FloMASTER Motor Temperature Result
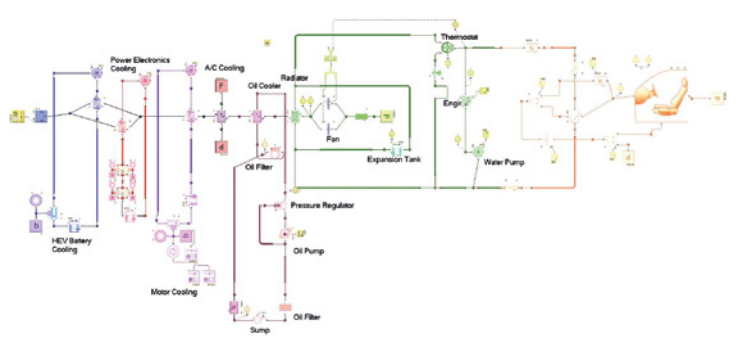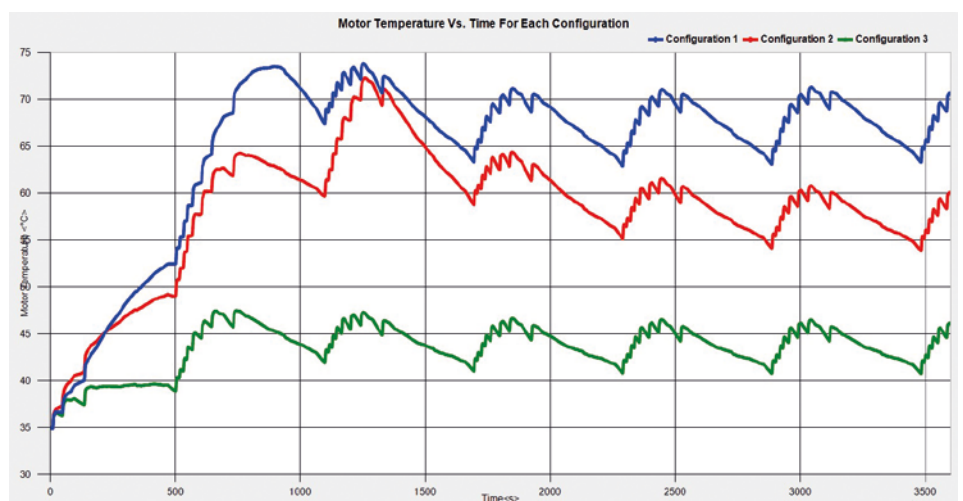
motor based on the efficiency maps from MotorSolve and the motor speed and torque from the drive cycle,

- A controller specifying the motor speed based on the drive cycle,
- A controller specifying the motor torque based on the drive cycle,
- A gauge reading the temperature of the motor and feeding it back for calculation of the thermal load, and
- A controller calculating the thermal load based on the motor speed, torque, and temperature.

This motor cooling sub-system can then be incorporated into the larger vehicle thermal management model. With the setup previously described the most likely place to connect this sub-system to the large model is through the heat exchanger since it will likely share under-hood airflow with the other sub-systems in the model. (Figure 4)

Case Study
Adding the motor cooling circuit means the model can now investigate how cooling the motor will affect other parts of the vehicle and vice versa. As an example, three different configurations were explored:

- Configuration 1 has a separate cooling loop for the motor directly after the power electronics,
- Configuration 2 combines the motor and power electronics into a single cooling loop, and
- Configuration 3 places the motor cooling loop at the front of the under-hood air path.

Figure 5 shows the results of the motor temperature for each of the configurations. Overall the temperature is lowest for configuration 3 since it is the first system in the cooling pack and thus has the coldest air. Configurations 1 and 2 have a similar rise at the beginning of the drive cycle but configuration 2 levels are 8-9°C cooler due to the positioning, even though it is in the same loop as the power electronics. FloMASTER's versatility as a system level thermo-fluid solver, enables a wide range of designs to be considered in the vehicle thermal management area. As these systems become more complex, it is important to identify where to get performance data from, such as MotorSolve to ensure accurate system simulation results.

FloEFD helps Dr. Schneider's mission:
To make the Car the Best Place in the World

By Enrico Lorenz, Research & Development, Dr. Schneider Unternehmensgruppe GmbH
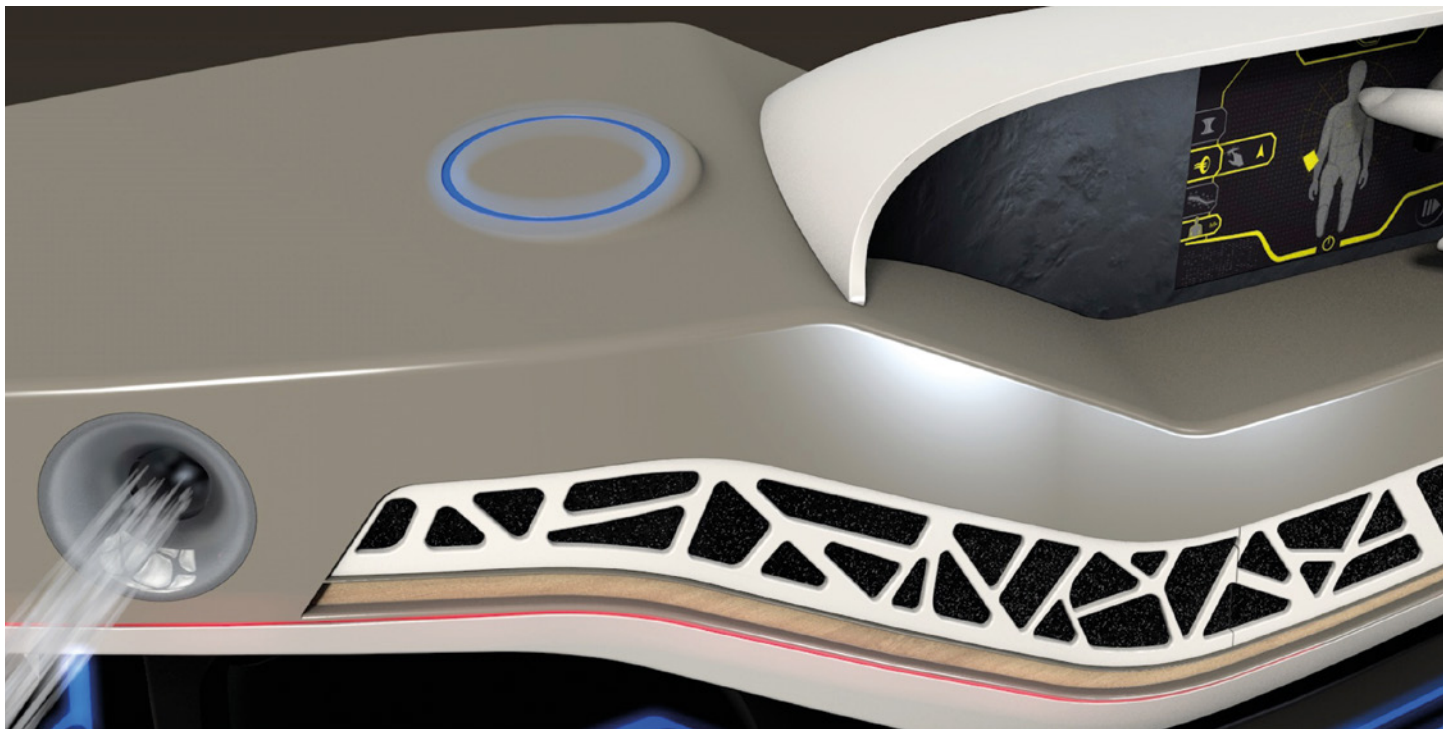
Dr. Schneider, a successful family-run business, located in Kronach-Neuses in Germany, supplies and develops vehicle plastics components and systems for renowned automotive producers all over the world. The entire process chain is handled within the group, from research and design to prototype construction. (Figure 2) Dr. Schneider has more than 3,900 employees and 90 years of experience in the plastics field, 60 of which are in the automotive industry.

Dr. Schneider's primary products are visible parts for the car interior: air vents (figure 1), stowage boxes, kinematic components, bezels, covers and trims, grills and window frames.

As the automotive market expands and grows, product development times are dramatically reduced. For many projects even the use of prototyping is no longer an option, making the need for reliable, fast and accurate simulation tools essential to overcome these challenges. Furthermore, frontloading the Computational Fluid Dynamics (CFD) simulation into the product development phase is crucial to the success at Dr. Schneider. Mentor Graphics' FloEFD tool is used mainly for the simulation of the air vents, one of Dr. Schneider's core products.

Figure 1. Extract of Dr. Schneider's products: air vents

"With FloEFD we can shorten product development time, quickly find appropriate design variants, save costs and explain and present the flow behavior of our products to our colleagues and customers."

Enrico Lorenz, Research & Development, Dr. Schneider Unternehmensgruppe GmbH

As FloEFD can be directly embedded into Catia V5, CAD models were used directly in the program with no need for additional geometrical preparations. Airflow distribution is investigated at a very early stage and must adhere to strict customer targets and specifications. For the example shown in figure 4, the influence of a bezel was investigated. The two variants of this broadband vent, with and without bezel, were simulated. The broadband vent variant including the bezel shows a better distribution of the airflow. The flow angle into the lower area is enlarged. Additional experiments in the lab using fog to visualize the air flow confirmed the FloEFD predictions. (Figure 5)

Enrico Lorenz, Simulation Engineer, explains: "We make up to 100 FloEFD simulations per month per license. We need fast, robust and accurate simulation results. In addition we need an efficient way to create the result reports and presentations". In combination with the batch run functionality which allows automatically runs of many variations, the pictures for comparing the defined
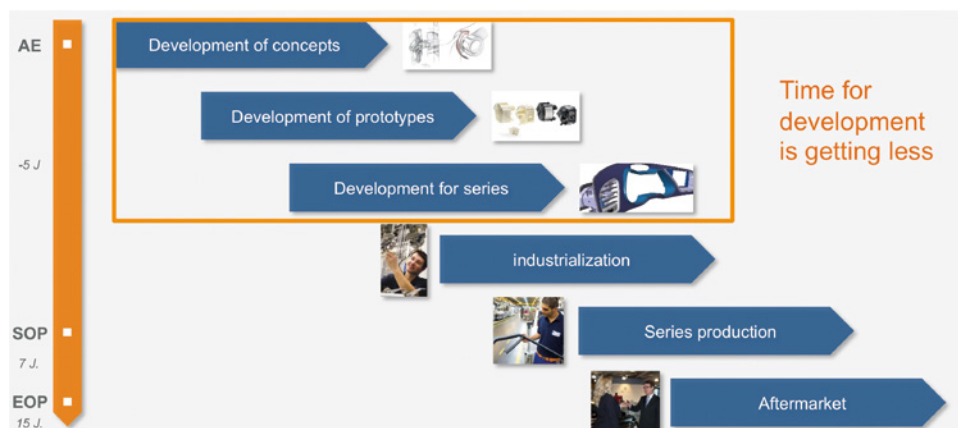

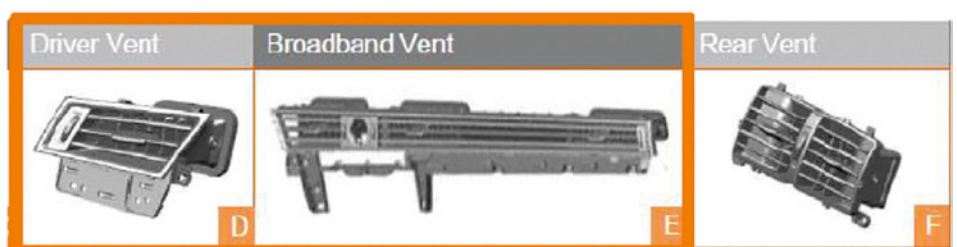**Figure 2.** Todays product development process

Figure 3. Driver, broadband and rear vent

> *"FloEFD predicts what we need, so it helps us to make the car the best place in the world."*
>
> **Enrico Lorenz, Research & Development, Dr. Schneider Unternehmensgruppe GmbH**

results items are created automatically. The influence of design changes on the fluid flow behavior can immediately be identified. (Figure 6)

One of the major tasks is creating MS PowerPoint presentations for internal purposes and for customer presentations. This might take more time than the simulation itself. For this reason, a VBA code is generated by the Dr. Schneider engineers which automates this work in MS PowerPoint.

With FloEFD embedded in Catia V5, Dr. Schneiders' engineers are able to meet today's requirements of short development times and fulfill the strict targets of automotive manufacturers.

Does the airflow directability of the air vent reach the targets set by the customer?

Figure 4. Broadband vent and airflow

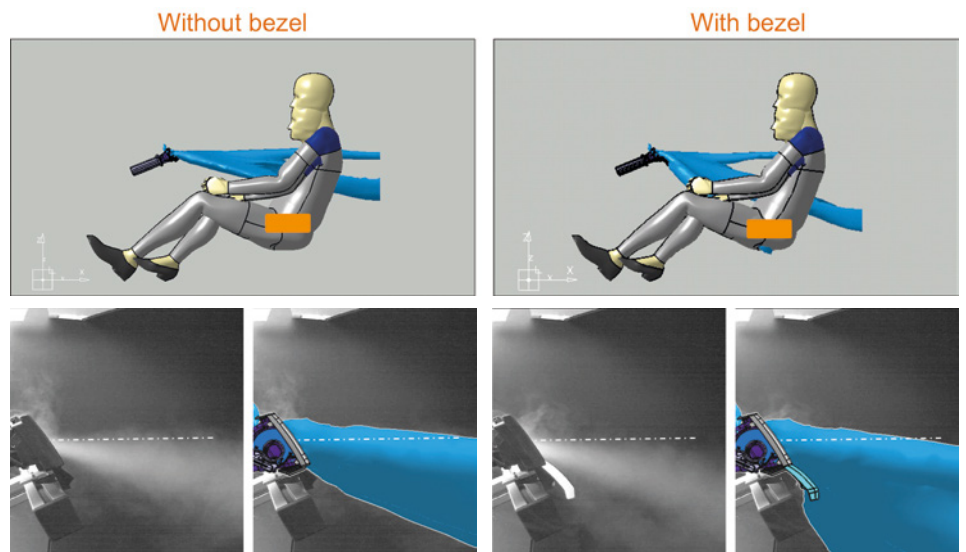

Without bezel   With bezel

Figure 5. Comparison of the broadband vent without and with bezel
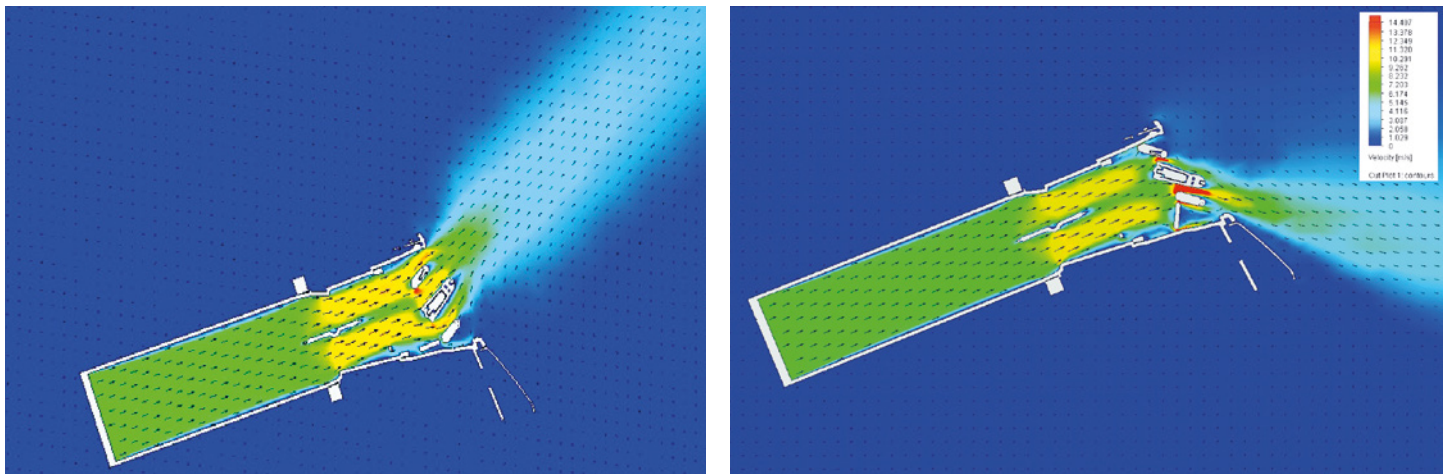

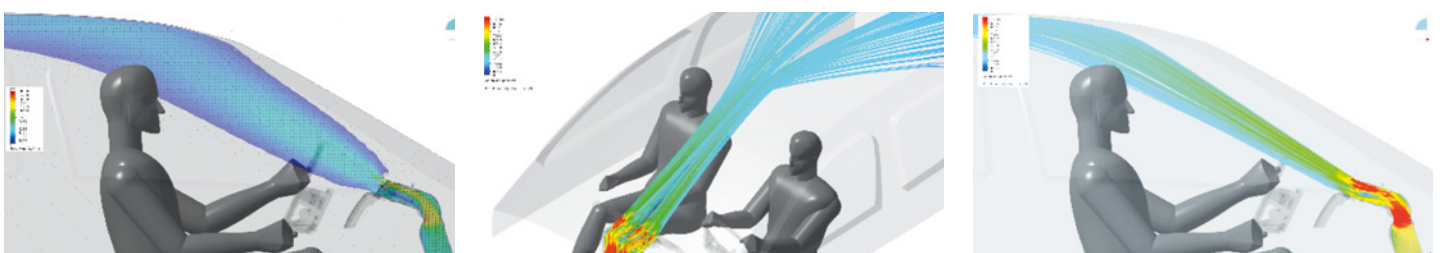**Figure 6.** Cut plots showing the velocity for different variations

Figure 7. Airflow distribution in the car interior

Paul-Henri Matha, Lighting Expert, Groupe Renault

Q. Tell our readers a bit about Groupe Renault?
A. Groupe Renault is a long established €45bn/yr French multinational automobile manufacturer that makes a wide range of cars, and vans (no trucks). It is a top ten OEM supplier and an international alliance with Nissan in Japan that makes us number three in the world, with subsidiaries that include Dacia and Renault Samsung Motors. We are strongest in B and C category segments cars like the Renault Clio, Megane, Scenic, Espace and Kadjar. We have been a pioneer in automotive styling over the years and our 'C' shaped headlight assemblies based on Light Emitting Diodes (LEDs) are a signature part of our marque these days.

Q. What is your background and your current role as a Lighting Expert in Renault?
A. I actually trained as a Mining Engineer before I joined Renault in 2000 to become part of their, then, small lighting group where I have risen to become the resident Lighting Expert in 2015. My role includes technologies and processes associated with our global lighting design activities with a primary focus on optimizing our simulation and test workflows thereby reducing costs in manufacturing. My work has a real impact on the financial bottomline at Renault. I also constantly try to think 'out of the box' and seek technology innovations that helps keep us ahead of the competition in a very competitive sector.

Q. Tell us about the Automotive Lighting Design Group in Renault-Nissan?
A. We have a large dispersed group around the world with most based in Paris but other significant groups in Korea, Romania, Brazil and India. We are closely linked to the Electronics Design Group inside Renault. We cover both simulation and test and deal with suppliers which Renault holds to very high specifications for incoming components and assemblies.

Q. How does your role influence the bottom-line at Renault?
A. A big part of my role is to understand the supply chain for lighting inside and outside Renault to manage and reduce costs. To do this properly, especially with suppliers, you have to have pre-development technical knowledge of all components and things like their thermal performance. With the advent of LED lights we can save on CO_2 emissions versus the old halogen lamps we used to employ. But also in
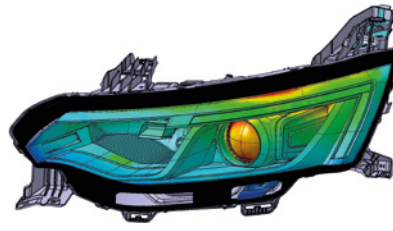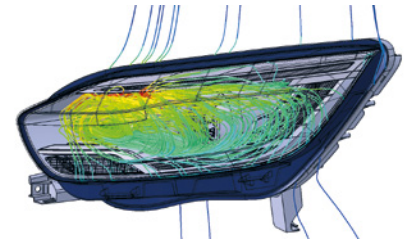

Figure 1. Renault Laguna Headlight assembly thermal analysis (left) in FloEFD and airflow pathline details (right)

the size of the headlight assembly package, such that it can be several centimeters shorter than before, for instance. It is essential to manage costs early in the design cycle with preferably multiple loops to optimize designs. Questions we might want to ask include 'If you change the temperature of a bulb will it fail?', 'Can we design for a smaller heatsink with less weight?' etc. Designing our headlamp LED arrays so we can go down from five to three LEDs yet maintain lighting quality and thermal levels can save several Euros per headlight in costs. That soon mounts up over large production runs. At Renault we have reduced our headlamp costs by 50% between 2014 and 2016 and we are aiming for a further 50% reduction in costs for our Generation 3 LED headlamps by 2018-2020.

Q. Why did you select FloEFD® as your headlight thermal analysis tool?
A. Well, first we correlated FloEFD with experimental measurements and it was very good. The big advantage with FloEFD we found is that you don't have to do meshing and you can save a lot of time at this stage of CFD. Because it is embedded and highly integrated into CATIA, our preferred MCAD tool, one thermal engineer can be over twice as productive. It also moves the analysis tool further up the design sequence. Invariably, we can do many more design loops of increasingly more complicated designs with FloEFD. We shoot for hundreds of simulations versus two or three in the past in our design optimization. With FloEFD's vapor absorption, deicing and condensation capabilities it is very well suited to our head and tail lighting applications in future.

Q. How does thermal modeling of headlights fit into the other physics simulations Renault does?
A. Of course we have to do EMC (electromagnetic confirmation), structural analysis, vibration and optical modeling (using Lucidshape) associated with each headlight design. And, naturally, a headlight is close to the engine underhood cavity which can produce surface temperatures of 70 – 80 °C which we have to take into account. Hence, we have to devise simulation workflows that accommodate all our different tools to make sure the boundary conditions for each tool is correct. Managing our software and the transition between them is becoming ever more important.

Q. There are a lot of new technologies coming to automotive lighting – what do you see as the most significant?
A. If I look to the horizon we all see electric vehicles and autonomous driving coming to the industry plus laser lighting and OLEDs (Organic LEDs). All of these will pose different lighting challenges I think. Laser lighting is being used in high-end automobiles, but we are not sure how much it will impact the market. At the moment it is only used for high beam headlights and there are questions over the efficiency of light emission in terms of lumens/watt. Mood lighting is being used today throughout all car ranges and in terms of thermal impact, it is not that significant due to it being low power. However, if they get hot the driver needs to turn them off and driving in tunnels may require them on automatically for instance. In terms of OLEDs, there is talk of V2X (vehicle to exterior) applications, but there are questions over OLED thermal reliability and the quality of the light source degrading over time, plus they are relatively expensive. In terms of electric vehicles they are easier to design in terms of lighting compared to conventional internal combustion engines as there is no hot engine cavity nearby plus condensation tends to be less of a problem. Finally, autonomous vehicles will pose a whole new set of regulatory lighting challenges. With no driver in such a vehicle, how do you light up a vehicle so that it is apparent to other drivers that it is autonomous? Do you have external red and green lights for instance? How do you determine standards between countries? All these need to be determined internationally still.

Q. Where do you see Thermal Analysis going in future at Renault Automotive Lighting?
A. We are in the business of managing headlight thermal and optical reliability. A good example of this is a Matrix Beam headlight with ten LEDs for instance. What if some LEDs are on and some are off during a normal drive cycle? At the moment we deal with steady state CFD simulations but in reality transient behavior will become more and more important in determining headlight lifetimes of up to 10 -15 years. Ultimately my dream is to push CFD down to the design engineer such that they would have a specification for a headlight and they could figure out for a given junction temperature at the LEDs, what size of heatsink, the overall size of assembly, and the number of LEDs that will be necessary to perform the specification well.

Driving down **Automotive Headlamp costs** at Renault

By Paul-Henri Matha, Lighting Expert, Groupe Renault

Automotive headlight design is an important part of the Renault brand these days and our 'C shape' headlights are a signature part of the appeal of our cars. About 30% of the cost of automotive headlight assemblies can be found in the mechanics and 70% in the electronics. Hence, any savings that can be made on the electronic side will have a profound influence on the overall cost of these units. This article will outline how we have broken down our headlamp costs and used thermal analysis tools to incrementally optimize headlight designs to achieve a 50% cost reduction in the two years from 2014 – 2016 and how we intend to halve it again in the next few years.

In Generation 1 of our full LED headlight assemblies we looked at six of our C and D-segment vehicles from the Espace to the Koleos. (Figure 1) We first standardized all platforms to one common height sensor, one common static leveller, one common DRL/low beam/high beam driver, one common central connector, and common low and high beam modules with two suppliers for each. We did this in one year by examining the partition of costs and standardized about 60% of the components of our headlights. (Figure 2) It can be seen that the plastics we used only made up about 30% of the overall assembly price. The volume effect is the main cost factor for a headlamp's part price as is its supply entry ticket. However, by moving from Halogen headlights in 2012 (see figure 3) to LED based headlights in 2014 the overall costs went up four-fold. This in itself gave us the impetus to see if we could cut costs in Generation 2 of our headlight evolution.

We focused our Generation 2 headlamp effort on our popular Segment B car, the Renault Clio, which was going through a

facelift and stylistically we wanted to move it to our LED based C-shape DRL lighting. (Figure 3) There were four pillars to our Generation 2 strategy:

1. Be the first generalist automotive OEM with full LED headlights in this B-Segment car,

2. To reduce by a factor of two the headlight part price between Generations 1 and 2,

3. To have a better LED lighting performance than the Clio Initiale (which had Xenon 25W lights), and

4. To reduce overall headlight assembly depth by 50mm.

We standardized the Clio on a common LED Electronic Control Unit (ECU), a common height sensor, and a common
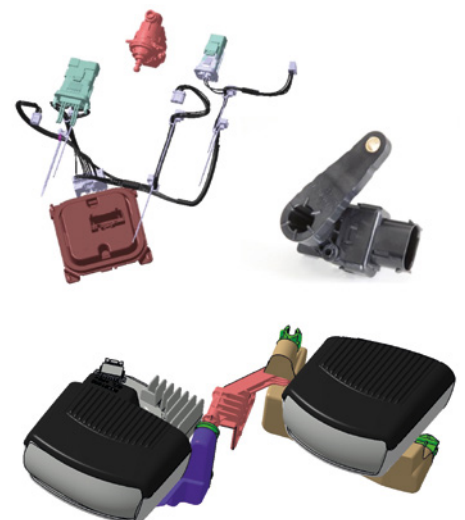
**Figure 1.** C and D-segment vehicle headlighting in this study
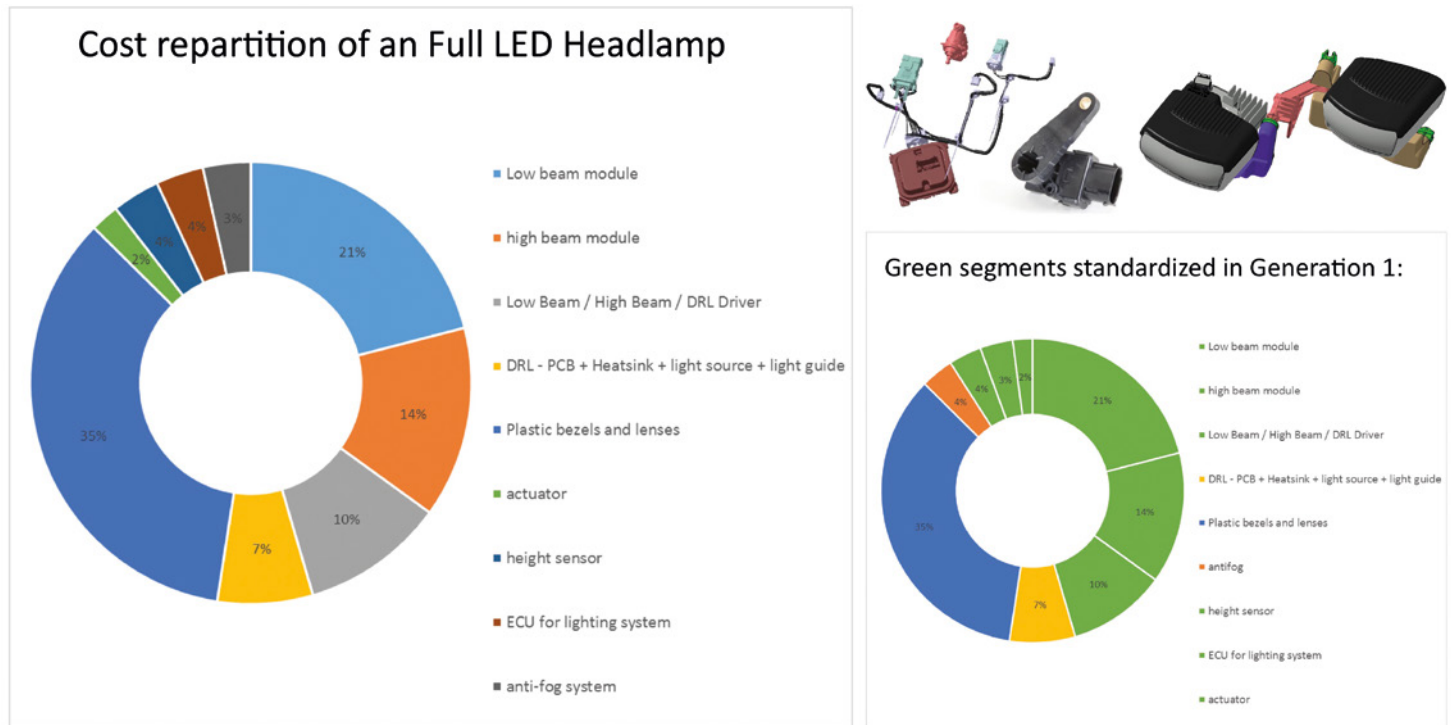
Figure 2. Headlight components standardized in Generation 1 versus overall cost partition of a Headlight Assembly

leveller. We then focused on the LED Low Beam light and reduced its price to 30% by reducing the number of LEDs, the size of the heatsink by 30%, and improved the optical system. By doing all these things (see Table 1) we improved the LED light flux by 33%, and reduced the assembly from eight to five LEDs. We also increased optical efficiency by 25% and produced an overall assembly size reduction of 50mm. With the thermal improvements to the LEDs we were able to increase the LED current, increase the maximum junction temperature usage and the flux derating at a lower ambient temperature (Table 1). Similarly, with the associated heatsink design, we were able to get better junction temperature management and better derating management through our detailed thermal simulations. (Figure 4)

With respect to the overall headlamp package size, figure 5 shows the 50mm depth saving we were able to achieve between Generation 1 with a halogen headlamp and Generation 2 with a LED headlamp due to a better designed assembly. Figure 6 shows typical CFD simulations for a halogen headlamp in Mentor Graphics' CAD-embedded software, FloEFD®, illustrating the complex air flows and thermal effects to be found on the surfaces in the assembly.

Looking deeper at our general CFD-based thermal analysis approach to headlamp
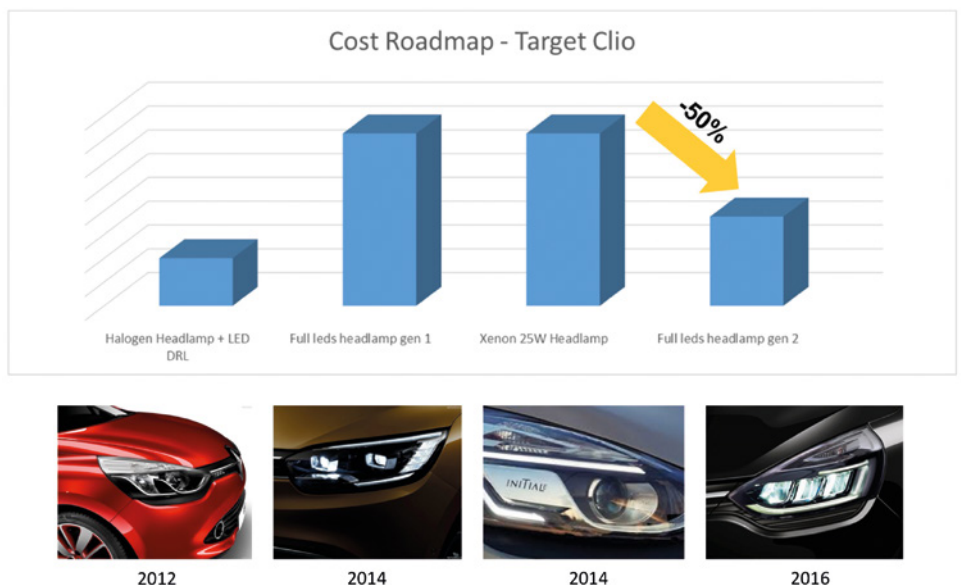
Figure 3. Renault Clio Headlamp changes and cost reductions from 2012 – 2016: Generations 0 to 2

Solution	Current (mA)	flux / LED	Number of LEDs	Tj @ 23°C T° ambient	Start of derating
LED Low beam Gen1	800 mA	200lm	8	120°C	T° ambient 60°C
LED Low beam Gen2	1A	270lm	5	130°C	T° ambient 50°C
LED High beam Gen1	800 mA	200lm	4	120°C	T° ambient 60°C
LED High beam Gen2	1A	270lm	4	130°C	T° ambient 50°C

Table 1: LED solution evolution from Generation 1 to 2 for the Renault Clio Headlamp

design that typically is used to optimize designs, we would normally be interested in predicting lighting performance at 23°C outside the headlamp in ambient air and up to a maximum of 70°C for the outside temperature for the outer boundary of LED reliability. To validate our simulations, we therefore carried out some experimental tests where we fixed the ambient temperature outside the headlamp at 23°C and installed eight thermocouples outside the assembly (see figure 7) for a car with its engine on and off.

Figure 8 shows thermocouple time traces for both the engine on and car stationary for 3hr 30mins; then lights switched on for 1hr 30mins with the engine on and stationary, and then the lights on and engine driving for 1hr 30 minutes. It is clear that the temperatures can reach over 50°C inside the headlamp when the engine is idling and the lighting is on for a prolonged period. In addition, headlamp surface temperatures can rise to 65°C in certain idling conditions. With other tests we were able to show that with just a low beam on for an hour, the temperature inside the headlight went to 20°C and with both low and high beam on for an hour an extra 5°C in temperature was measured.

We also carried out a series of tests where we evaluated the effects of engine idling and lights either on or off by looking at Rjth of an Altilon LED with 3K/W and 3 chips @ 1A and for a Delta (Tjunction – Tcase) of 20°C. We were able to show that for ambient temperatures of 70°C and with both low beam and high beam lights on, together with the engine on that the junction temperature of the LEDs comes very close to the worst case scenario of 150°C. We concluded that it was not possible to design a LED system if we were to take into account all the use cases. The OEM must therefore define the best compromise. For example, at 23°C, after one hour engine idling, lighting performance was shown to be at 100%, but if the ambient temperature rose to 50°C for the same situation the lighting performance would go down to 80%. In order to respect this specification we concluded that a thermal sensor had to be added to the PCB so that the current could be reduced if the temperature at the LED was greater than a threshold we would define. We could then do a thermal derating and a flux derating of the full LED headlamp.

Going forward, we are putting in place an action plan to deal with simulation and testing of lighting in transient drive cycle

Figure 4: Renault Clio Headlamp heatsink weight evolution Generations 1 to 2
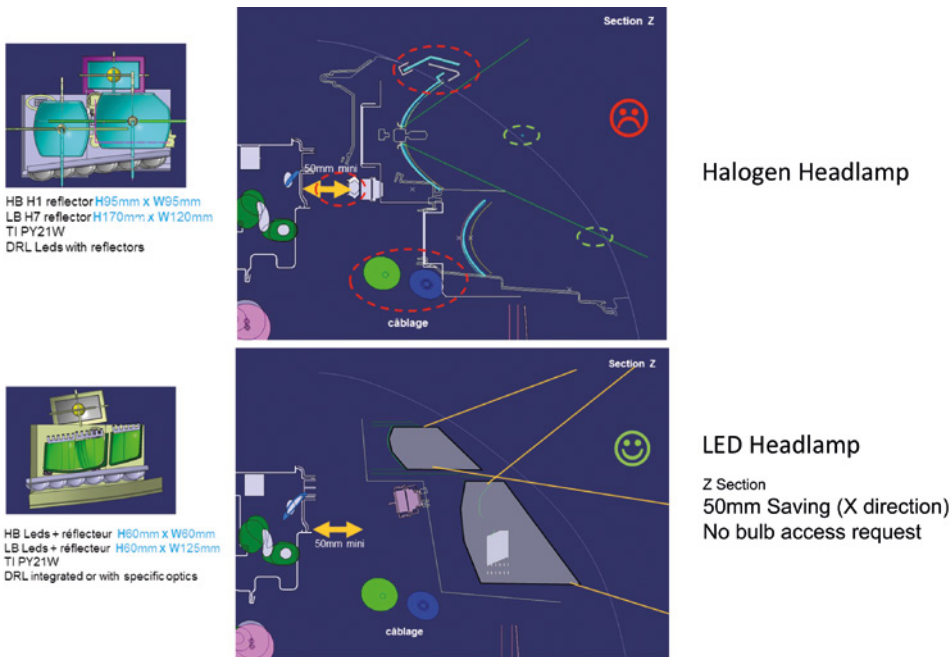

Figure 5: 50mm Headlamp Package saving between Generation 1 (halogen) and Generation 2 (LED)

Figure 6: FloEFD Thermal Predictions for a Renault Halogen Headlamp Assembly
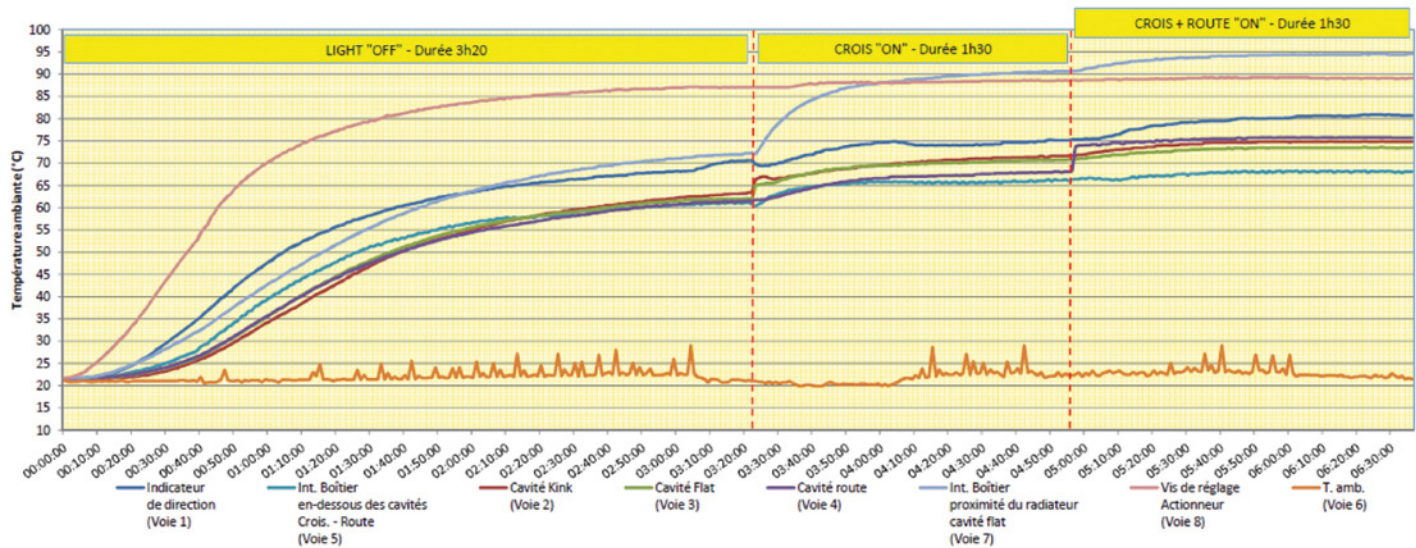
Figure 7: Location of the eight thermocouples for the Ambient Temperature Headlamp Engine Tests

modes. (Figure 9) As an OEM we want to be able to simulate the impact of car speed on its lighting's thermal performance, and in particular the thermal variation due to speed of each of our engines. This will make thermal CFD software key for lighting engineers in future.

We also need to be able to model the nearby engine bay's thermal behavior in parallel with the headlight simulation as they affect each other. And we also see the need for thermal management inside the headlamp when thermal inductors will be present. In short, Renault believes that the OEM should be responsible for the complete thermal system associated with headlamp design. To do so will make the OEM a market system leader.

Our immediate goal in the Renault Lighting Team with Generation 3 of our project is to increase the LED flux of headlamps from 270lm to 320lm by 2018 – 2020 and introduce new LED Drivers to deal with higher power, plus we are aiming for the introduction of Turn Indicators and AFS functionalities, as well as overall assembly size reduction. Finally, we are aiming for a Height Sensor regulation evolution. Our eventual target is to get our full headlamp assembly to reduce in price by another 50% bringing it to the levels we saw with halogen headlamps five years ago. (Figure 10)

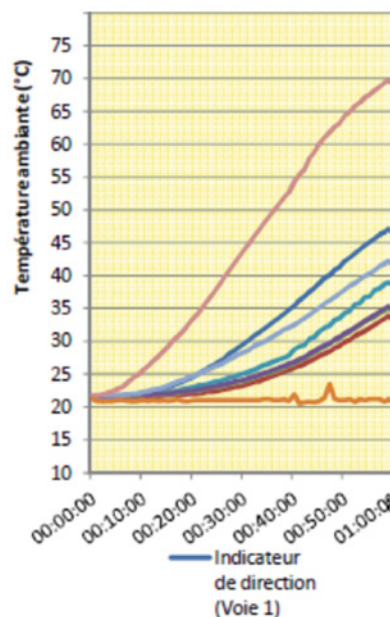**Figure 8:** Thermocouple Temperatures outside the Headlamp Assembly for Various Engine on and light on/off scenarios

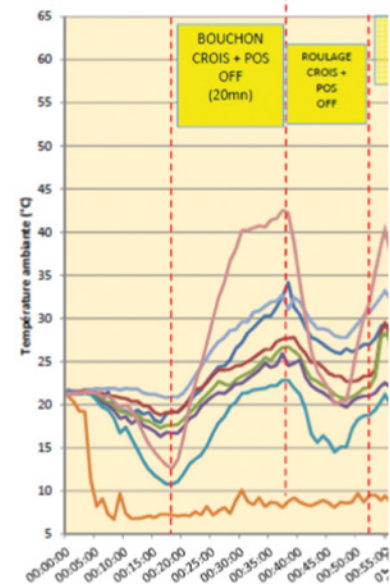**Figure 9:** Headlamp Temperature Measurements for Engine Idling and during a Car Drive Cycle
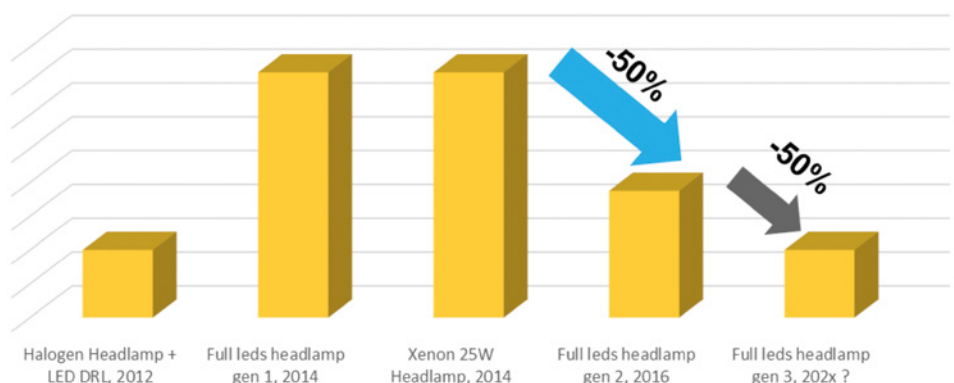

Figure 10: Renault Headlamp Cost Reduction Roadmap to Generation 3 Headlighting

How To...

Characterize an Automotive Thermostat for Thermo-fluid System Simulation

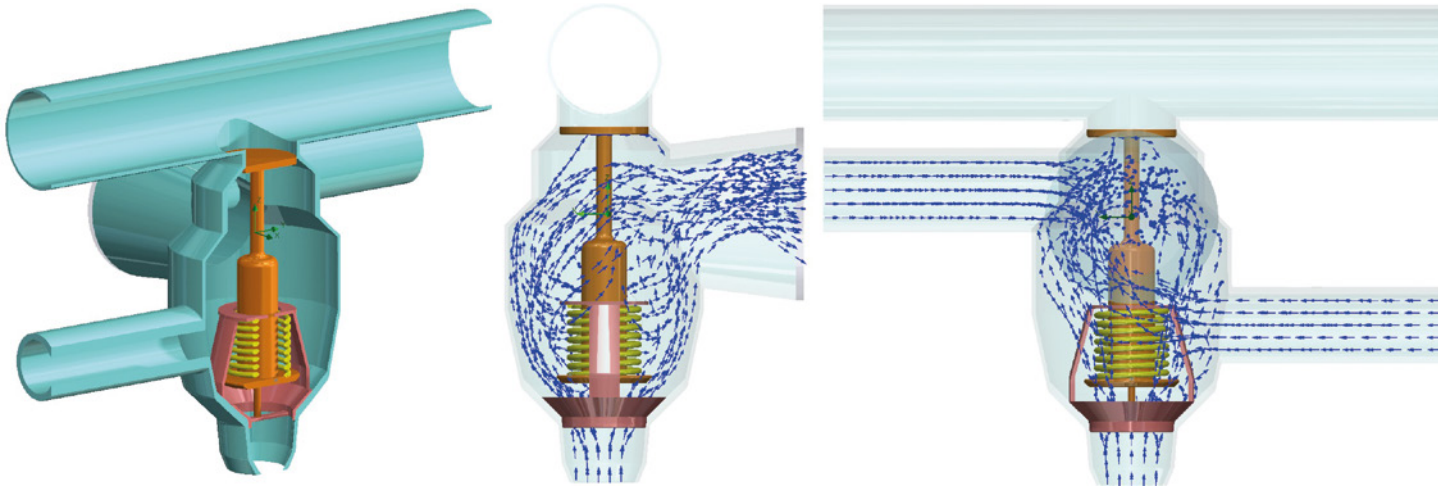By Doug Kolak, Technical Marketing Engineer, Mentor Graphics

Figure 1. Thermostat Model in FloEFD

Automotive thermostats are one of the most important components in a vehicle thermal management system. It is responsible for maintaining an acceptable working temperature in the engine both to prevent catastrophic failure and keep it operating as efficiently as possible. As vehicles have become more complex with their cooling systems, so too have thermostats. These parts are no longer as simple as a single flow path in and then either flow to bypass or the radiator. It is easy for these components to now have at least three or four inlets and multiple outlets.

This increased complexity creates more complex 3D flow patterns that are not accounted for in any standard FloMASTER component model. Engineers could try to replicate the number of flow arms using discrete losses, but this does not allow for the interaction of the effect on pressure drop that the differing flow rates in all the arms have in reality, e.g. Venturi effects. This is where applying simulation based characterization can increase the accuracy of automotive cooling circuit simulations. In fact this is something Sudhi Uppuluri of Computational Sciences Experts Group has expressed,

"When modeling multi-arm junctions such as automotive thermostats and pump housings, characterizing individual flow paths as parallel and independent losses can give rise to 15 to 20% error in predicting mass flow rates through an outlet. This
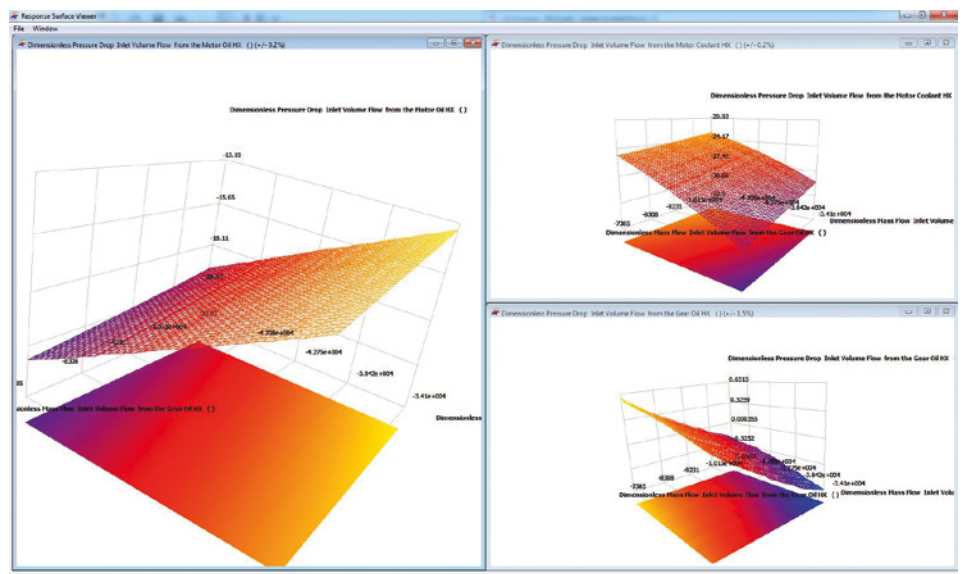
Figure 2. Response Surface Models for Pressure Drops

error is eradicated by considering the effect of changes in branch pressure drops with changing flow rates in the other branches. Using FloEFD to perform full spectrum 3D CFD characterization of the housing and integrating inter-dependent flow channel interactions into a FloMASTER N-Arm component improves simulation accuracy, confidence and trust reducing physical testing times and ultimate time to market."

FloEFD Model Setup
As an example, figure 1 shows a five arm thermostat with four inlets (from the radiator, gear oil cooler, engine oil cooler, and radiator bypass) and one outlet to the engine. The

goal is to characterize this component for use at maximum flow rate to the radiator, so an assumption can be made that the radiator bypass is fully closed. This simplifies the problem to a four-arm component with three inlets and one outlet.

The next step is to determine what the bounds of the characterization should be. At this point in the design the expected coolant flow rates should be known, and if they are not, thermal balance for each of the cooling loops could be done to estimate these values. With this information it is important to give a range of values centered on the expected flow rate. The range can

vary based on how well the system and component are known but for this example a range of +/- 20% is applied and shown in Table 1. In addition to the flow rates, a reference arm must be specified which in this case will be the thermostat outlet. This arm has an environmental pressure of 101325 Pa which will remain fixed through all of the simulations.

Design of Experiment Setup

These values can then be entered into FloEFD using the Characterization option for the type of Parametric Study. Once the values are entered, a number of experiments is required, in this case 120 simulations were run. FloEFD then creates a Design of Experiments (DoE) that randomly and equally distributes the combinations of flow rates throughout the characterization space. The DoE can then be run with the results presented as dimensionless flow rate and dimensionless pressure drop. These values have been non-dimensionalizes based on the fluid properties to remove any dependency on density and viscosity. This means when using this characterization in FloMASTER it is not critical to use a fluid with the exact same fluid properties.

Once all of the experiments are finished successfully, the Response Surface Models (RSM) can be created. These response surfaces are N-dimensional mathematical 'surfaces' that relate an output to multiple inputs. The first thing to check with the RSMs is the error in their mathematical fitting. The amount of error that is acceptable is a subjective decision, but for this scenario < 5% is considered acceptable which all three RSMs and under. If further refinements need to be done, additional experiments could have been added to the original DoE with the new points fitting into the original distribution. There is also the option to visually inspect the RSMs as shown in figure 2.

Response Surface Model Export and Import

Assuming everything is acceptable the RSMs can then be exported to FloMASTER as a ".flonarm" file. This file is actually an FMU adhering to the FMI standard, but augmented to also include additional information that is used by FloMASTER such as the area of each arm and the 3D representation of the geometry for visualization in FloMASTER.

To create the thermostat component in FloMASTER, "New FloEFD N-Arm Component" can be selected from the Launchpad. Once the file is loaded and the import is successful, the branch data and

hydraulic limits are available for review. At this point the 3D visualization is also available to identify each arm and also to create a component symbol as seen in figure 3. The 3D representation can be rotated and zoomed to get the best angle, and the camera icon at the top can be used to take the image. Once this is complete, the component will be saved into the FloMASTER database for use by anyone with access to it.

With the component in the FloMASTER database, it can be used in any model with a simple drag and drop similar to standard FloMASTER components. In this example, it is added to an automotive vehicle thermal

management model and connected to the appropriate parts of the model as seen in figure 4. An initial run results in a system that is operating well with-in the bounds of the characterization. This process allows for increased accuracy in the pressure drop through the thermostat when compared to previous ways of modeling in FloMASTER and thus a more accurate representation of the system behavior.

Download the White Paper:

Simulation Based Characterization. A 3D to 1D System Level Thermo-Fluid CFD Workflow: http://bit.ly/2nwjEmV

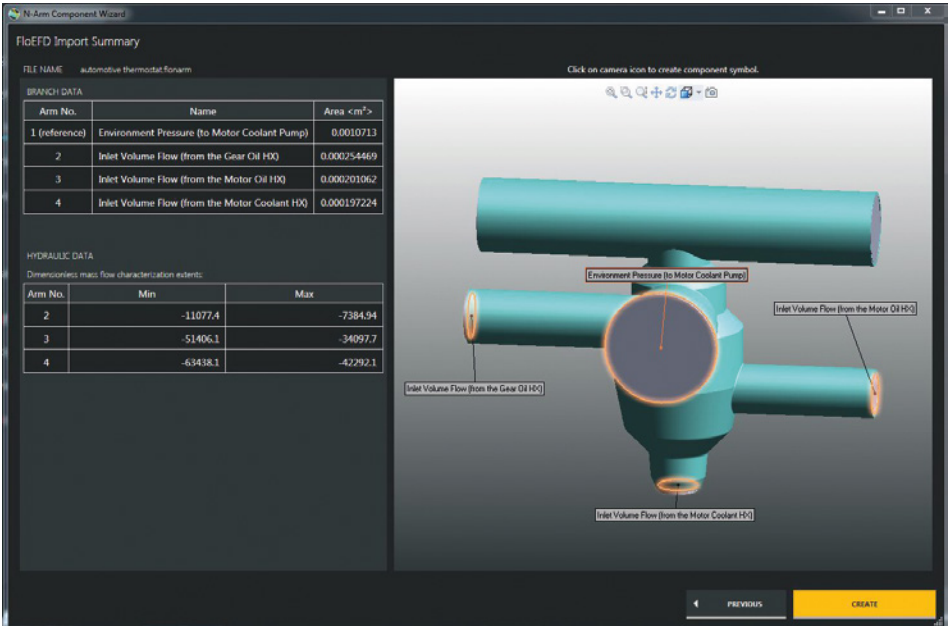| Parameter	Min Value (L/min)	Max Value (L/min)
Gear Oil Cooler Flow Rate	9.6	14.4
Motor Coolant Flow Rate	48.4	72.6
Motor Oil Cooler Flow Rate	39.4	59.4

Table 1. Oil Flow Rate Values

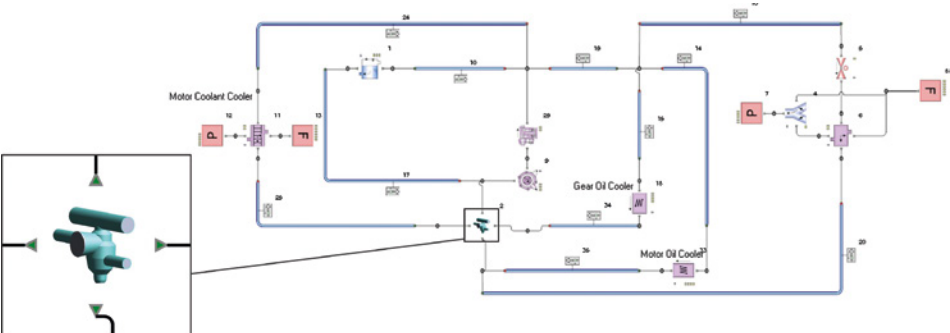**Figure 3.** FloMASTER N-Arm Creation

Figure 4. FloMASTER Cooling System Model with FloEFD Thermostat

System Level Evaluation of 4-Quadrant Mixed Flow Diffuser Pump Behavior Using CFD

By Doug Kolak, Technical Marketing Engineer, Mentor Graphics

This work, "System Level Comparison of 4-Quadrant Mixed Flow Diffuser Pump Behavior Using CFD", is a derivative of "Investigation of the 4-Quadrant behavior of a mixed flow diffuser pump with CFD-methods and test rig evaluation", by S. Höller, H. Benigni, and J. Jaberg, IOP Conf. Series: Earth and Environmental Science 49(2016) 302018, DOI: 10.1088/1755-1315/49/3/032018, used under Creative Commons 3.0.

When looking to analyze a thermo-fluid system one of the most important aspects to consider is: what will cause fluid flow in the system. This may be as simple as imposing a flow rate or using a difference in pressure due to elevation, however one of the most common real-world methods of generating fluid flow is through the use of pumps. Generally the behavior of centrifugal pumps is well known under normal operation of forward flow with a forward rotational direction of the pump. This is the most common usage for a pump and is usually well defined in terms of pump head and efficiency from the manufacturer.

However, there are scenarios where the pump will need to run outside of this normal operating mode, such as when the direction of flow or rotation change. An example of this is a pump trip, where to reliably calculate system transients like maximum or minimum internal pressures it is necessary to obtain performance data for all quadrants of operation. While it is possible to determine this information through physical testing, it is expensive, so the ability to generate accurate 4-quadrant pump characteristics using Computational Fluid Dynamics (CFD) can be valuable.
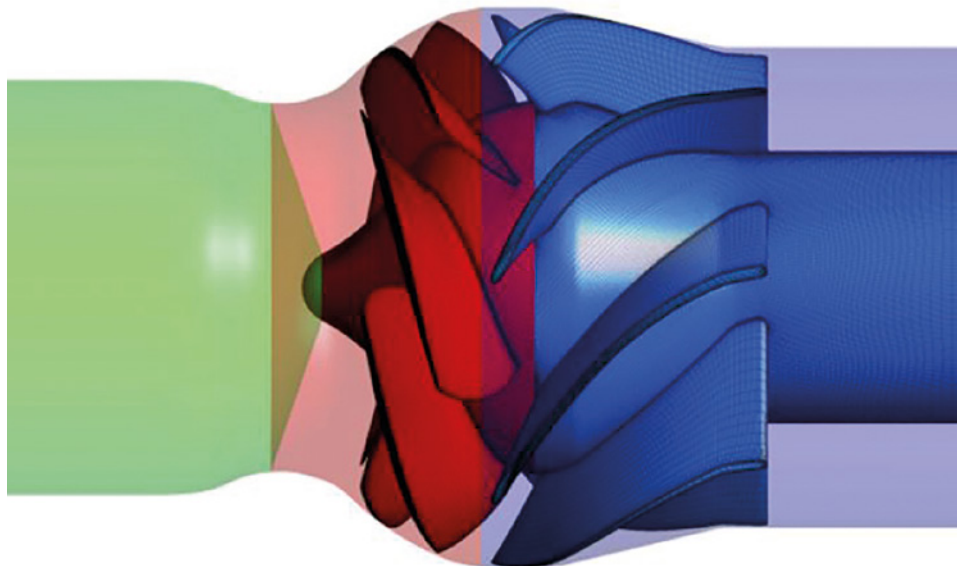

Figure 1. CFD Model of a Centrigual Pump

The simulation was carried out using a full 360° model with traditional 3D CFD software. The model consisted of the suction bell domain including an inlet extension, the impeller domain, and the stator domain including an outlet extension as shown in figure 1. The inlet boundary condition was a specified mass flow rate and the outlet boundary condition was defined as a static pressure. An entry and exit length of five times the respective diameters was used to help redevelop the flow profile.

The experimental measurements were made at the Institute of Hydraulic Fluid Machinery at Graz University of Technology. Since a full size prototype pump with a mechanical power of over 1500 kW would exceed the capabilities of the test facility, a 1:3.6 model
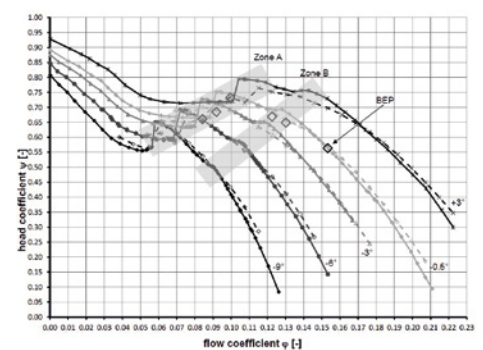

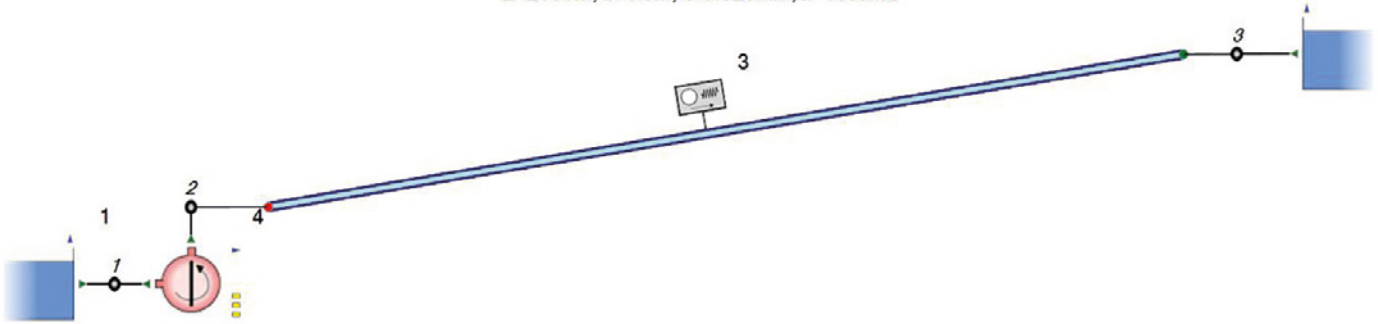**Figure 2.** Head Curves for Different Blade Positions

scale was chosen. To accurately compare the results of the CFD analysis and the physical test, the test results were scaled up using IEC60193. As shown in figure 2, the results of the simulation and the physical test showed good correlation.

L=2000m, d=1.5m, k=0.025mm, a=1000m/s

Figure 3. FloMASTER Pump Trip Model

To further demonstrate the effectiveness of creating this performance data with 3D CFD a pump trip simulation was conducted using FloMASTER. The goal being to evaluate the effect of discrepancies between the experimental and the numerically calculated pumps. The system level thermo-fluid model shown in figure 3, contains two reservoirs connected by the pump and piping with a static head difference of 22 meters. The mixed flow pump is connected directly to the outlet of the lower reservoir and will operate at 507 rpm. The best efficiency point for the pump is at 5m3/s which produces a head rise of 27m. The outlet of the pump is connect to the downstream reservoir by a 2000m pipe, with a diameter of 1.5m and an absolute roughness of 0.025mm. To account for the transient nature of the scenario, the method of characteristics is used for the pipe with a combined wave speed of 1000m/s specified. Finally the inertia of the pump including the drive is set to 1000kgm2.

The analysis is conducted for 120 seconds with the pump tripping after five seconds. Two different pitch angles were analyzed in this way, 0° pitch angle and -9° pitch angle, the results are shown in figure 4 and 5. The graphs compare the system transients for flow rate (Q), pump rotational speed (n), and pump outlet pressure (p) for both the experimental curve and the CFD generated curve.

As expected the decreasing rotational speed once the pump has tripped results in an immediate pressure drop at the outlet of the pump. The flow rate decreases at a lower rate than the pressure due to the inertia of the fluid mass inside of the pipe. During this initial phase of the simulation the graphs show there is virtually no difference in any of the three parameters between the experimental and CFD pump models. However, once the pump changes the direction of rotation and the direction of flow reversed, a turbine runaway condition starts
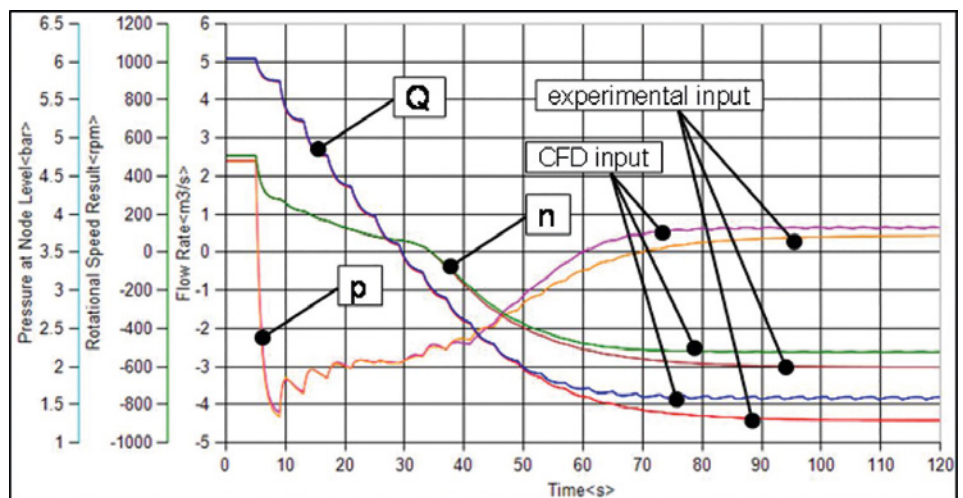
Figure 4. 0 Degree Pitch Results
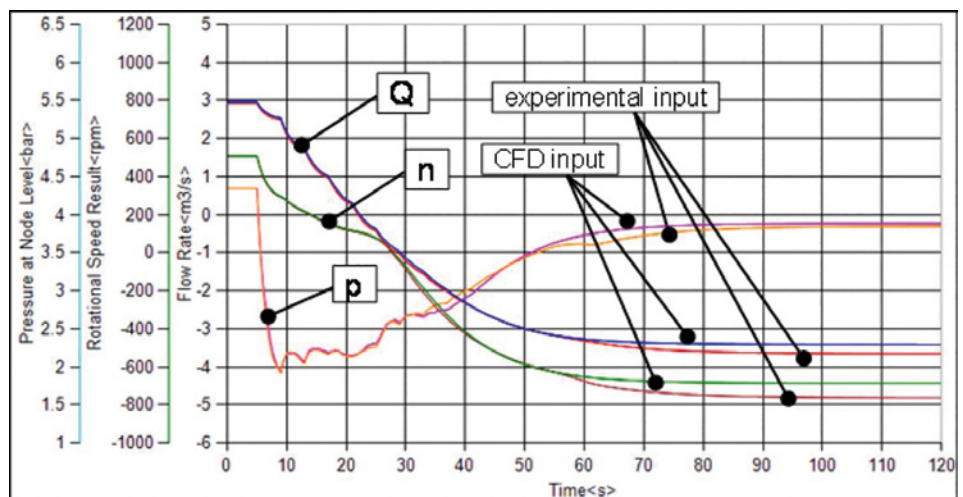
Figure 5. -9 Degree Pitch Results

to occur. At this point a slight difference in the rotational speed and flow rate becomes evident. This difference is likely an effect of the inaccurate prediction of the pump behavior in the CFD calculations near the turbine runaway point.

Ultimately the results from the CFD pump characterization provide comparable behavior to the experimental results when used in FloMASTER for a pump trip analysis, thus providing a reliable option for obtaining pump performance outside of the normal operating range.

"With FloEFD, the configuration of the simulation is made from within the CAD software, which eliminates the need for exporting/importing geometry. The software also has features such as automatic meshing, a case configuration wizard and integrated post processing, all from within the CAD software."

Arne Lindgren, Halmstad University, Sweden

Image Credit: Koenigsegg Automotive AB

Sports Car Brake Cooling Simulation with CAD-embedded CFD

By Arne Lindgren, Halmstad University, Sweden

Brake cooling is a crucial area in motorsport and sports car engineering. A recent thesis project by Arne Lindgren of Halmstad University in Sweden considered different cooling solutions for the extreme conditions of super cars. The project, conducted for super car manufacturer Koenigsegg Automotive AB, had the objective to design an efficient brake cooling solution for their latest model, the Regera. (Figure 1)

Regera, which means "to reign" in Swedish, is the first Koenigsegg car with hybrid-technology, the combined power of its internal combustion engine and its electric motors exceeds 1,500 horsepower. Such a powerful car needs effective and reliable brakes. During a braking event from 300 to 0 km/h, the average brake power is over 1 MW in the Regera.

Koenigsegg Automotive AB is a Swedish company founded in 1994 by Christian von Koenigsegg. The first prototype was completed in 1996 and the series production of their CC8S model started in 2002 [2]. The Koenigsegg CCR became the fastest production car in 2005 and the CCX model took the Top Gear lap record in 2006 with a time that wasn't beaten for over two years. In 2014 the One:1 model was introduced, the world's first production car with a hp-to-kg curb weight ratio of 1:1. The company employs approximately 120 staff including an engineering department which consists of about 25 engineers.

Lindgren evaluated several brake cooling designs for the Regera in his thesis. For

his CFD simulations he used FloEFD™ embedded in CATIA V5 from Mentor Graphics – experimental testing being deemed too expensive and lacking in acquisition of certain flow data [1].

While dedicated brake cooling is not necessary for ordinary passenger vehicles, it is a huge challenge for sports cars that must tolerate racing conditions. The cooling effect of the ambient air is normally sufficient for ordinary car brakes during normal driving conditions. Modern road vehicles are equipped with internally vented brake discs (at least at the front axle, and usually also at the rear). The internal vanes help to pump air through the disc, internal channels are where the biggest heat dissipation takes place [1].

Over-heating of brakes can lead to a number of problems:

- Friction material degradation;

- Thermal stress in the brake disc, which can lead to distortion and stress cracks; and

- Brake fluid vaporization in the brake caliper.

These failures can lead to partial or complete loss of braking, which is very serious.

With regard to racing cars and cars for track driving, this issue becomes more complex. Special cooling ducts which direct ambient airflow to the brakes are used to ensure sufficient cooling performance taking into account the more frequent braking intervals that occur during track driving.

Brakes are mainly cooled through the heat transfer method called convection, where a fluid absorbs heat and transports it away from the hot object. Lindgren focused his work on improving the convective air cooling of the brakes, and limited his studies to the front axle brakes as this is where heat generation is at its greatest. The brake cooling solution that was used on the previous generation of Koenigsegg cars was used as a baseline for the cooling simulations.

The baseline design consists of inlet ducts in the front bumper of the car (that captures ambient airflow) and flexible hoses that channel the air to ducts (or nozzles), which are mounted on the wheel bearing carriers and direct the cooling air towards the center of the brake discs. (Figure 3) For the simulations, CAD models of the relevant geometry were provided by Koenigsegg which were used for the embedded CFD simulations.
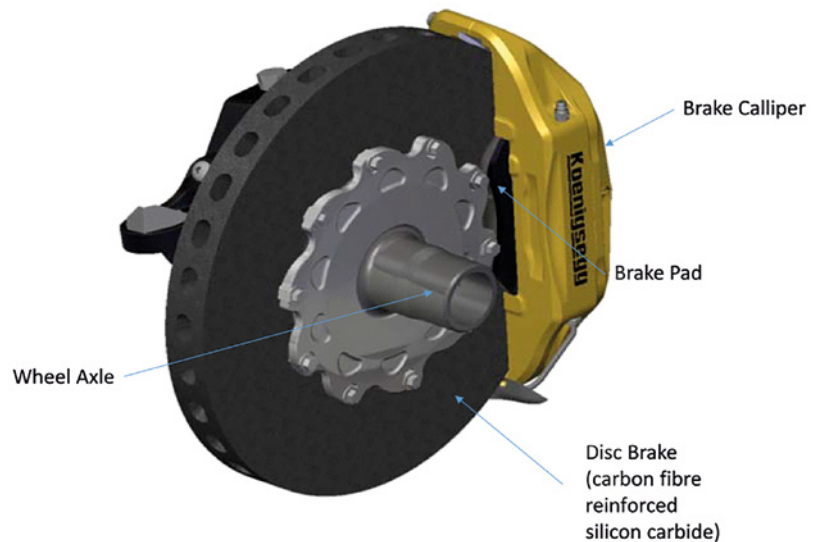

Figure 1. Koenigsegg Regera

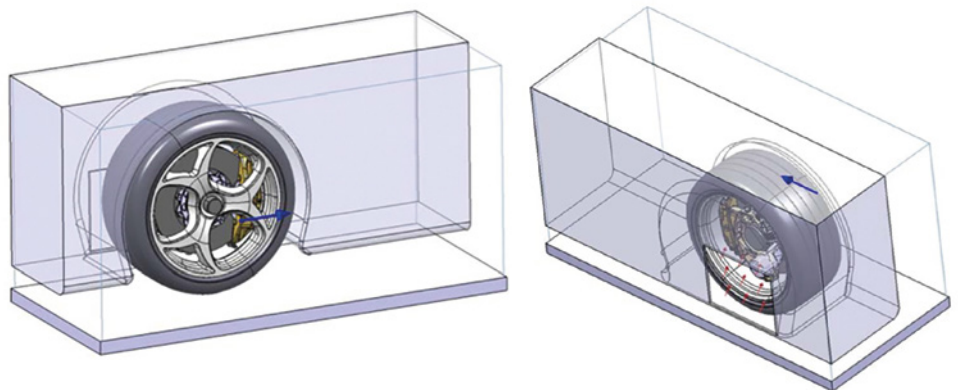**Figure 2.** Koenigsegg Regera front brake.

Figure 3. Brake cooling duct mounted on a Koenigsegg Regera upright (the baseline design). (Klingelhoefer, 2013, Ref 3)
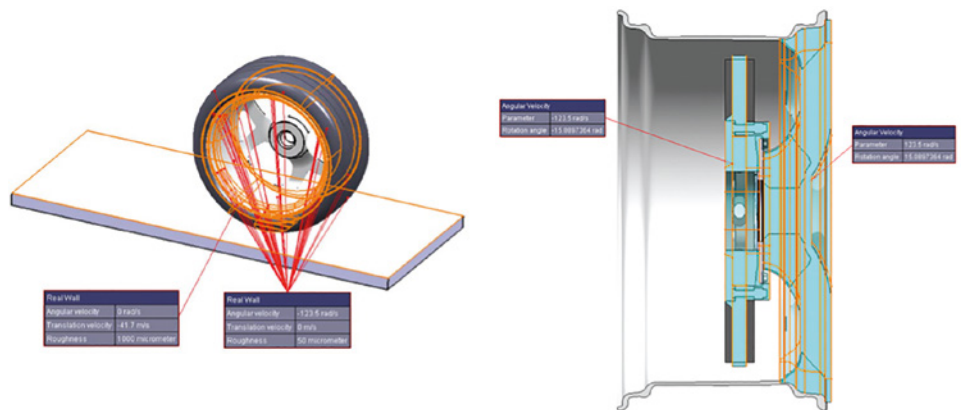
The main geometries used in the simulations were:

- The brake discs made of Carbon fibre-reinforced silicon carbide (C/SiC), diameter 396 mm and thickness 38 mm, equipped with radial ventilation channels;
- The brake pads;
- The brake caliper;
- The upright (or wheel bearing carrier);
- The hollow wheel axle;
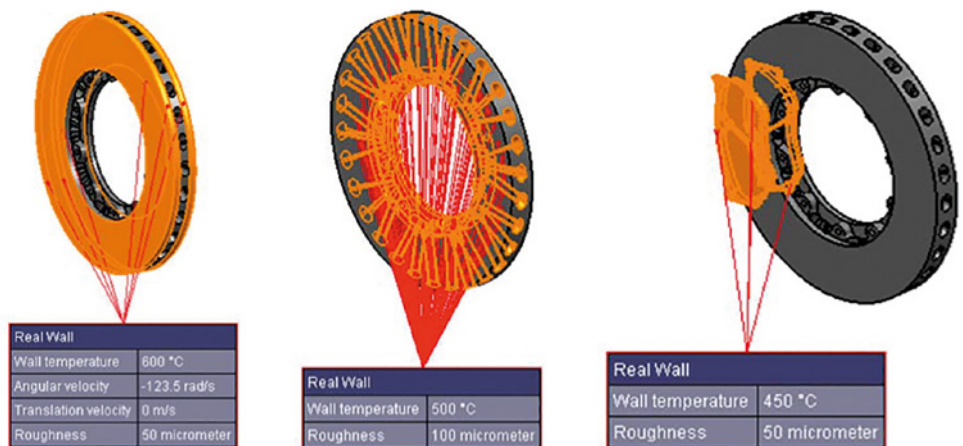- The 19" wheel rim with tire; and
- The wheelhouse geometry.

After simulating the baseline configuration, different brake duct concepts were generated and their cooling effect was simulated. The same computational model was used for both baseline and concept simulations, only the brake duct geometry and, naturally, the position of the duct inlet boundary conditions were changed. The simulations were conducted directly within the 3D geometry models in the CATIA V5 embedded FloEFD™ CFD software. This allowed for efficient simulation of complex geometries. An efficient and productive workflow was found as a result of the automatic meshing function, the case configuration wizard, the post processing features, and because geometry could be modified directly within the CAD environment [1].

As to the objective of the project was to investigate many concepts, a reasonable calculation time was required. Therefore, a complete simulation of the entire vehicle was not expedient. A partial car body with wheelhouse was used as well as wheel and the brake as assemblies (figure 4) with similar dimensions and ground clearance as the Regera.

The ambient velocity was defined as 150 km/h, which is a typical average speed on a race track. An additional airflow from the radiator was applied on the inboard side of the wheelhouse (figure 4, red arrows). The

Figure 4. The geometrical wheelarch model (blue arrow indicates ambient airflow direction)

Figure 5. Wheel and ground boundary conditions. Rotating regions highlighted in turquoise

Figure 6. Disc and pad with FloEFD wall boundary conditions
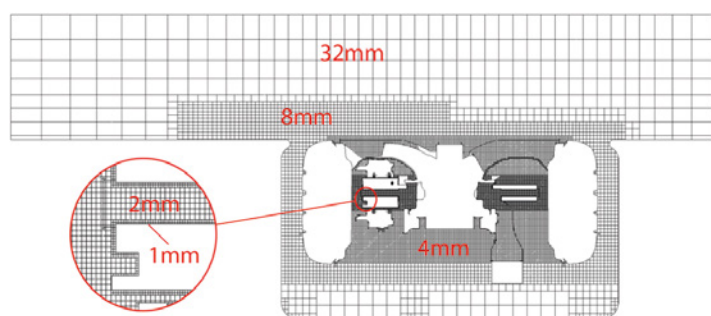
Figure 7. FloEFD Computational mesh of the Wheel, Brake Disc and Wheel Housing
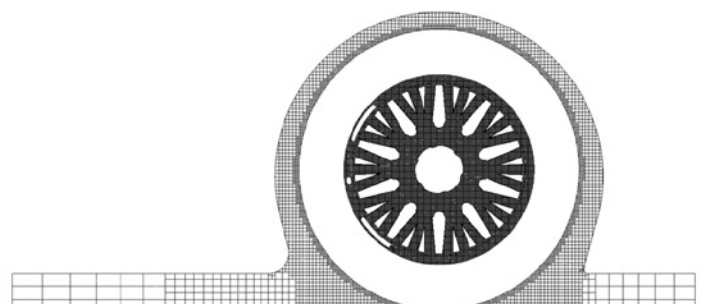
airflow through the flexible hose from the inlet ducts in the front bumper was modeled as a pressure to get a realistic flow rate for all possible brake duct designs. The rotation of rotationally symmetric geometries, such as the tires and brake disc friction surfaces, were defined with wall conditions. The FloEFD sliding mesh approach was applied to the non-rotationally symmetric parts. A 3D body (rotating region) is used to define which geometries should rotate, in this case the rim spokes and brake disc channels. A translation velocity of 150 km/h was applied to the ground (figure 5) to include ground effects. Only convection was considered for the CFD simulations as this is the easiest heat transfer process to influence and has a proportion of about 60 – 90 % of the total heat dissipation. The surface temperatures applied on the surfaces of the parts (figure 6) were based on values recorded by Koenigsegg during track testing. The simulation was conducted with approximately 3.5 million cells (figure 7) using the FloEFD two-scale wall function technique, which enables the use of a coarser mesh than would be otherwise necessary in traditional CFD codes.

The concepts were based on Lindgren's own ideas, observed brake cooling designs, and observations in other applications while taking into account only concepts that are possible to manufacture. 12 different concepts were investigated using the described FloEFD boundary conditions. With the given settings, the simulation time was approximately 24 hours on a computer with a six-core Intel Xeon E5 CPU at 3.5 GHz and 32 GB RAM.

The baseline simulation results are shown in figure 8.

Each concept was compared with the baseline concept. The investigations focused on the cooling of the brake discs as most of the braking energy goes into the discs. The approach was to increase the convective cooling by breaking up the temperature boundary layer, which can be done by using high air velocity or by introducing turbulence. In addition, other design criteria were considered to ensure that the solution withstands forces, vibrations, and temperatures etc., that occur in driving conditions.

The investigations showed that a local improvement of the airflow often led to worse heat dissipation in other areas simultaneously. The airflow rate was simply not sufficient to improve the cooling over larger surfaces.

Another early discovery was that the design of the cooling channels in the brake discs could be improved. But the brake disc design was outside the scope of this project so it was not studied further. The breakthrough was the idea of putting the brake duct inlet in the center of a wheel axle that has radial channels. This resulted in higher hose flow rate because the radial channels in the axle and the brake disc work together as a centrifugal fan. Finally, this concept was supplemented by a "passive" cooling design (not relying on airflow from the hose), realized by two ring-shaped plates perforated with slots. (Figure 10) The simulations showed that these plates improved the cooling of the discs friction faces, but Lindgren expresses
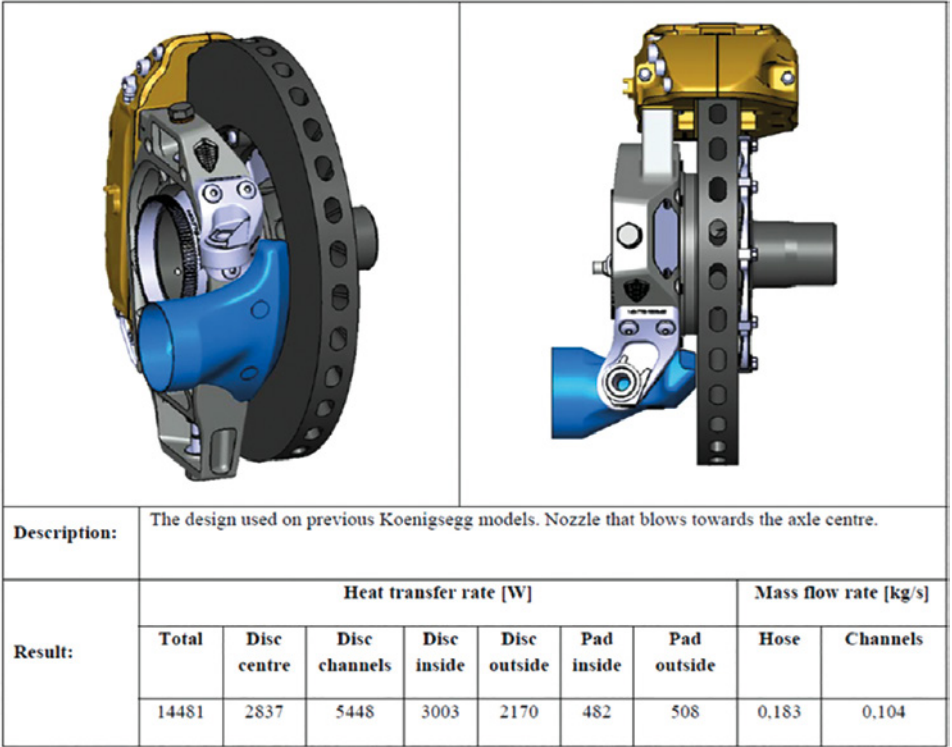

Description:	The design used on previous Koenigsegg models. Nozzle that blows towards the axle centre.								
Result:	**Heat transfer rate [W]**							**Mass flow rate [kg/s]**	
	Total	Disc centre	Disc channels	Disc inside	Disc outside	Pad inside	Pad outside	Hose	Channels
	14481	2837	5448	3003	2170	482	508	0,183	0,104

Figure 8. Baseline brake duct highlighted in blue and table with the numerical results from FloEFD

Concept 8								(Section view)	
Description/ Idea:	Inlet duct in the centre of a modified axle with radial channels, the through hole is plugged. The brake disc centre is closed off so no air is escaping there.								
Difference from baseline	**Heat transfer rate**							**Mass flow rate**	
	Total	Disc centre	Disc channels	Disc inside	Disc outside	Pad inside	Pad outside	Hose	Channels
	14%	34%	19%	-2,0%	1,9%	4,8%	6,1%	41%	48%
Comment /Analysis:	Good overall improvement, better cooling on most surfaces. Axle channels and disc channels are working like a centrifugal pump and increases the hose flow rate which benefits the cooling.								

Figure 9. Overall view and FloEFD results for concept No. 8

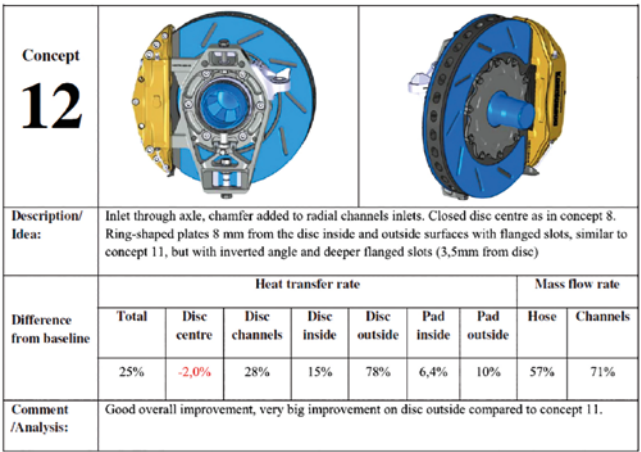| Concept 12									
Description/ Idea:	Inlet through axle, chamfer added to radial channels inlets. Closed disc centre as in concept 8. Ring-shaped plates 8 mm from the disc inside and outside surfaces with flanged slots, similar to concept 11, but with inverted angle and deeper flanged slots (3,5mm from disc)								
Difference from baseline	**Heat transfer rate**							**Mass flow rate**	
	Total	Disc centre	Disc channels	Disc inside	Disc outside	Pad inside	Pad outside	Hose	Channels
	25%	-2,0%	28%	15%	78%	6,4%	10%	57%	71%
Comment /Analysis:	Good overall improvement, very big improvement on disc outside compared to concept 11.								

Figure 10. Overall view and FloEFD results for concept No.12

skepticism to these results as the simulations didn't include radiation (in reality the plates would reflect heat back to the disc). Concepts 8 and 12 were the most promising, although concept 12 needs further analysis or testing to see the effect of radiation. The designs of the concepts and the results given as the difference in percent from the baseline values are shown in figures 9 and 10. Concept 8 has the advantage that only a few relatively simple additional parts are needed.

From the almost infinite number of possible cooling solutions, 12 concepts were analyzed (figures 11 - 13) and compared with the baseline design from Koenigsegg. The two most promising solutions lead to an overall thermal improvement of 14% and 25%. Concept 8 was proposed as an enhancement, which had the hose inlet in the center of the wheel axle thus directing the cooling air through radial channels to the brake disc. FloEFD simulations indicated that the proposed design should result in 14% higher heat transfer rate compared to the previously used cooling solution. In addition to these cooling ducts, some passive cooling devices could also be considered in future.

In this study FloEFD was able to provide trend predictions within engineering timescales for a wide range of concepts although it was recommended that finer meshes and radiation effects be examined more in the future which require more computational resources. However, the CFD results described here indicate that when compared to brake cooling with the previous Koenigsegg ducts analyzed as a baseline, new concepts could be created, analyzed and developed in an easy iterative process. The simulations with the CATIA V5 embedded version of FloEFD made these investigations possible because creating a real prototype of each concept would lead to high cost and time requirements. The most promising solutions can now be investigated deeper in terms of structural analysis, manufacturing processes, and finally produced as a prototype.

References

[1] "Development of Brake Cooling", Arne Lindgren, Bachelor Thesis in Mechanical Engineering, 15 credits, Halmstad 2016-05-20:

http://www.diva-portal.se/smash/get/diva2:938489/FULLTEXT01.pdf

[2] Koenigsegg website: http://koenigsegg.com/
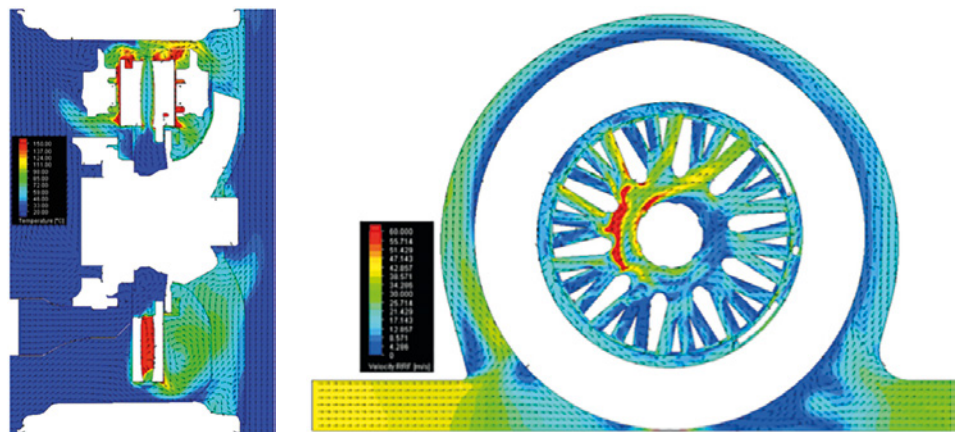
Figure 11. Baseline Case (a) temperature cut-plot on a horizontal plane through the wheel, and, (b) vector velocity on a vertical plane through the disc channels.
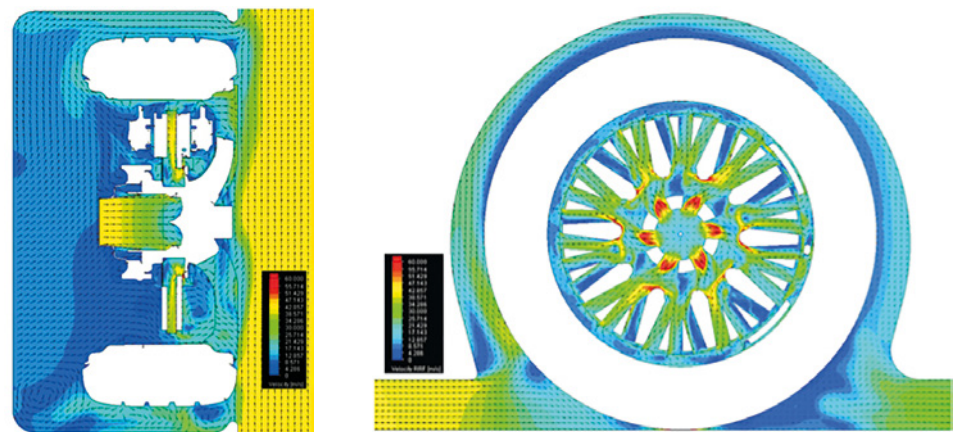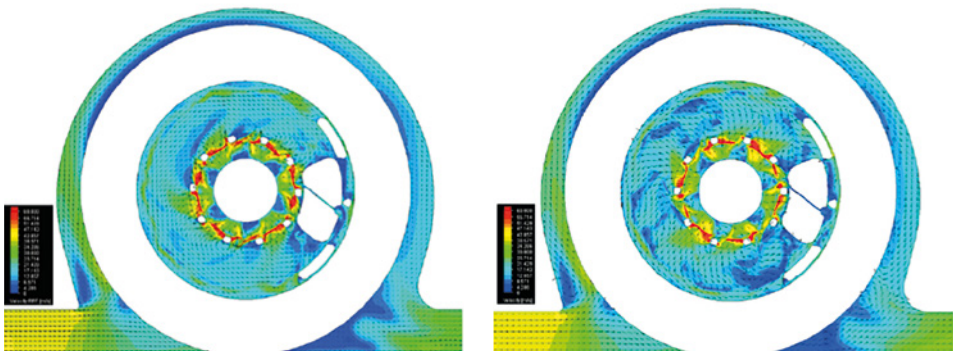

Figure 12. Concept 8 velocity cut-plot horizontal plane (a) through the wheel, and, cut-plot vertical plane through disc channels (b).
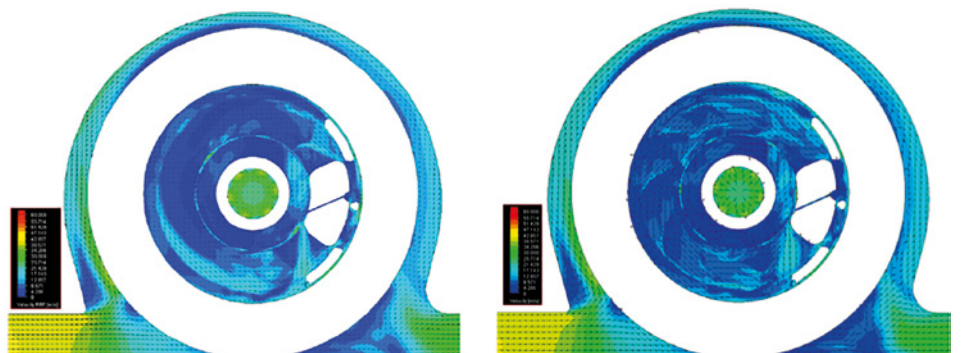
Concept 8, velocity 1 mm inside disc

Concept 12, velocity 1 mm inside disc

Concept 8, velocity 1 mm outside disc

Figure 13. Comparison of Concept 8 and 12

Concept 12, velocity 1 mm outside disc

Winging It!

FloEFD® provides Accurate and Fast Flight Load Data for Aircraft Wing High Lift Devices at Irkut

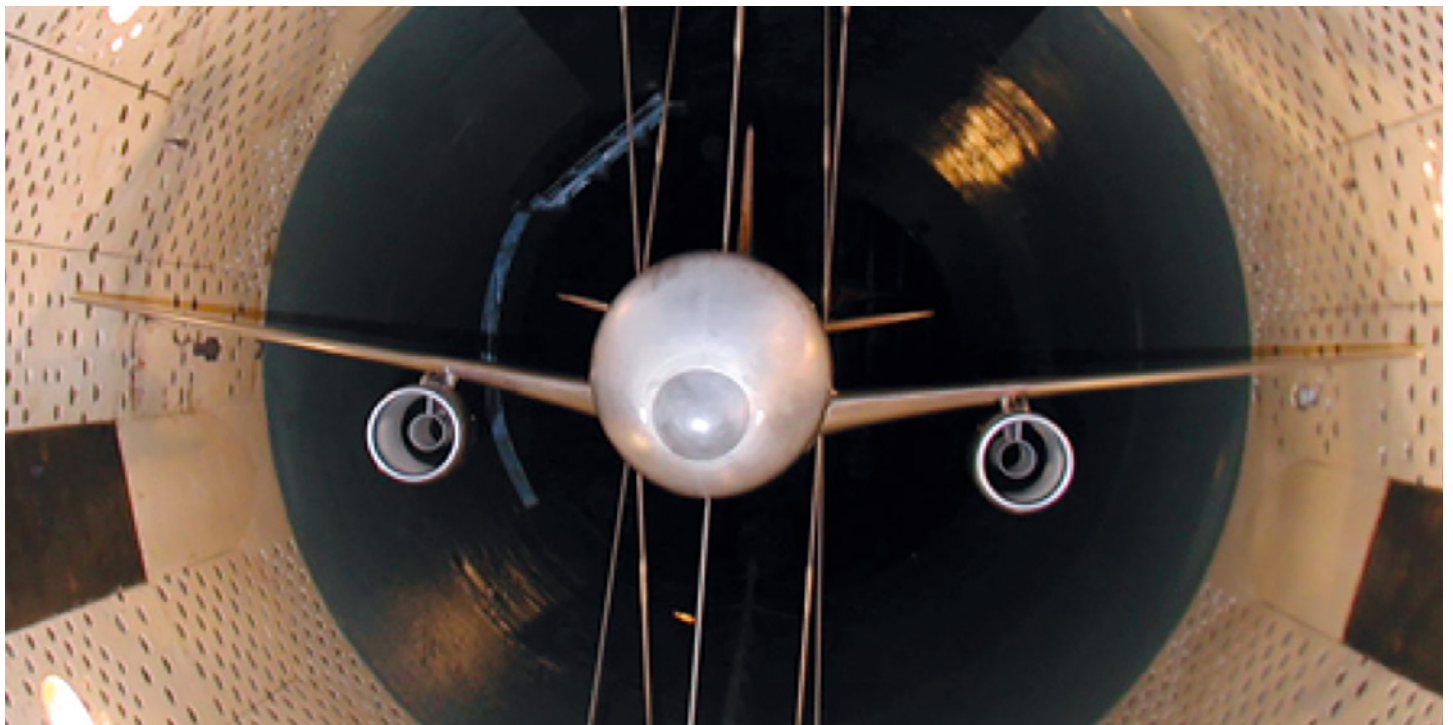By Andrey Chuban, Lead Design Engineer, Irkut Corporation

Figure 1. Typical tube experiment for a scale model aircraft

Engineers at Irkut Corporation were looking for a way to get better external aerodynamics data than what they were currently able to get from tube experiments. Tube experiments consist of building scale models of the aircraft and measuring values in a wind tunnel. This approach is expensive and has some inherent disadvantages. These include low Reynolds numbers and higher airflow turbulence intensity for scale models vs. full size aircraft. There are also inaccuracies due to the scaled geometry such as radii and points where different structures such as the wings and fuselage meet. Finally, tests run in different wind tunnels can produce varied results. To solve these issues Irkut turned to CFD as
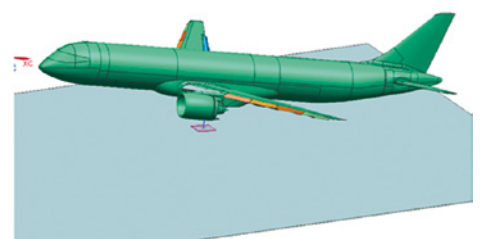

Figure 2. 3D CAD model of aircraft

an alternative approach. As part of this the CFD tools needed to be validated for this use, the tools tested included Mentor Graphics' FloEFD and Ansys' CFX.

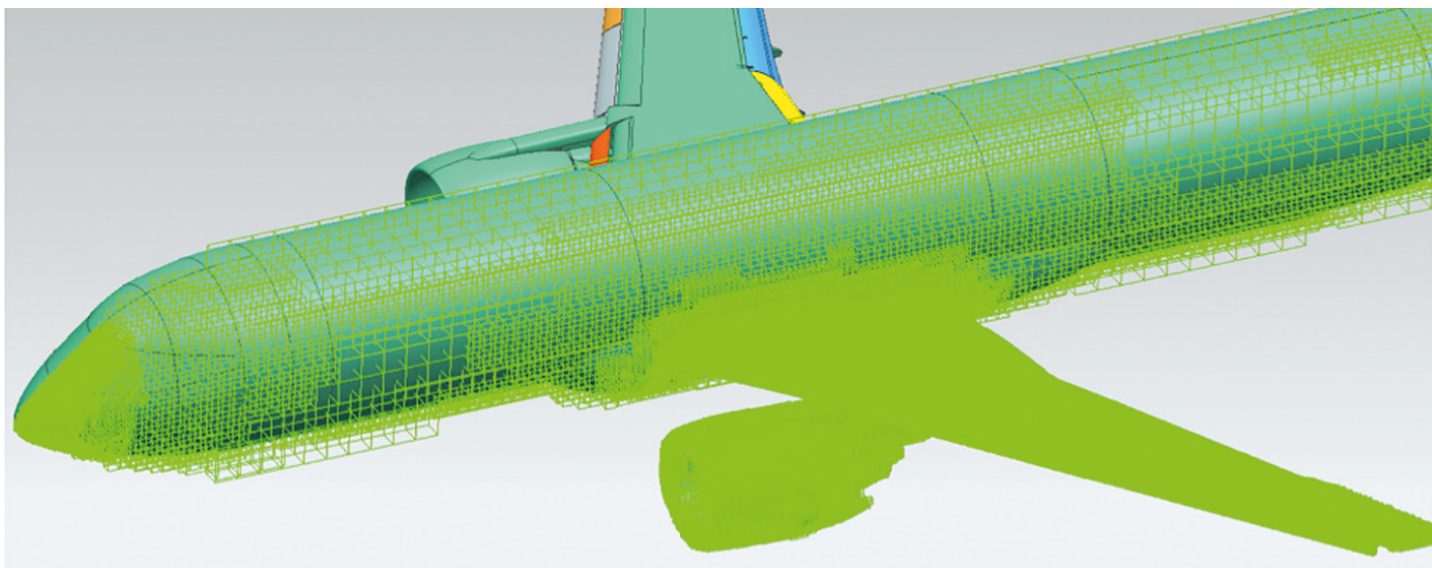The criteria for validating the tools were:
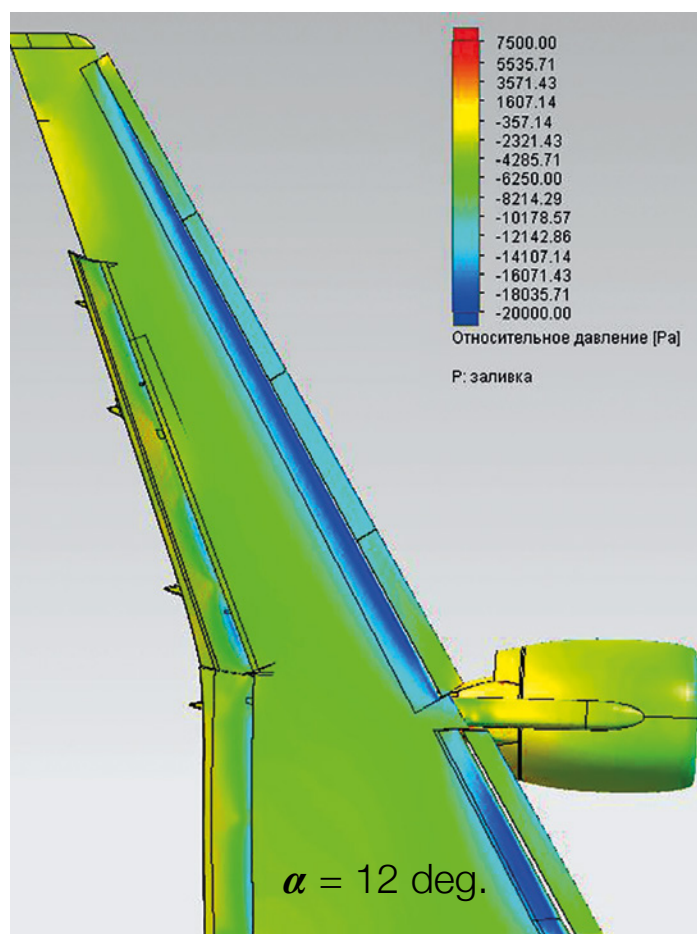
- Obtain the computational results close to those of the tube experiment,

- Provide loads for the flight modes and configurations, that were not tested during experiments,

- Compare solutions with or without ground effect simulation screen, and

- Compare the FloEFD results with the load data obtained with CFX.

Figure 3. Final Mesh after a single adaption

α = 7 deg.

α = 12 deg.

Figure 4. Computation Results: ΔP on Wing Surface

The FloEFD software was installed on a double Xenon powered computer with 48 Gb RAM. The mesh size was limited to 4 million cells (about 1.4 million before mesh adaptation process). The density of the mesh was organized with the help of volumetric zones to meet the basic rule: very dense mesh in areas with large airflow speed gradients.

After construction of volumetric zones around the nose of fuselage, high lift devices, wing with engine and whole aircraft a basic mesh was refined automatically. The picture in figure 3 presents the final mesh after a single adaptation.

The simulation was then run for two angles of attack, 7 degrees and 12 degrees and several computational results were examined. The first result studied was the ΔP on the wing surface. This showed an increase of pitch angle leading to the growth of negative relative pressure along the wing leading edge surface and upper surface of
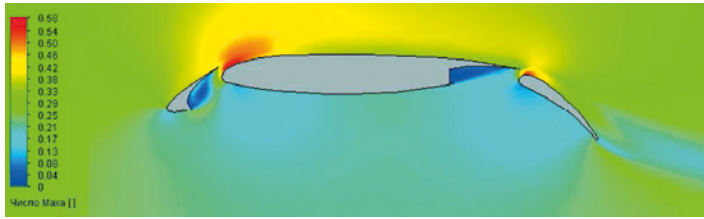
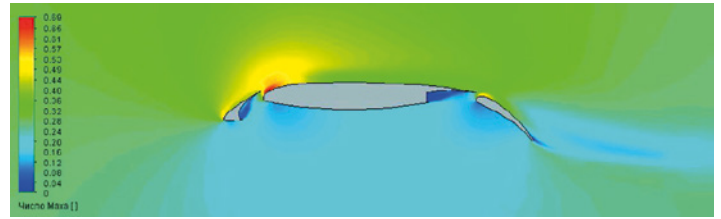**Figure 5.** Computation Results: Mach Number Distribution along Wing Airfoil

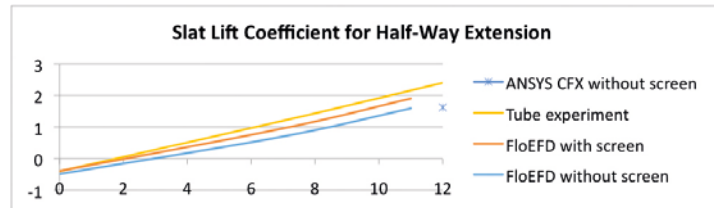**Figure 6.** Results Comparison: Slat Drag Coefficient

Figure 7. Results Comparison: Slat Lift Coefficient
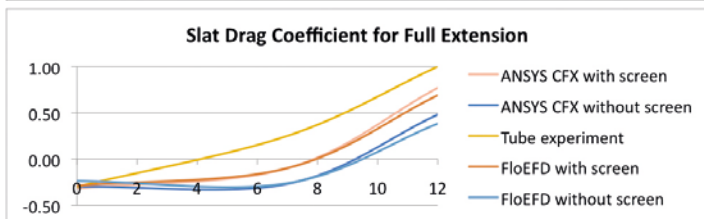

Figure 8. Results Comparison: Flap Drag Coefficient
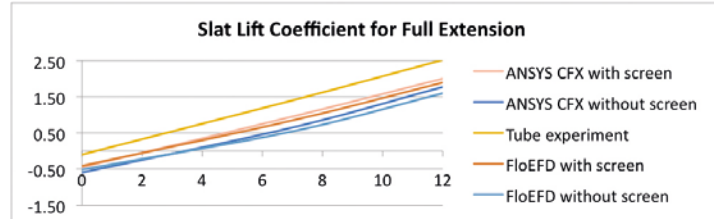

Figure 9. Results Comparison: Flap Lift Coefficient

the slats. So slat loads are the function of an angle of attack.

The relative pressure on a bottom wing surface doesn't really depend on the angle of attack; flap loads are almost independent of the angle of attack.

Next they examined the Mach number distribution along the wing airfoil. In case of a full flap extension, a high pitch angle may provoke flow separation on the flap's upper surface. The relative pressure growth on the upper surface led to flap loads decrease.

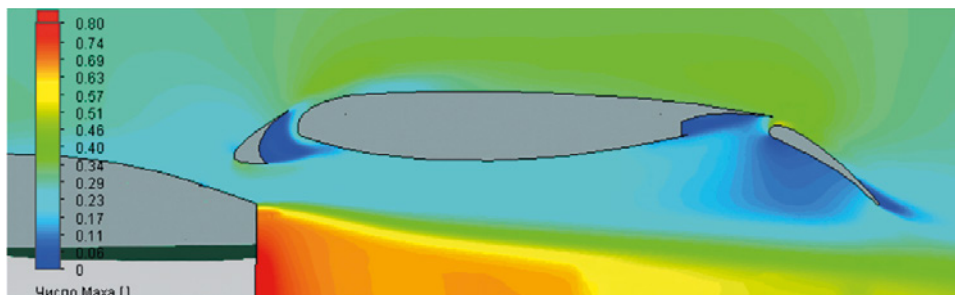Since the experiment was run with the

Figure 10. Engine Thrust Effect: Flow Stagnation on the Flap Bottom Surface

ground effect simulation screen, a plate was added to the FloEFD model to capture the screen effect. This resulted in an almost doubling of drag load level with

screen presence.

The drag and lift coefficient plots illustrate that qualitatively identical airflow around

the slat in the half-way and fully extended positions.

The addition of the screen also greatly raised the slat loading, but for flap, the opposite is true.

The flap lift coefficient is especially affected by screen, they observed a 15% load decrease at high angles of attack.

The next stage of the validation was to consider the engine thrust effect. The tube experiment was also done with the engine simulator which demonstrated a 10% increase of flap lift at high angles of attack. To investigate the engine thrust, effect the boundary conditions at the inlet and outlet of the engine were added to the model. This led to flow stagnation on the flap bottom surface.

FloEFD also shows a flap load increase during computation with the engine thrust taken into account, but the gap between the results with and without thrust tends to decrease with the angle of attack growth.

The spoilers, release effect at a small angle, (within 10 degrees) results in a substantial increase of outward flap loading. Wherein large spoiler release angles greatly disrupt the flow around the flap, causing a reduction of flap loading. The main problem for the flap release kinematics designer is a huge tangent load increase after spoiler release.

10 degree spoiler release causes flow separation on the flap aft edge and flow acceleration on the leading edge.

The tube experiment and FloEFD calculations show large increase (four times for FloEFD) of flap drag load for half-way extraction configuration and about 20% increase of lift load. For the outward flap tube experiment, results differs from CFD calculations due to slightly different flap release angles of a tube model and real aircraft.

The final criteria studied was the Reynolds number effect. The tube model's small scale leads to a difference in Reynolds number of a flow around the model and the aircraft. To determine the effect of the Reynolds number, the scale model was calculated in FloEFD. The results of the calculation of the aircraft and a scale model were almost identical.

Conclusions

- The FloEFD results satisfactorily correlate with the experimental data which are very close to the results of ANSYS CFX calculations. The size of the CFX mesh used for calculations was about 18 M cells, so these flow computations took too much time and required a very high-capacity equipment. Each FloEFD calculation took about six to eight hours on a standard workstation.

- The ground effect simulation screen greatly affects the drag coefficient of the slat and must be accounted for during calculation. Outward flap loading is highly dependent on spoilers release. The inner flap load growth due to the
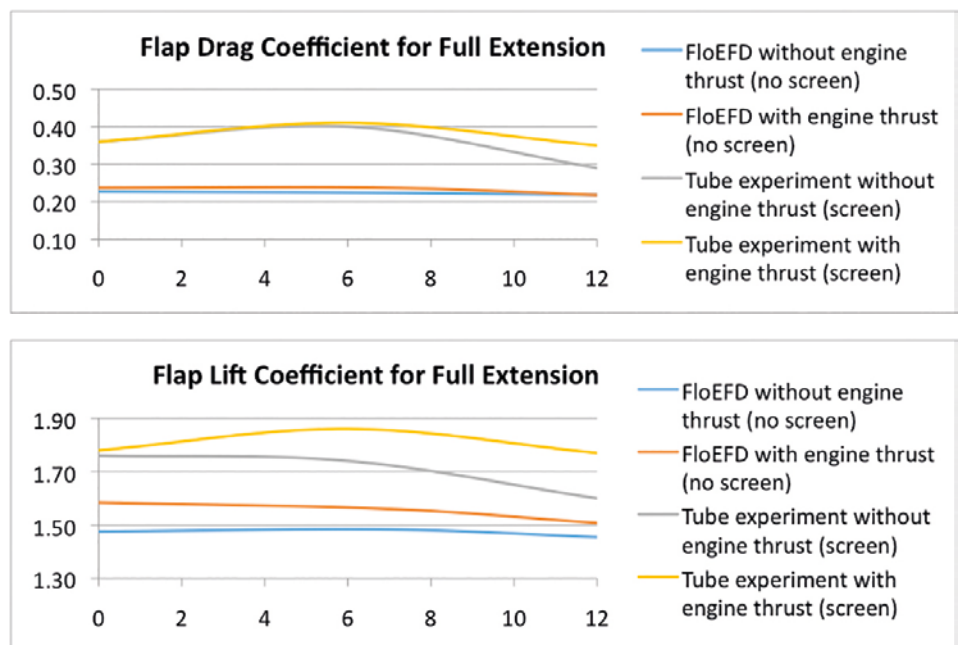
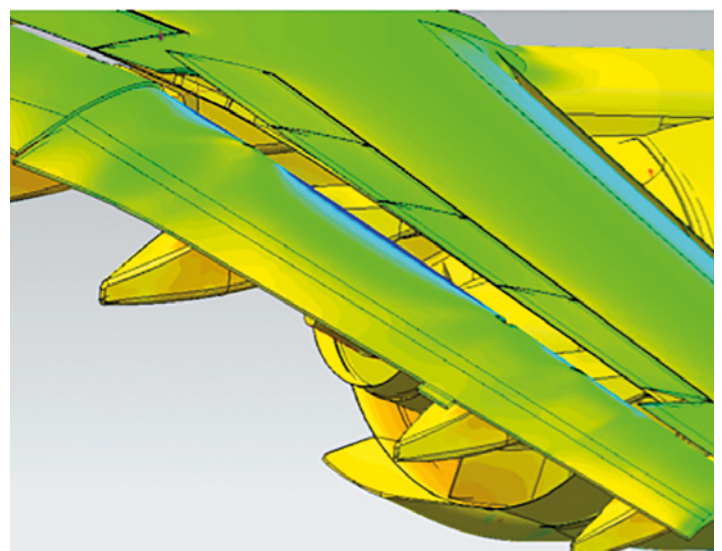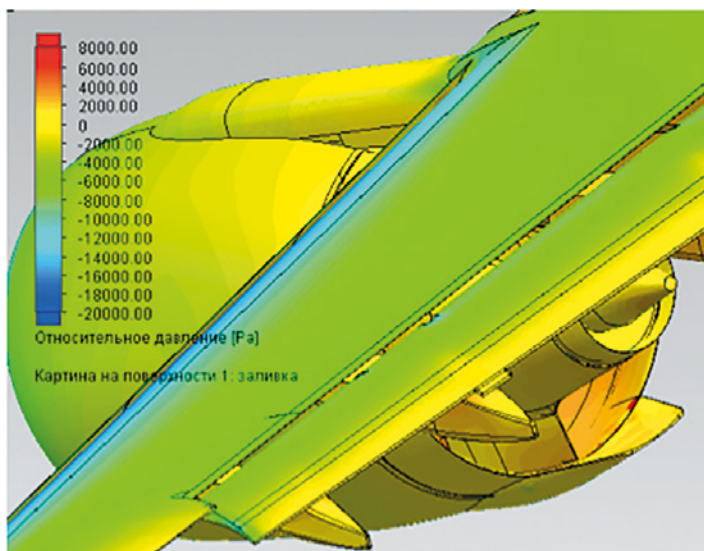**Figure 11.** Engine Thrust Effect: Flap Drag Coefficient

Figure 12. Spoilers Release Effect: Negative relative pressure growth on flap leading edge after spoilers release

engine thrust increase must also be considered.

- The difference between the experimentally defined and FloEFD and ANSYS CFX computed loads raises the question about the load data source at the aircraft design stage. On the one side there is a traditional distrust in CFD results and on the other side there is a difference in Reynolds numbers and geometry between the tube model and the real aircraft.
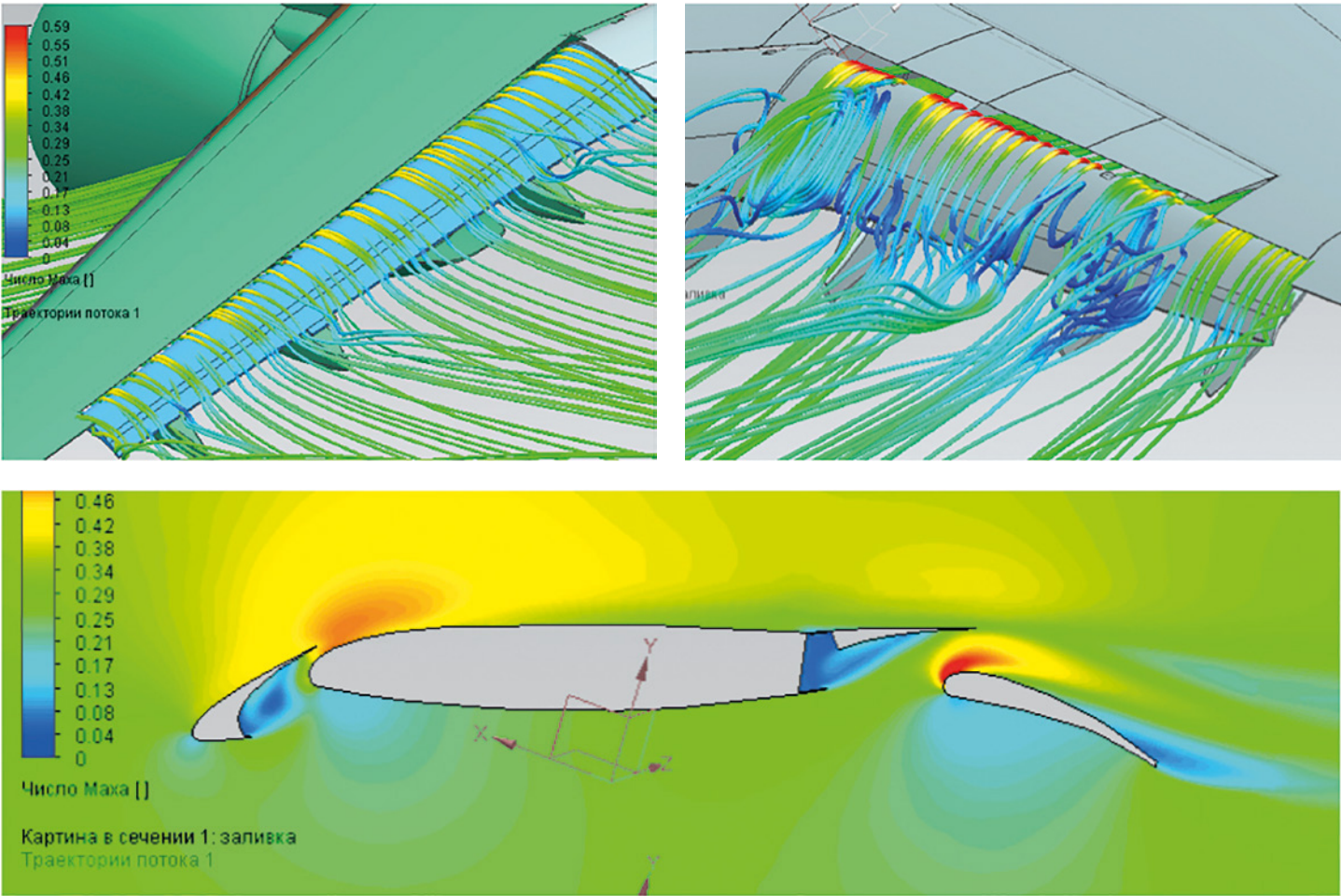

Figure 13. Spoilers Release Effect: Flow separation on the flap aft edge and flow acceleration on the leading edge
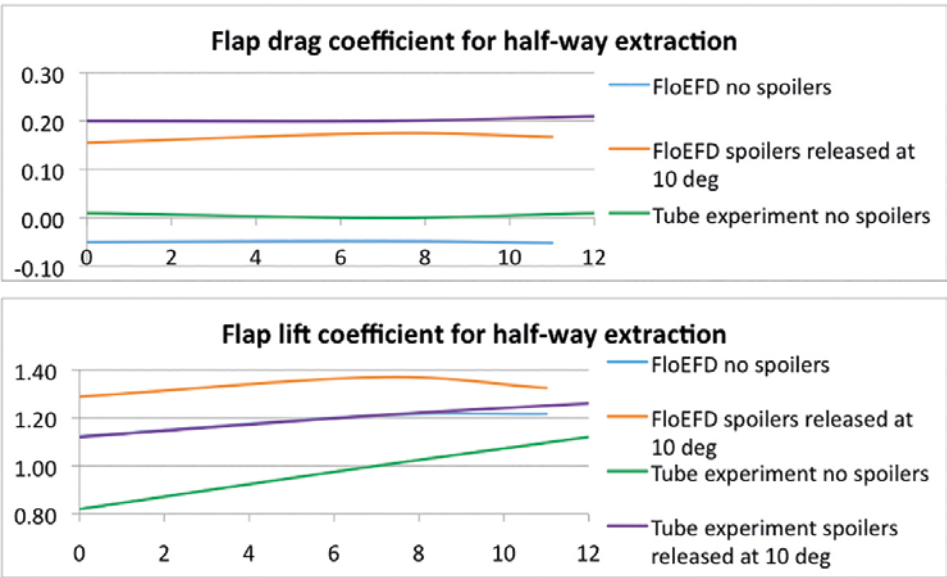

Figure 14. Spoilers Release Effect: Flap Drag Coefficient

	Scale model	True model	Δ
Slat drag coefficient	-0,11	-0,08	37%
Slat lift coefficient	0,91	0,96	5%
Flap drag coefficient	0,02	0,02	0%
Flap lift coefficient	0,89	0,96	7%

Figure 15. Reynolds Number Effect: Comparison of scale model to True Model

Figure 2. BOSE Automotive Audio Amplifiers

Bose Automotive Systems

Finding new ways to make our Products Cool!

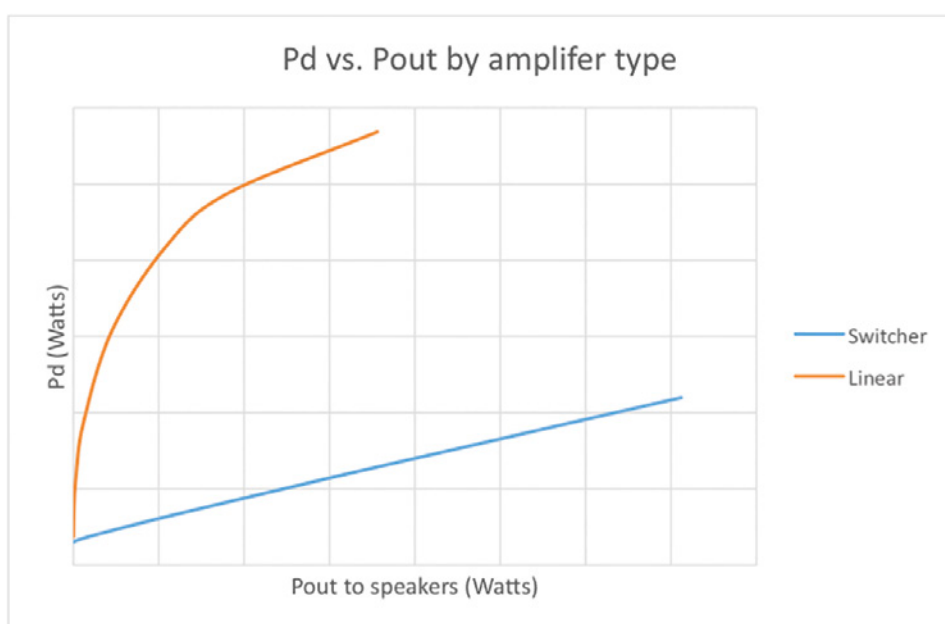By Brad Subat, Mechanical Engineer, Bose Automotive Systems

Figure 1. Power Dissipation vs. Amplifier Output Power

Like many industries these days, it is vital to maintain class leading technology and deliver products to market in less time. For Bose, one instrumental tool has been Mentor Graphics thermal analysis software, first FloTHERM and more recently FloEFD. We switched to FloEFD since it handles our more complex geometry and has the benefit of being embedded in our CAD tool (NX). While these tools provide great insight into the thermal design of products, we enter a new project with a bias to use previous designs which brings us to this article.

More than a year ago, I was intrigued by the first Mentor Graphics blog (of what became a several part series) on "Organically Grown 3D Printable Heatsinks". So, while the example was nothing like our actual products, I could see that this technology (once matured) could help us
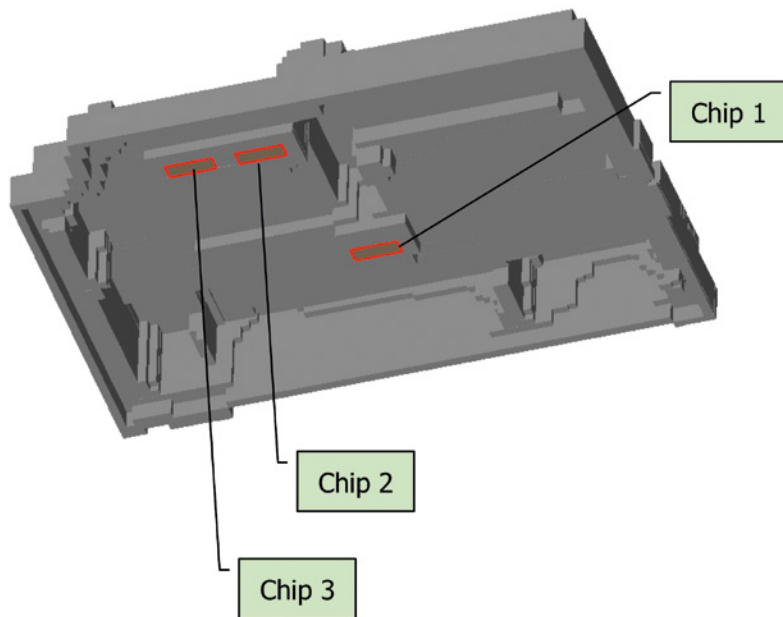
Figure 3. Power Amplifier Heat Source Locations
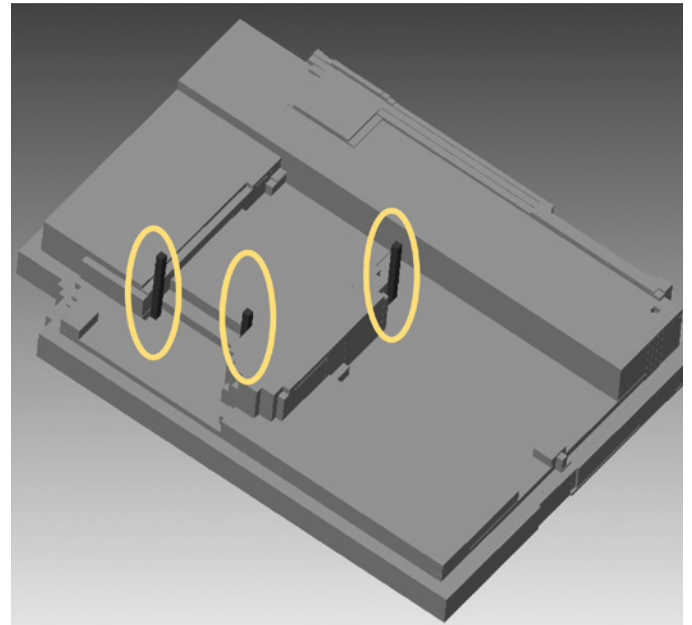
Figure 4. Starting Rod Locations

meet our goals in future years. At Bose, we believe we have "Better products through research", so while a tool might be effective today, we are drawn to developing better tools for the future. I then reached out to Mentor Graphics to propose we start an industrial research collaboration where this automated "growth" approach could be applied to something closer to our products. They would focus their algorithm development on our design space, while Bose would provide feedback and testing at critical progress points.

Designing products for the automotive audio market has many constraints and competing goals. In respect to our amplifiers, we design them to work within a wide temperature range, with high product reliability and nearly perfect initial quality. In the thermal realm, there are a few main components that dominate our designs; power amplifiers, voltage regulators and digital signal processors. Traditionally, the largest power dissipating (Pd) devices are power amplifiers. There are two main technologies that are used in the automotive industry, linear (Class AB) and switching (Class D), figure 1 Linear power amplifiers are less efficient but historically have been more cost effective. In recent years, the industry has focused on improving the cost effectiveness of switching amplifiers and the cost gap has narrowed significantly. The graph below shows the power dissipation differences versus power out for these types of power amplifiers. On both axes, there can be endless discussions on what
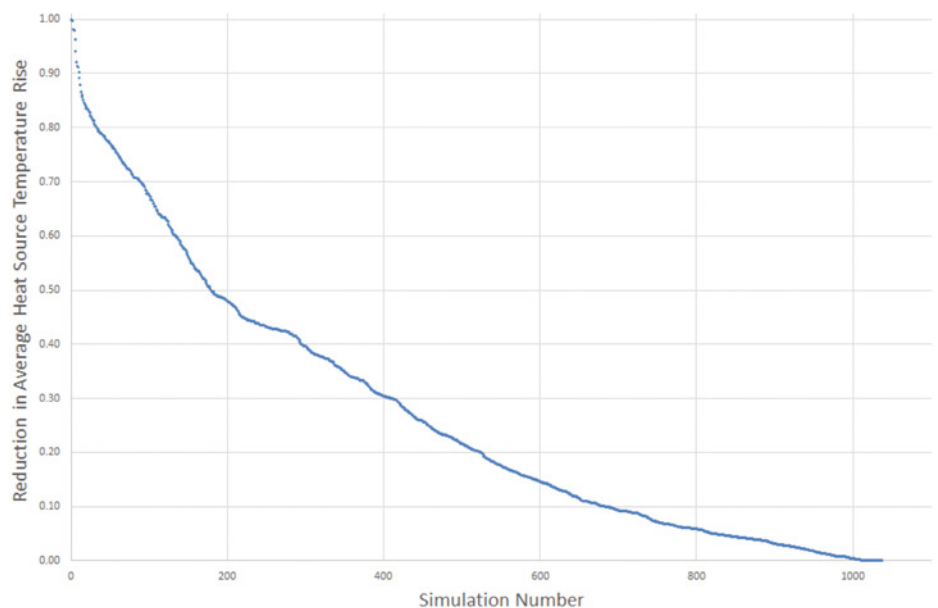
Figure 5. Reduction in Average Power Amplifier Temperature During Growth Process

variables and conditions should be used to produce this data, so, focus on the relative differences.

For the purpose of this initial investigation, the simplified model only had linear power amplifiers as components (figure 3) and a uniform heat source was spread over the simplified PCB.

Bose's current design methodology for our amplifiers is to use die cast housings (both aluminum and magnesium) for five, of the six, sides of the enclosure. The blank

canvas of this growth study was a minimum nominal wall shell around a typical size PCB. We included a few thick sections for heat spreading and added three starting rod locations (figure 4) from which the algorithm builds.

In automotive, part re-use is important, so car companies typically choose to have us design a housing that can work in several orientations. This allows them to have design freedom from vehicle to vehicle in regards to the amplifier location and orientation. During a standard development

many orientations are considered. To simplify this initial study, only the fins up axis orientation was considered for "growth" since it usually is the hottest orientation.

Figure 5 shows how the heat source temperature drops, as the heatsink grows. The sharper the initial drop, the greater the effectiveness of the added material. As the growth continues, the rate of temperature reduction slows. If the slope becomes very small, this indicates that you are having to add a lot of material for a small temperature reduction. An ideal thermal design would still have a large slope once the thermal goals have been reached.

Figure 6 shows a few steps of the growth.

With the simulations in and showing favorable results, it was time to do actual thermal testing to see if this innovative simulation technique would correlate well. Before machining our test housings, the grown design was adapted in our CAD tool to account for high level die casting design rules:

- **Fin spacing:** Tool steel is the inverse of your part, so between fins there needs to be enough tool steel to provide cooling and strength during the die-casting process. If pushed too far, the standing steel can break during production requiring major repair or early decommissioning of that cavity.
- **Draft:** Like plastic injection parts, die-casting needs a taper so it can be pressed out of the tool.
- **One area not addressed, was mold fill.** In high volume, automotive die casting process use an extremely short high pressure process to inject molten metal into the tool that can cool or trap air in a complex geometry.

As seen in figure 7, these results are very encouraging for this additive technology, as the unaided design used less material and has a similar thermal result. For thoroughness, we also tested the machined housings to confirm our selected orientation was indeed the hottest.

As with any research, it leads too many other areas to explore. So as Mentor Graphics was working on growing a heatsink, they decided to work on an optimization algorithm in parallel, which was subtractive by removing material from the design. This algorithm was applied to the "grown" heatsink tested above. The graph figure 8 to the right shows the increase in
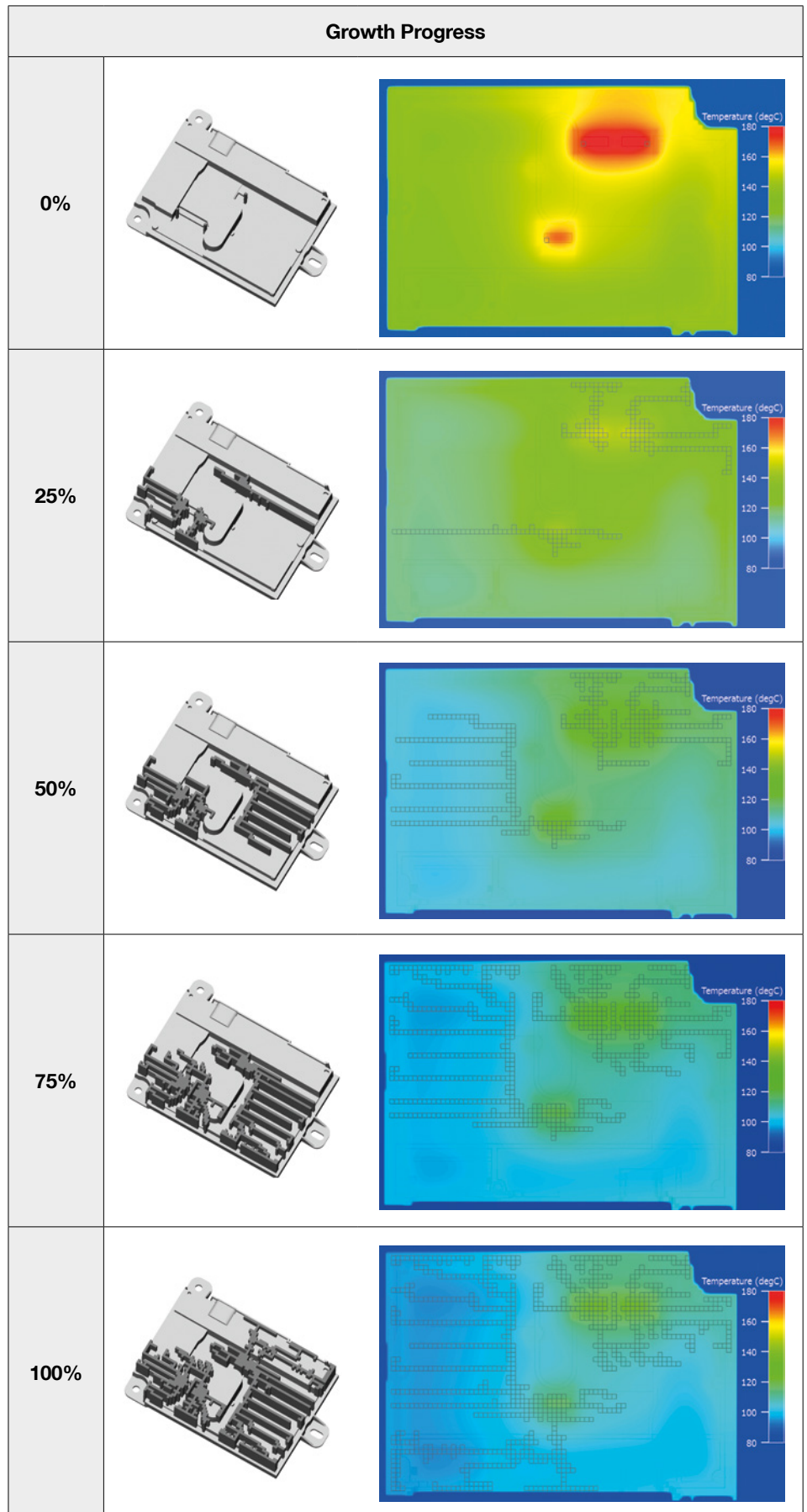

Figure 6. Fin Growth and Temperature Distribution During the Growth Process

"What was seen as an interesting idea over a year ago by Mentor Graphics and Bose for a autonomously grown heatsink, has now proven to be possible technology for the future."
Brad Subat, Mechanical Engineer, Bose Automotive Systems

	Predictions and results:				
	Heatsink volume (mm^3)	Fin only surface area (mm^2)	PA1 (C°)	PA2 (C°)	PA3 (C°)
Existing design (Prediction)	268,475	100,904	119	124	117
Grown (Prediction)	236,833	76,921	120	122	114
Delta	12% less	24% less	1 Hotter	2 Cooler	3 Cooler

Figure 7. Existing Fin Design vs. Grown Fin Comparisons
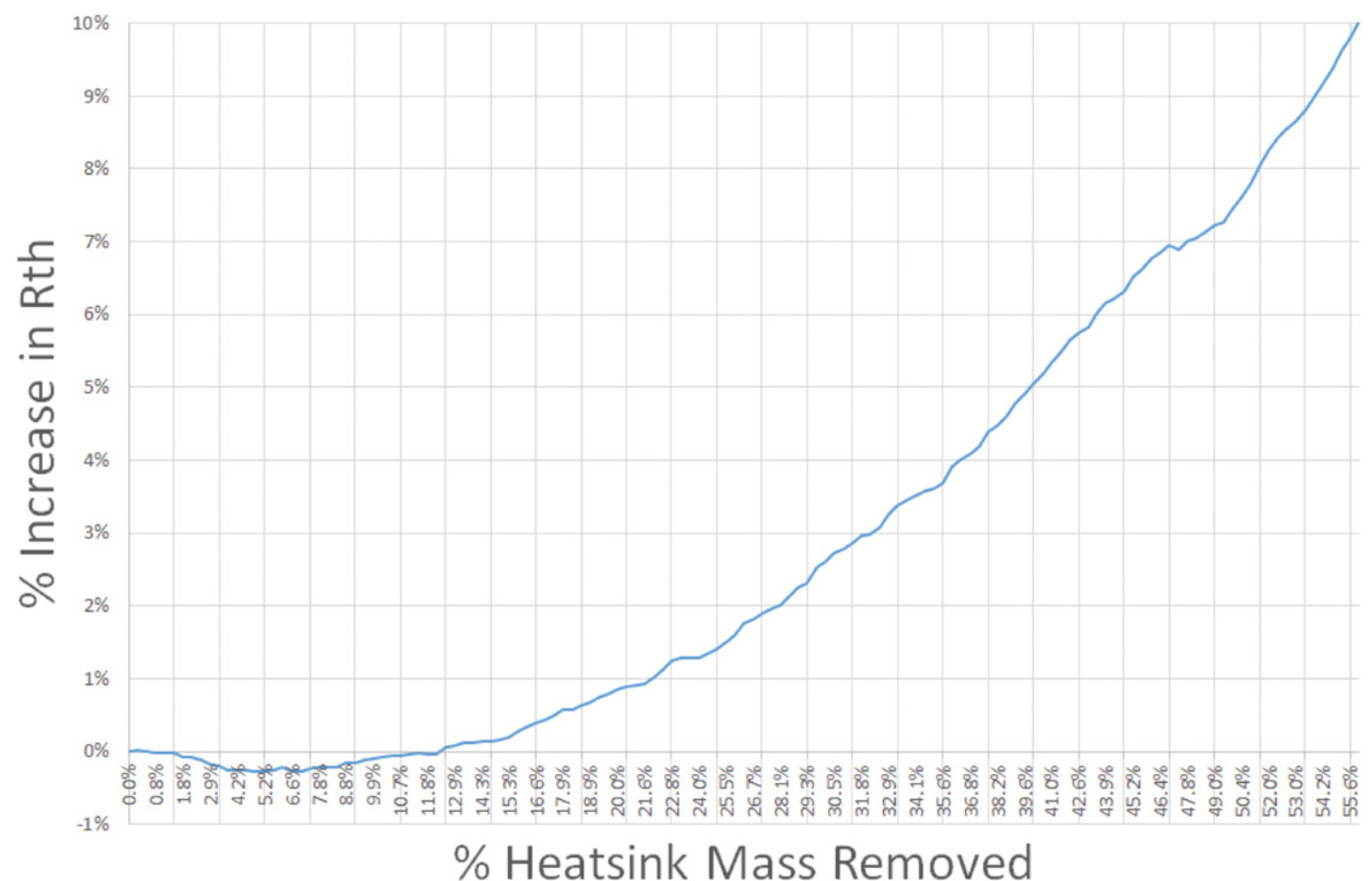

**Figure 8.** Increase in Thermal Resistance vs. Heatsink Mass Removed

the housings thermal resistance versus the amount on heatsink fin material removed. In this specific design the initial removal of heatsink material is predicted to actually lower the thermal resistance (cooler). Figure 9 shows the optimization of the fins and predicted temperatures at several stages.

We decided to test at 22% since there was a small leveling in the rise of thermal resistance. (Figure 10)

Again, the results are very encouraging for this subtractive algorithm, as heatsink material can be removed for minimal temperature rise. So if you have a product with thermal margin and are looking to optimize it, this technique might be immediately interesting for you.

A special thank you to the Mentor Graphic team this past year for their hard work, vision and passion for this collaborative project. What was seen as an interesting idea over a year ago by Mentor Graphics and Bose for a autonomously grown heatsink, has now proven to be possible technology for the future. I look forward to the next steps in refinements from Mentor Graphics to see if we can establish the confidence needed to add to our product development tools in the future.
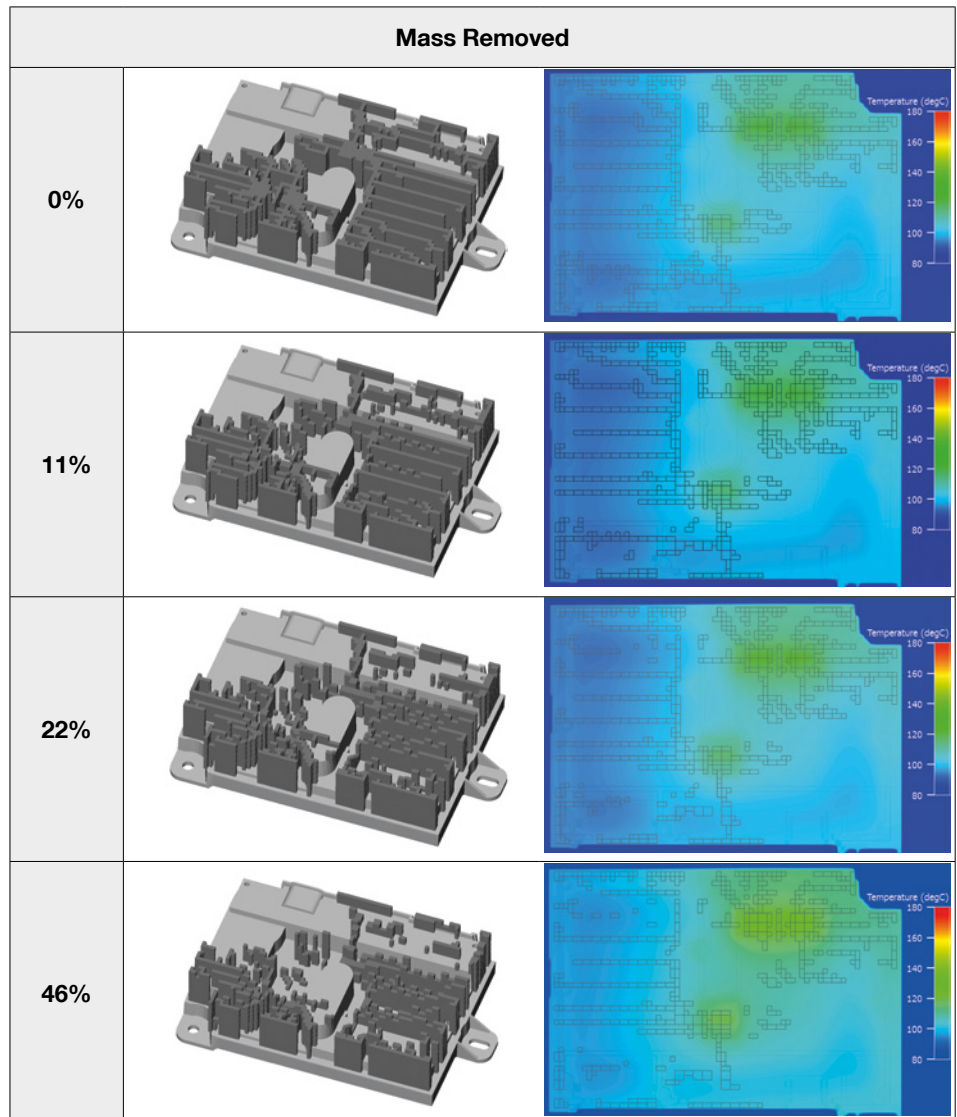
Figure 9. Fin Geometry and Temperature Distribution (Hardly Changing) During the Fin Mass Reduction Process

	Heatsink volume	Fin only volume	PA1 (C°)	PA2 (C°)	PA3 (C°)
Existing design (Prediction)	268,475	100,904	119	124	117
Optimized (Prediction)	219,114	62,268	122	123	117
Delta	18% less	38 % less	3 Hotter	1 Cooler	No Change

Figure 10. Grown Fin Design vs. Mass Reduced Fin Design Comparisons'

The growth methodology involves a series of sequential FloTHERM simulations. The pin with the largest thermal Bottleneck number is identified and another pin added to its coolest side. The process is then repeated. If the addition of a pin causes an increase in the thermal resistance then that pin is removed and a pin addition to the next largest thermal Bottleneck location is attempted instead.

The subtraction methodology starts with a tessellated discretized definition of the heatsink. An initial simulation identifies the portion with the lowest thermal Bottleneck, that portion is removed, the model re-simulated and the change in thermal resistance noted. The process is repeated, building up a graph relating the change in thermal resistance to the decrease in heatsink mass.

Both methods are implemented using an Excel front end, VBA and FloTHERM's FloXML and FloSCRIPT technologies. The processes are fully automated, not requiring any manual intervention due to the stability and robustness of FloTHERM's meshing and solver.

Electrothermal Simulation Study by ZFW

Successfully carried out with MicReD® Power Tester and FloEFD™

By Christian Rommelfanger, ZFW
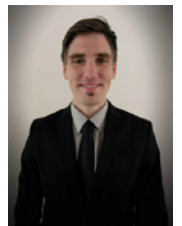
ZFW, Zentrum für Wärmemangement (Center for heat management) based in Stuttgart, specializes in comprehensive services in heat management and lifetime testing of components and systems. No matter the industry, our clients all basically want the same thing: a fast and simple solution for a specific thermal problem. We rely on a fast and easy to use CFD system that is capable of handling different applications as our consulting projects are spread through almost every industry sector, from automotive to production systems, and usually our clients give us a call when a project is time critical. That's why we use congruent CFD software to give our customers a fast and reliable answer to their questions. Besides simulation we offer our clients a wide range of measurement techniques and test benches. We think, in a modern engineering department, simulation and measurement needs to fit closely together to work effectively.

In power electronics, it is critical to have a tight fit between simulation and measurement. Even small differences in the simulation can have a big difference in predicting the lifetime of a component. Within an industrial project, ZFW conducted a detailed electrothermal simulation study of a bridge rectifier as an example for the use of coupled simulations to get more
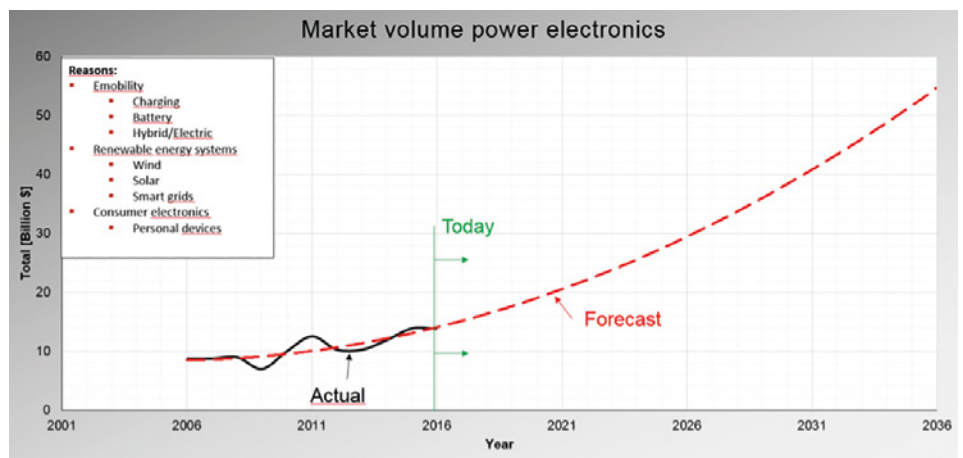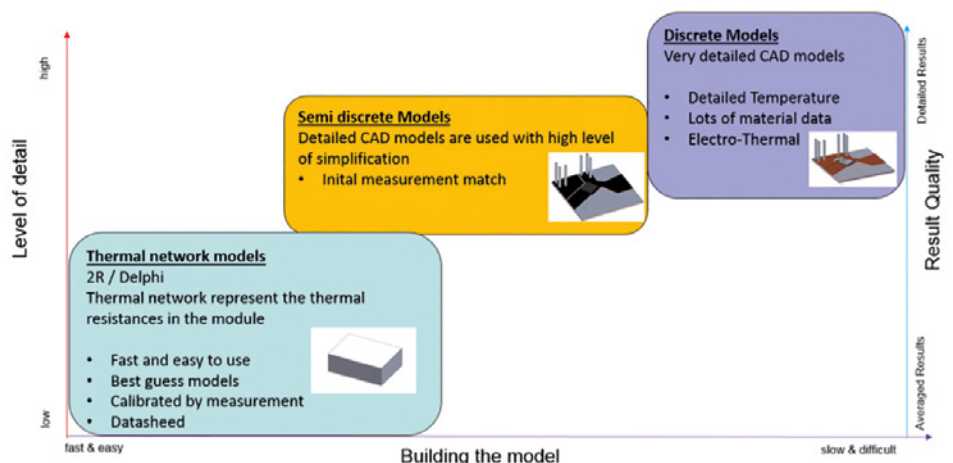

Figure 1. Forecast of the power electronics market

Figure 2. Level of Detail – Model building – Result quality

Types of power electronics			
Input	Output	Name	Application Example
AC	DC	Rectifier	E-mobility, renewable energy systems or industrial applications. Exchange between AC and DC electricity (socket <-> battery)
DC	AC	Inverter	
DC	DC	Converter	In mobile phones to maintain the voltage at a fixed value independent from the state of charge
AC	AC	Converter	Change of frequency or voltage, for example in power distribution network for change utility frequency 50 Hz to 60 Hz power grids

Table 1.

accurate results for reliability prediction of power electronics.

The forecast of the power electronics market predicts a rise of 200% in the next ten years. (Figure 1) There are several reasons for the increased demand in power electronics, such as the rapidly increasing market for e-mobility, the strong demand for renewable energy, and the uprising market for personal devices – just to mention a few. In most of these applications clients have high requirements on the sustainability of the device.

Keeping in mind that the rule of thumb of a 10 K change in temperature leads to almost 50% change in lifetime, it becomes clear that even with typical errors from thermal simulations, the error in the lifetime prediction can be worse. A 5% error in power losses within the device can have a serious impact in lifetime prediction. Usually our customers have +/- 10% error in their power loss prediction.

That's why it is very important for engineers to have accurate models for reliability prediction in early stages of development. Furthermore, it is crucial to have good and accurate boundary conditions that match the application.

In a nutshell, power electronics means the application of solid-state electronics to control electric power. In modern industry, there are plenty of applications where power electronics helps to control power. AC/DC rectifiers are used to change the alternating current of the electricity grid network to direct current for loading the battery of an e-car. In personal devices like mobile phones, DC/DC converters are used to maintain the voltage at a fixed value independent from the state of charge of the battery.

Figure 3. MicReD Power Tester

Most companies use the basic empirical based Coffin-Manson model (Equation 1) and add specific influences in the equation that they observed in experiments.

$$N_f = a* \Delta T^n$$

N_f: Cycles to Failure
a,n: Empirical Parameter
T: Temperature
Equation 1

A typical addition to the Coffin-Manson

law is an Arrhenius approach (Equation 2) to implement the influence of the average junction temperature to the lifetime prediction.

$$N_f = a* \Delta T_j - n*e^{\frac{E_a}{K*T_m}}$$

E_a: Activation Energy
K: Empirical Parameter
T_m: Average Temperature
T_j: Junction Temperature
Equation 2

The MicReD® Power Tester was used to determine the empirical coefficients in the Coffin-Manson equation. As well as for many additional parameters for various types of customer based lifetime laws. There are many different strategies to determine the constants in the lifetime laws for components, such as constant temperature change or constant current and so on. Which tactic is the right one always depends on the specific application. Assuming the following constants for a given application, that fit the basic Coffin-Manson law, we arrive at the results that a change of the Junction Temperature of around 10 K leads to about 44% change in lifetime (Equation 3).

$$\text{Coffin–Manson: } N_f = a * \Delta T^n$$

$a = 10000000000$

$n = 2{,}7$

$N_f (80\ °c) = 72720$

$N_f (70\ °c) = 104288$

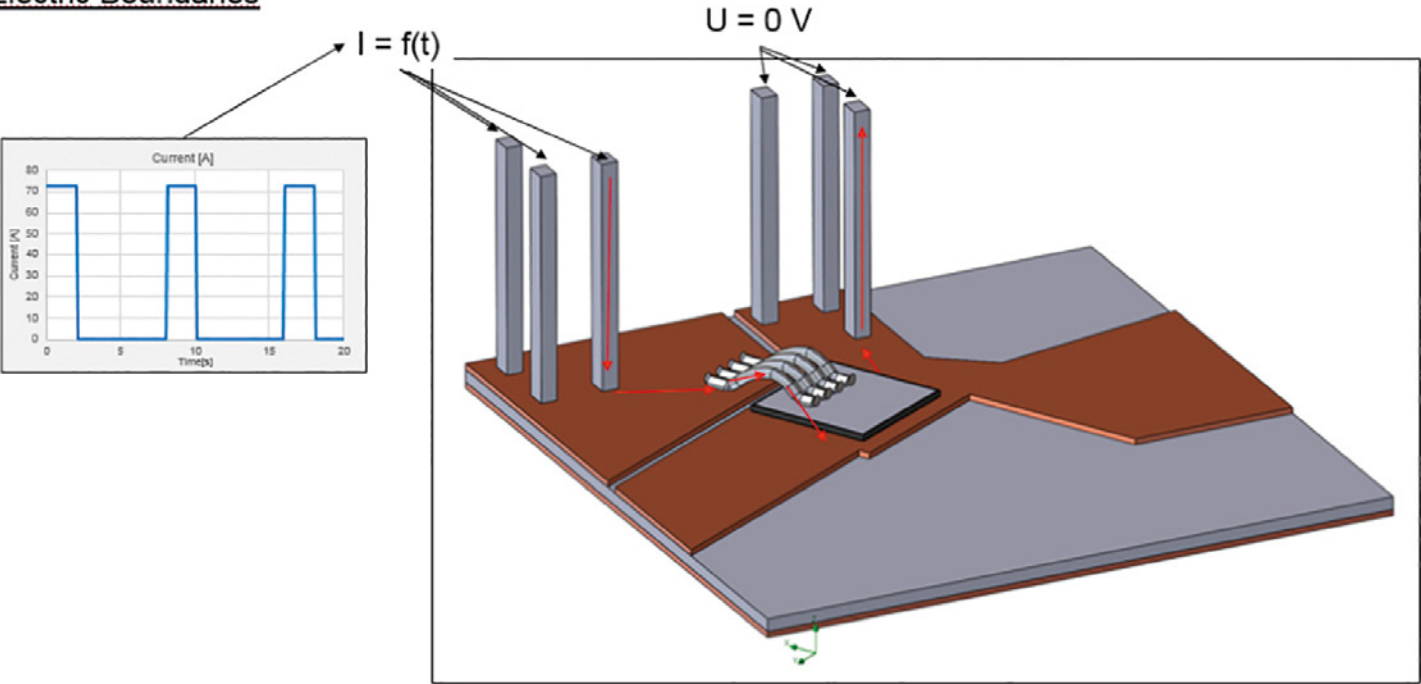**Equation 3**

Electric Boundaries

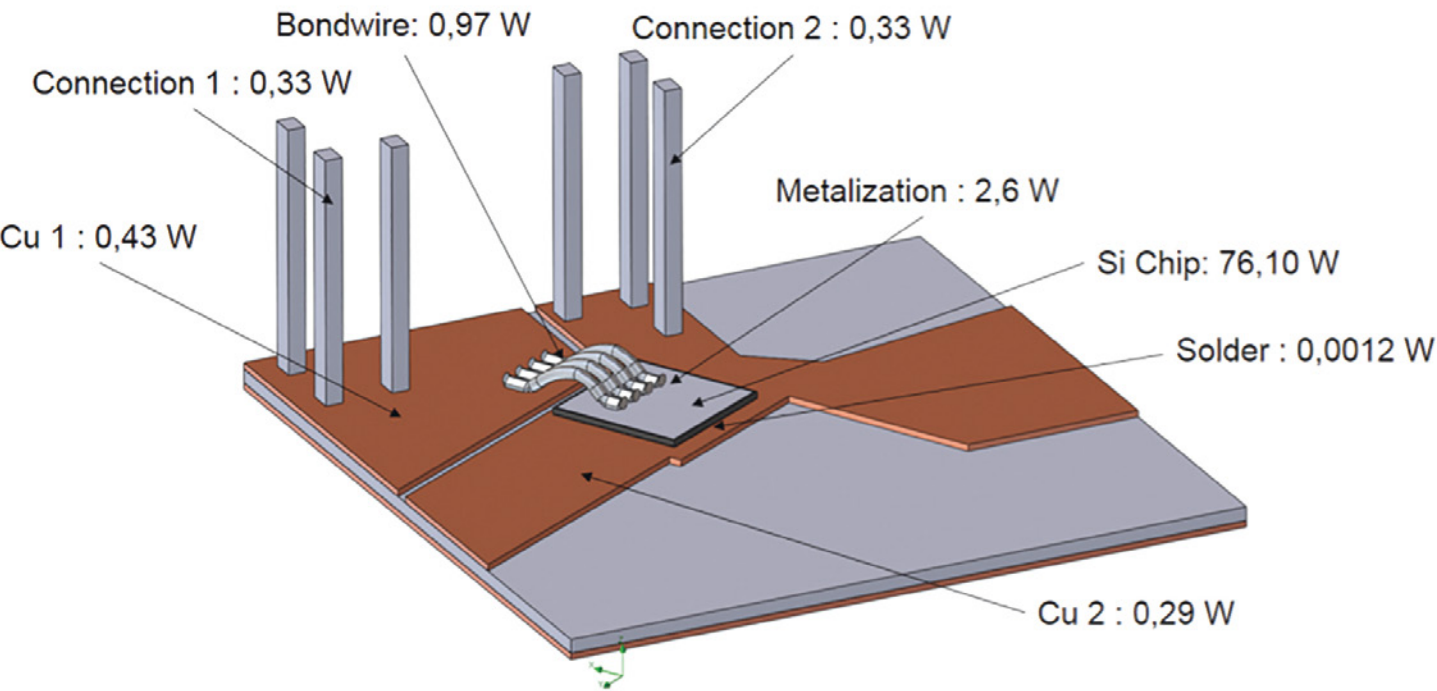**Figure 4.** Electro-thermal simulations in FloEFD

Figure 5. Detailed Power loss distribution increases design accuracy

"With these findings from the study, using the combination of the MicReD Power Tester and FloEFD, reliable simulation models can be created and used in the future."

Christian Rommelfanger, ZFW

As mentioned before, a 10 K change in temperature leads to almost 50% change in lifetime. Because of this relationship between temperature and lifetime, it is critical to have accurate models for electronics. The results of thermal models can be improved by coupling the thermal simulation with an electric one.

Figure 4 shows an overview of how electro-thermal simulations works with FloEFD™. The geometry is based on a single diode of a bridge rectifier. The electric boundaries are three power steps in 20 seconds with a length for each power step of two seconds. The thermal boundary is a fixed temperature at the bottom of the device.

The 3D electric simulation can predict the actual Joule heating in every part of the system. Two-way coupling between electric and thermal simulation works in two directions. It enables the direct transfer from the power losses due to Joule heating into the thermal simulation (figure 5) and the temperature for predicting the temperature dependent electric resistance into the electric simulation.

In the Si-chip itself power loss is 76,1 W. A stand-alone thermal model that would use the overall power loss of 81,6 W, as a volume source in the silicon would lead to an error of 7%. This leads to a temperature error of 8,4 K, assuming a junction temperature of 120°C. Calculating the lifetime with the error of 8,4 K would result in a 50% error in lifetime prediction.

The temperature dependent electric resistance of the silicon chip is calibrated through a parameter study of the measured $R_{SD_{on}}$ in the MicReD Power Tester for a given current. In the post process of the electric simulation the voltage drop in the Si-chip can clearly be seen.

In the thermal simulation, the distribution of the temperature through the diode is shown. Notice that the bond wire works in this transient load chase, due their thermal capacity as a heatsink. Comparing this simulation with measurement results in the MicReD Power Tester the error in temperature at the junction is less than 1K.

Conclusion

In reliability investigations of power electronics, it is important to have accurate temperature field prediction in the Si-Chip. Ordinary thermal models give a good insight in the temperature distribution in an electronic system, but when it comes to component reliability detailed electric/thermal studies need to be done due to their sensitivity to temperature. To simulate the thermal chip behavior, it is very important to have reliable material data. A parameter study that compares a measured voltage drop to a simulated voltage drop can help to characterize the material value. The error with a calibrated electro/thermal model can be less than 1K if the baseplate temperature is fixed (coolplate) and the heat losses occurs due Joule heating. The methodology used in this example isn't just for diodes it can transferred to MOSFETs and similar devices as well.

With these findings from the study, using the combination of the MicReD Power Tester and FloEFD, reliable simulation models can be created and used in the future.

References
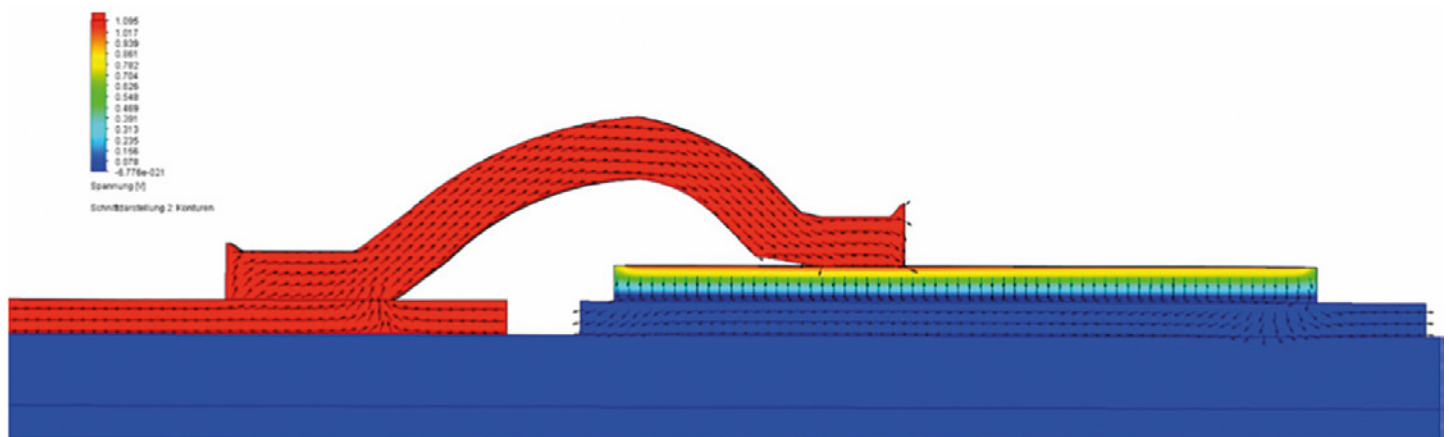
https://www.zfw-stuttgart.de/
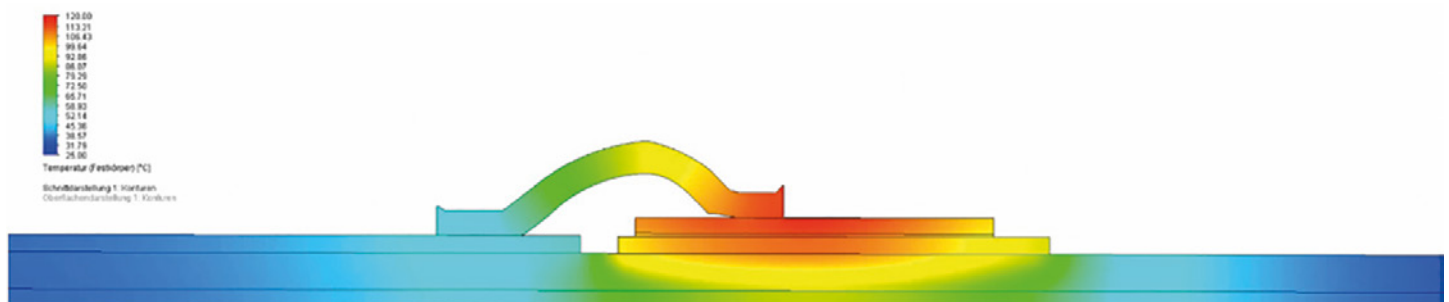

Figure 6. Voltage drop

Figure 7. Temperature distribution

A Unique Design to Generate UAV Electrical Power in Flight

By Guy Wagner, Electronic Cooling Solutions and Travis Mikjaniec, Mentor Graphics

As smaller UAVs are designed with more sensors and communications technology for longer missions, the additional electrical power to run them drives the need to generate onboard electric power. One way to create onboard electrical power would be to harness the remaining 80% "waste energy" produced by the two-stroke engine.

A team of engineers from Electronic Cooling Solutions and Ambient Micro designed, built, and tested an exhaust-heat thermoelectric generator (EHTEG) that can be incorporated into a UAV design to harvest and convert this waste energy into electrical power in flight [2] .

There are several sources of energy loss in a small engine all in the form of heat. The main sources are the heat rejection from the cylinder and cylinder head, loss from friction, and the heat of the exhaust stream. Though the heat from the exhaust system is the only truly usable heat source.

The EHTEG had several requirements:

- Mechanically robust and integrate into the aircraft without compromising flight safety,
- Extract the required heat without impairing engine performance,
- Provide the largest possible temperature differential across the thermoelectric modules while operating within the maximum temperature limits, and
- Designed with minimal weight and aerodynamic drag.

Figure 1. UAV with the EHTEG attached on top

Designing the Interior and Exterior TEGs

Heat exchangers on the inside of the muffler absorb heat from the exhaust as it flows through. The heat passes through exchangers to 2inch. square TEGs mounted on the outside of the UAV and finally passes through another row of heat exchangers to the open air. As the TEGs are exposed to the temperature difference between the hot inside exhaust air and the cool outside air, they generate electric current. The greater the temperature difference, the more current is generated.

The team modeled the thermal design of the system using Mentor Graphics' FloTHERM® Computational Fluid Dynamics (CFD) modeling software [1]. They simulated airflow on the outside (cool air) and the hot exhaust inside to estimate the temperature difference, which enabled them to optimize the internal and external fins of the heat exchanger and the number and location of the TEGs.

They built engineering models of several likely EHTEG configurations and ran them on a test stand using the same engine and propeller that is used in a MLB Company Bat4 UAV. The models were validated for a range of operating parameters that simulate flight conditions

The engineers used FloTHERM software that models conduction, convection, and radiation as well as the fluid flow of both the external cooling air and the hot internal

exhaust gas. They created virtual models of the exhaust system and performed thermal analysis and test design modifications quickly and easily before building any physical prototypes. The results of the CFD models correlated well with those obtained on the engineering test bed.

The engineers used the internal volume and length for the muffler recommended by the manufacturer to make the system act as an efficient expansion chamber exhaust system. These were used to develop the first half-symmetry CFD models that would determine the number of TEGs needed to optimize the electrical output with minimal weight. The model is symmetrical, so building a half-symmetry model reduced the number of elements down to 1.04 million cells with no loss in accuracy.

The fin parameters of the internal and external heat exchangers were kept relatively constant while varying the location of the heat exchangers and the placement of the TEGs. The goal was to maximize the temperature differential across each TEG to extract the most heat energy from the 455°C exhaust gas.

13 configurations of heat exchangers and TEGs were modeled in the first optimization study. They tabulated the power output from each configuration and chose the best configuration.

After optimizing the placement of the TEGs, it was found that the central fins on the interior heat exchangers disrupted the exhaust flow and the hot exhaust gas wasn't reaching the front end of the muffler. But if they removed the center fins, the exhaust gas would not channel down the center and the exhaust pulse would not reach the front end of the muffler. So instead of removing the central fins, they placed them in a semicircular pattern. (Figure 3) This configuration kept the exhaust pulse moving through the center of the muffler and it was able to curl back symmetrically as the hot gas flowed back along the outsides and through the fins.

The interior heat exchangers decreased in temperature as the hot exhaust gas flowed from the front through the fins to the rear of the muffler and then out of the vertical exhaust pipe.

The FloTHERM simulation was able to show the exhaust gas flow pattern for the heat exchanger with the center fins removed. (Figure 4) The flow pattern is disrupted
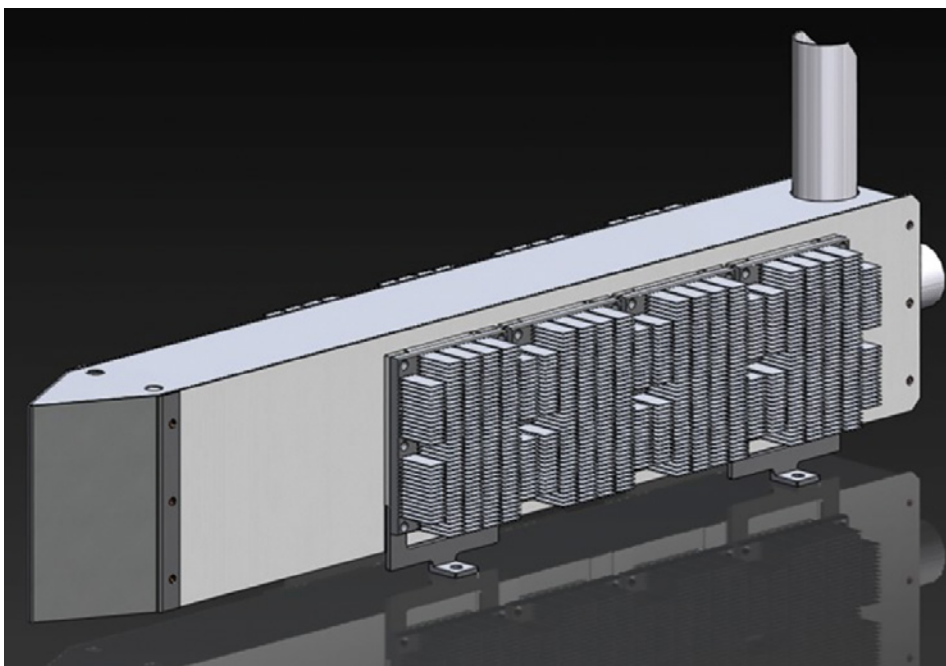
Figure 2. The positions of the external heat exchangers that resulted in the highest average power generation for the system
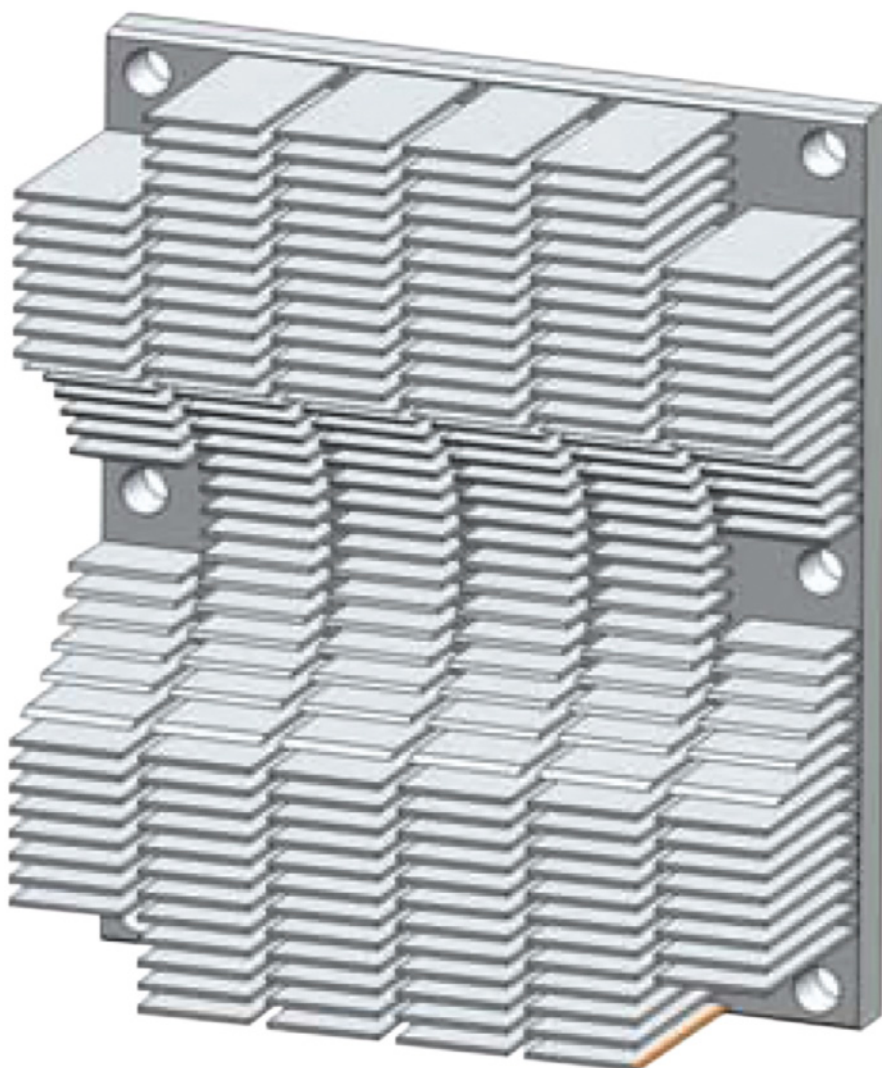
Figure 3. The interior heat exchanger with the fins in a semicircular shape in the center

before the exhaust stream reaches the front end of the muffler.

The simulations showed that when the semicircular-shaped fins are present, the flow pattern retains its shape all the way to the front of the muffler. (Figure 5) This allowed them to optimize fin placement.

Typically, the outside heat exchangers on TEGs are placed in a line. This causes an issue because the units toward the rear of the external airflow receive more preheated air than the heat exchangers that are upstream. This reduces the delta-T across the heat exchanger and the power output.

Therefore, nine configurations were analyzed to determine the optimum fin parameters for the external heat exchangers. The results were plotted against the total power generated by the TEGs. All of the custom heatsink designs analyzed out-performed the stock heatsinks for total power generation, but due to time and budget constraints, stock heatsinks were used for the first flight test model. This resulted in a reduced power output 11W compared to the custom heatsinks.

The outside TEGs were arranged in four columns by two rows on each side of the muffler. The TEGs maintained a cool side temperature below 58.3°C with external air at 18 °C and 22.3 m/s velocity, while keeping the hot side temperature below the maximum allowable temperature of 225°C. (Figure 6) The outside heat exchanger temperature ranges from 26.1°C on the leading edge of the front fins to 58.1°C on the base plate next to the hottest TEG.

Some of the first simulations demonstrated that the heat loss through all other surfaces of the muffler had to be minimized to maximize heat flow through the TEGs for maximum power generation. Mineral wool insulation was used on all the exposed surfaces to minimize the heat loss.

The power output of the EHTEG system was modeled by summing the power contribution of each pair of TEG modules. By first calculating the hot side and cold side temperatures of each TEG pair, these values could then be used to compute the open circuit voltage. The harvesting and power conditioning circuitry matches the equivalent series resistance for maximum power transfer; thus, the voltage of the load resistance is exactly half the open circuit voltage. This data defines the power harvested per TEG pair.
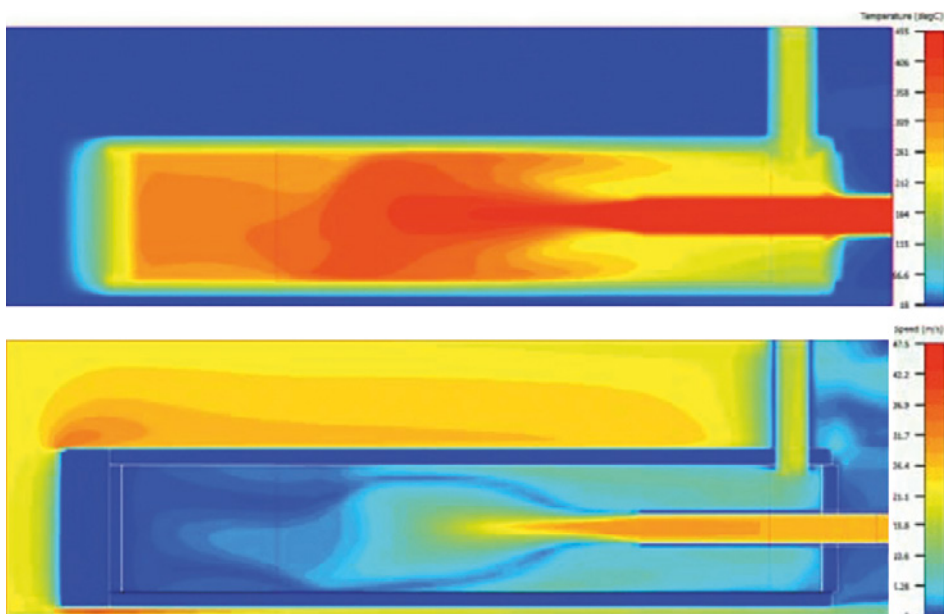

Figure 4. Thermal simulation shows the exhaust gas flow pattern without fins in the center
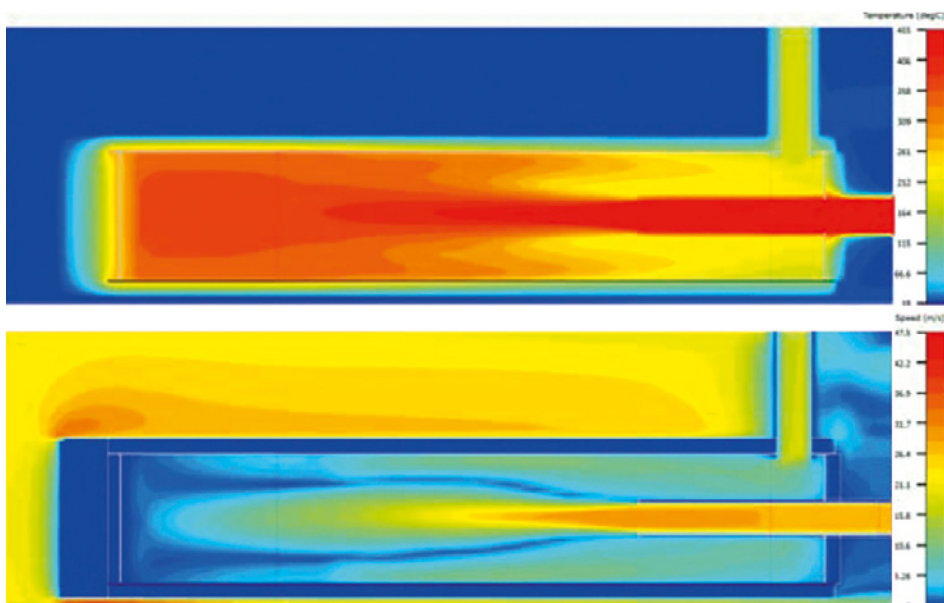

Figure 5. Thermal simulation shows the exhaust gas flow pattern with fins placed in a semicircle in the center

Mechanical Design
The mechanical design of the EHTEG had two main requirements:

- Able to support the thermal components and allow adequate flow of cold air around the external heatsinks, and
- Be lightweight with minimal frontal area to reduce aerodynamic drag.

The heatsinks were fastened from the outer (cold side) to the inner (hot side) forgings. The TEG modules were sandwiched between the outer heatsinks and the EHTEG sidewalls. They used a high-temperature thermal interface material at each interface in the thermal path to maximize heat transfer from the inner heatsinks through the thermoelectric generator modules and the outer heatsinks. Figure 8 shows an exploded view of the EHTEG.

Converting to Usable Electricity
The thermal environment of each thermoelectric module was slightly different because of its location on the EHTEG, so each module's output was also different from its neighbors. The input interface modules received the output from a pair of

modules and converted the input voltage to 12 V. The input module also automatically adjusted its input impedance to match the source impedance, thus operating at the maximum power transfer point.

The outputs of the input modules were combined and fed to a single 12-V bus regulator that provided a regulated 12-V output to external loads. An electronic load was included in the power conditioning electronics for testing purposes. The electronic load automatically adjusts its resistance to extract the maximum power available from the EHTEG system. The data I/O board provided voltage levels proportional to selected voltage and current levels for input to the onboard data-logging system.

In Summary
The team used FloTHERM to create virtual models of the exhaust system, analyzing various design configurations quickly before building any physical prototypes. And the results of the CFD models correlated well with those obtained on the engineering test bed. Since the TEGs are actually thermoelectric coolers run in reverse, their efficiency is only around 5%; that is, 5% of the heat energy flowing through is turned into electricity. If this efficiency rate can be doubled, the technology could be used in many practical and profitable applications. New commercial opportunities are spurring interest in thermoelectric power generation. The design techniques described here could be used to develop much higher power output thermal energy harvesting power systems.

References
[1] FloTHERM, http://www.mentor.com/products/mechanical/products/flotherm

[2] J. Langley, M. Taylor, G. Wagner, and S. Morris, "Thermoelectric Energy Harvesting from Small Aircraft Engines," SAE International, 2009.

[3] Marco Nuti, Emissions from Two-Stroke Engines, Society of Automotive Engineers, Inc., Chapters 7 and 9.

[4] Combustion Products Applet: http://www.engr.colostate.edu/~allan/thermo/page9/Combustion/combustion.html, Allan T. Kirkpatrick, Colorado State University, Fort Collins.
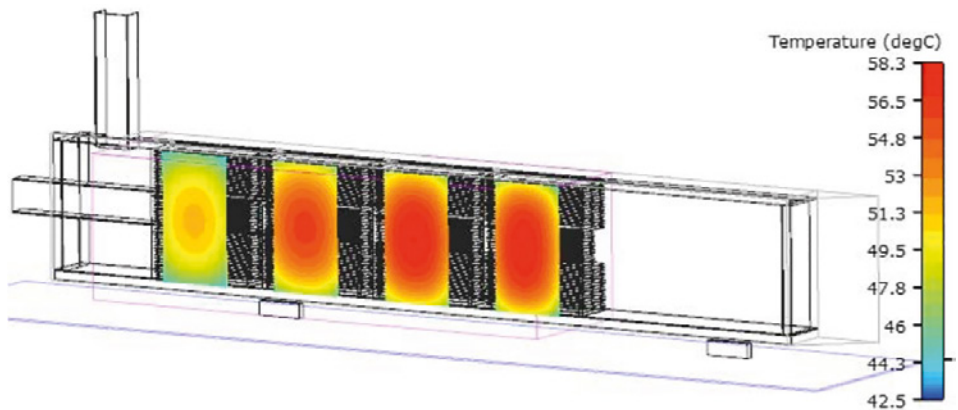
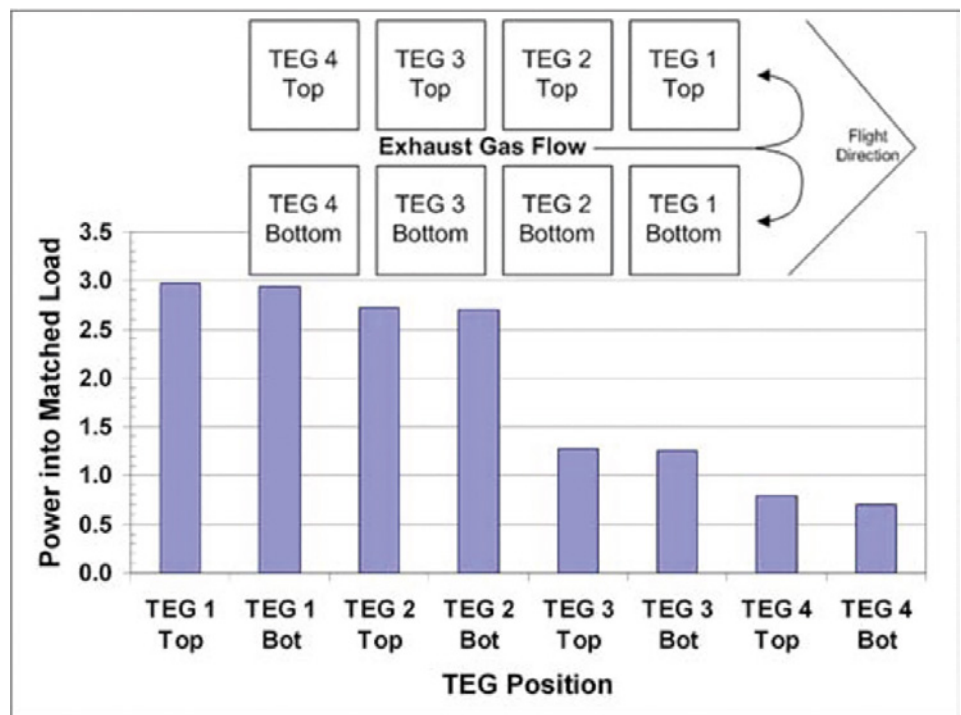**Figure 6.** Cool-side temperatures of the outside TEGs.

Figure 7. Single-side power output (W) for the flight configuration

Figure 8. The inside and outside of the EHTEG

Comparing FloMASTER ORC Results to Experimental Data

By Doug Kolak, Technical Marketing Engineer, Mentor Graphics

There is a strong current in the automotive industry today, pulling the future of vehicles more and more towards electrification. While this is a certainly a good direction, not only because of the need for lower emission rates and the reduced reliance on fossil fuels; there are still several obstacles that need to be overcome before the roads are dominated with these vehicles. As engineers continue to tackle these challenges, it is important to remember there are still opportunities to improve vehicles that use the internal combustion engine. Even with all of the optimization that has gone into these components in the past, approximately 60% of the fuel energy is lost through heat, friction, and exhaust loses [1].

There are a number of techniques currently being investigated that deal with capturing the energy of the exhaust gas. There are several options that fall under this umbrella of Waste Heat Recovery (WHR), these include: Exhaust Gas Heat Recovery, Thermo-electric Generators, and Organic Rankine Cycle (ORC). Each of these options does pose a number of challenges to system engineers, and this is particularly true of ORC systems since they are effected by both component and system layout design. However, when compared to other exhaust gas energy capture technologies, ORC has been shown to achieve efficiencies as high as 16% in automotive applications [2].

ORC systems are typically designed to recover waste heat from a process and subsequently used to heat a working fluid until it is a superheated vapor. The vapor is then sent through an expansion device such as a turbine, so that useful work can be extracted. To effectively design an ORC system, it requires that individual components are sized accordingly, that an appropriate working fluid is selected, and that system interactions, including a control strategy, are understood
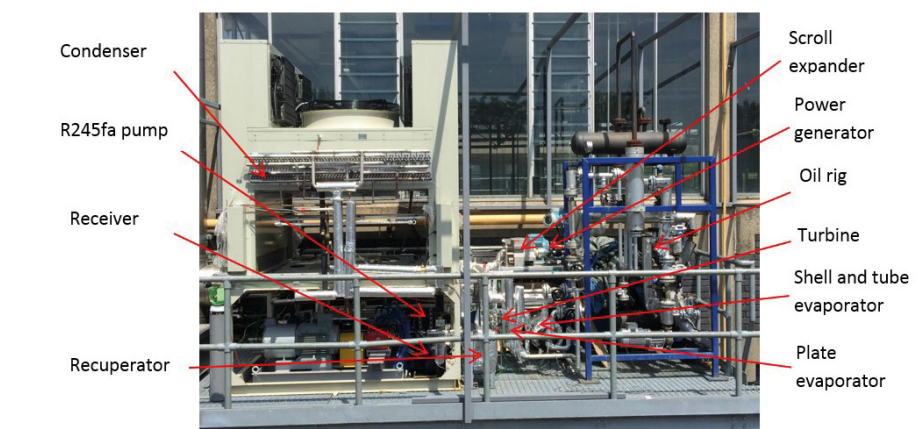

Figure 1. Brunel ORC Test Rig

and employed. For this reason, it is critical that a tool can quickly and accurately model these complex systems for evaluating designs and rapidly prototyping new concepts.

With the release of V8, FloMASTER has introduced functionality to fully model ORC systems so that engineers can consider key design parameters such as available superheat, high and low side system pressures, ORC fluid selection, pump type and performance, and heat source and expander selection. The tool was developed in conjunction with Brunel University in the UK, who ran extensive tests to evaluate accuracy and robustness. Installation of rig based pressure, temperature, and flow instrumentation has demonstrated that FloMASTER is capable of predicting overall system thermal efficiencies within 2% of expected values. In addition to the work with Brunel, FloMASTER can be compared to experimental work carried out by AVL Powertrain Engineering Inc. and published by SAE [3].

The system represented by the model shown in figure 2 is a typical ORC system that would be found on a heavy duty truck. Due to its common availability, ethanol is being used as the working fluid, and both the exhaust gas and the EGR gas are being used to
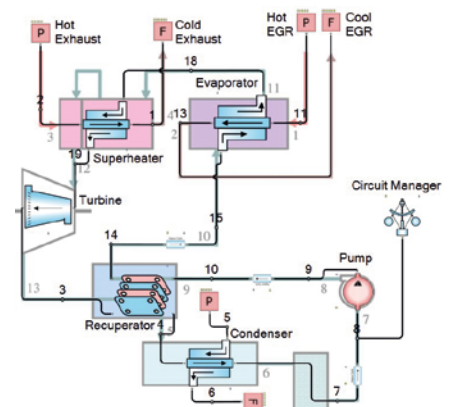

Figure 2. FloMASTER ORC System Model

heat to the fluid. The overall design goal of the system is that it must be able to extract 5 – 15 kW of energy from the turbine without having negative effects on the EGR or exhaust systems. As shown in figure 2 the system is laid out as follows:

- The pump is a positive displacement type pumping, delivering the required flow rate based on the pressure drop of the system,

- The fluid exits the pump and enters the recuperator where it is heated by hot ethanol coming out of the turbine,

- The warmer fluid then enters the evaporator

Figure 3. ESC Test Points

Figure 4. B50 Test Point Temperatures
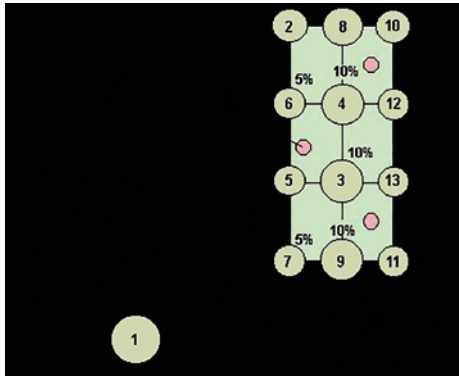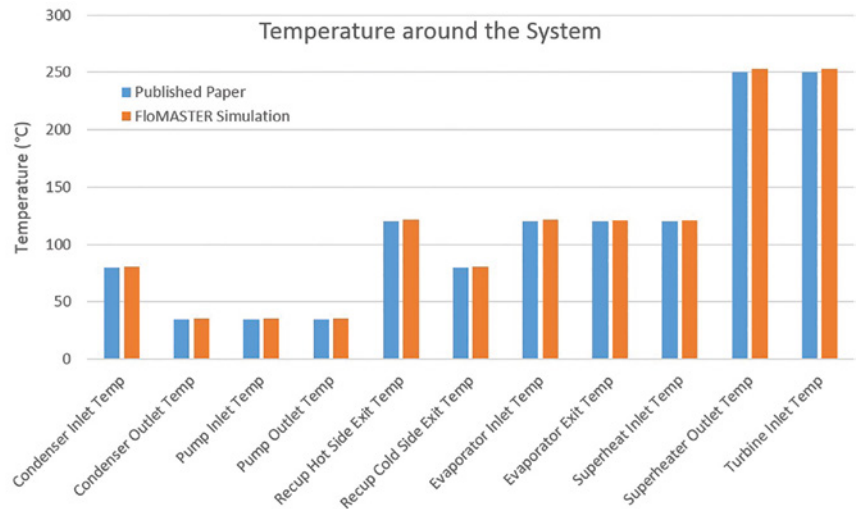

Figure 5. All Test Points Heat Inputs

where it is heated by the EGR gas until it changes phase to a vapor,

- The vapor then enters the superheater where it is heated further by the hot exhaust gas,

- The superheated vapor then enters the turbine where it is expanded. This expansion turns pressure energy into rotational energy which can then be translated into electrical energy by an attached generator,

- The still superheated vapor then enters the other side of the recuperator, warming the incoming liquid phase ethanol, and

- The ethanol then enters the condenser where it changes phase back to a liquid to begin the thermodynamic cycle all over again.

The FloMASTER model was constructed using all out-of-the-box vapor cycle components with no calibration required. For the recuperator, a plate frame heat exchanger was chosen, while a shell and tube component was selected for the other three heat exchangers.

As part of the study a number of simulation conditions were run based on the European Stationary Cycle (ESC). The European Stationary Cycle (ESC) is currently used across Europe and is a part of the Euro III emissions regulations. The European Transient Cycle (ETC) and the European Load Response (ELR) test cycles are also part of the 1999/96/EC directive. The ESC consists of 13 test points which are all run in steady-state. Figure 3 shows the test points recorded onto a graph of load vs. engine speed with the focus of the study on points B50, B75, B100, A100, and C100. These test points determined both the temperature and flow rate of the exhaust gas and EGR gas which directly determines the amount of heat energy available to the system.

Overall the agreement between the simulation results and the published experimental results is very good. The variation in temperature versus published results across all of the
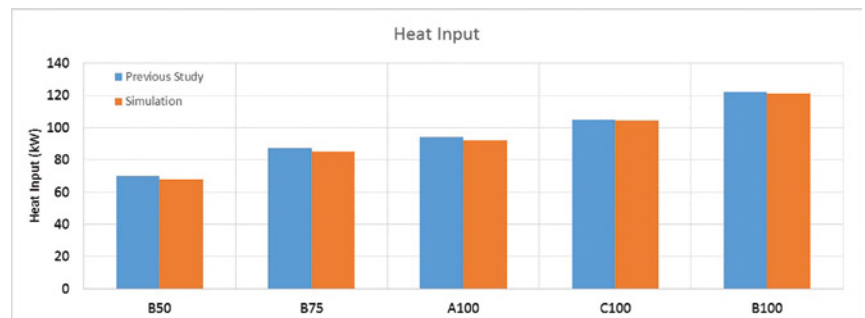
simulation, is never greater than 1.7%, Figure 4 shows the temperatures around the model for the B50 test point. The heat input across the simulations also shows very close correlation with the greatest deviation from the B50 test point at 3.34% with all cases shown in figure 5.

The other critical factors for the system is the power generated and the overall system efficiency. Table 1 shows the values for the B100 test case. Overall the study and simulations match extremely well except for the pump power, however this value is so small in the overall system it has minimal effect. This design for the B100 test point is able to deliver 13.54 kW assuming a 75% efficiency on the turbine, well within the desired range of the study. This leads to an overall system efficiency of 11.2%, both quantities well below 2% variation from experiment.

Developing ORC systems is both time consuming and expensive, but being able to frontload as much design work as possible through the use of 1D system simulation, such as with FloMASTER, can give companies the advantage of fewer physical prototypes and faster time to market.

Results	Previous Study	Simulation
Heat Input (kW)	122	121.21
Turbine Power (kW)	18.1	18.2
Pump Power (kW)	0.15	0.114
Condenser Heat Duty (kW)	N/A	103.26
Overall Energy Balance (kW)	N/A	-0.106
Net Rankine Cycle Power (kW)	13.42	13.54
System Efficiency (%)	11.0	11.2

Table 1. Power Generated and System Efficiency

References

[1]Furukawa, T., Nakamura, M., Machida, K., and Shimokawa, K., (2014). A Study of the Rankine Cycle Generating System for Heavy Duty HV Trucks. SAE Tech Paper, 2014-01-0678, doi:10.4271/2014-01-0678.

[2] Park, T. Teng, H. Hunter, G. Velde, B. Klaver, J. (2011) A Rankine Cycle System for Recovering Waste Heat from HD Diesel Engines - Experimental Results, SAE Int. Publication 2011-01-1337, doi: 10.4271/2011-01-1337.

[3] Teng, H., Klaver, J., Park, T., Hunter, G., van der Velde, B. A Rankine Cycle System for Recovering Waste Heat from HD Diesel Engines - WHR System Development, SAE int. Publication 2011-01-0311, doi: 10.4271/2011-01-0311.
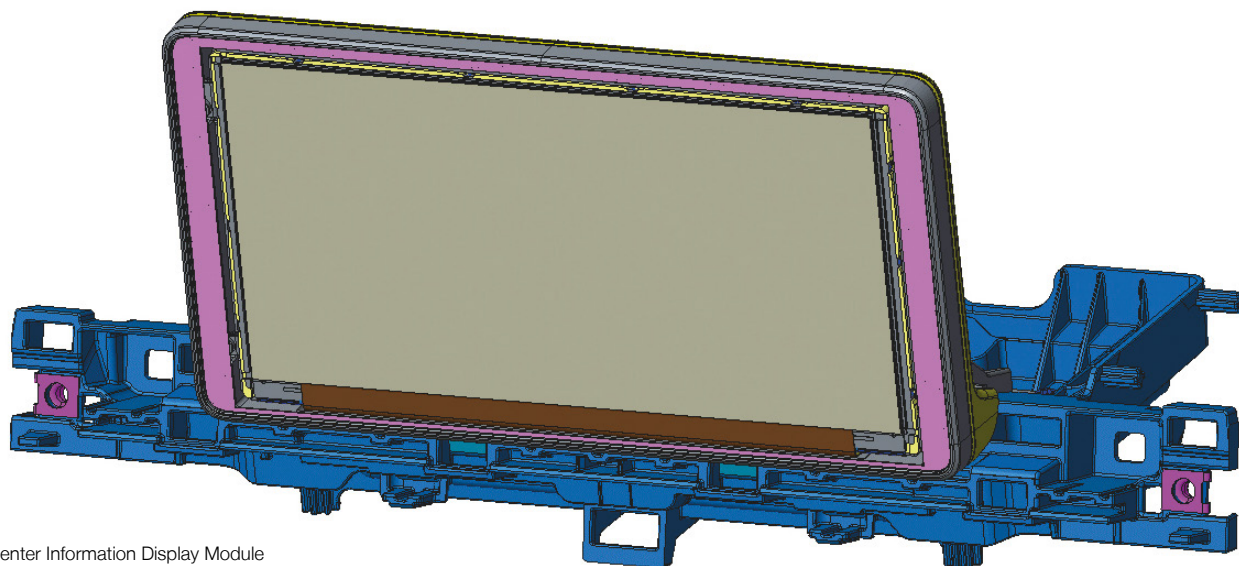
Figure 1. Center Information Display Module

Thermal Design Approach for *Automotive Display Integration*

By Clemens J.M. Lasance, Philips Research Emeritus, Consultant SomelikeitCool

Innolux Corporation is a world leading manufacturer of TFT-LCD displays, and supplies customers that include many of the world's leading information and consumer electronics manufacturers. Innolux Corporation employs more than 68,000 employees worldwide and is a leader in the global optoelectronics industry. Innolux actively recruit and train R&D talent to consolidate its prominent status in the industry. Innolux is striving to realize the ultimate in visual infotainment. Their unique intelligent management platform has not only enhanced the company's management capabilities, but also provides customers with prompt, accurate delivery information.

Engineers at Innolux Technology Europe B.V. were confronted with the challenge of how to solve expected thermal problems with the integration of a display-centered system into a high-end automobile. The thermal design philosophy behind the activities to be taken is the subject of this article.

A thermal model was already available based on the code CST Microwave which had an embedded thermal solver, with detailed MCAD data as input. However, there were some doubts concerning its accuracy for this application due to the fact that the code

does not solve the Navier-Stokes equations. Furthermore, its radiation treatment was not well-documented and caused further concern. Hence, as a starting point for the numerical analysis the CFD code FloTHERM from Mentor Graphics would be used.

The main objective was to provide preliminary models based on the available (but not sufficiently accurate) input data to study the feasibility of the proposed complete system as a sound starting point for subsequent discussions regarding design decisions with the customer. Tests on an available prototype were performed early on to provide a first-order comparison with the numerical models. In a later stage, experimental calibration by means of dedicated tests, such as thermal resistances and thermal conductivities and component thermal data, were required due to the inaccurate thermal data delivered. One key challenge was that the system was being designed to operate in an environment where the ambient could be as high as 70°C, while the testing had to be carried out at room temperature.

The numerical models were developed as a tool for optimization: sensitivity analysis of gap pads, wall thicknesses and thermal conductivities, PCB thermal data, boundary

conditions, coupling of elements to housing, decoupling LEDs from light guide, properties of the display stack, etc. These models were also to compare with dedicated tests to determine several unknowns, specifically the real-life boundary conditions and thermal interface resistances.

To get an idea of the CFD output, figure 2 depicts three screenshots for the three cross sections through the hottest point. The module is mounted vertically, showing the internal airflow, for a total dissipation of 18.5W.

Results were made available to the customer for several system test conditions, heat transfer coefficients on the external surfaces to represent natural convection, with and without radiation, various choices of gap pad, PCB data, thermal conductivity changes, etc. including component temperatures, which should be interpreted as local solder temperatures. An additional temperature rise caused by the internal thermal resistances of the components should be added, but this is only appropriate when reliable component thermal data is available.

A comparison was made between the existing model created using CST Microwave and Mentor Graphics' FloTHERM. After a series

of trials, a reasonable match was obtained between the two codes, for identical input data and boundary conditions. However, there were a number of reasons for not continuing to proceed with CST:

- The CST model does not solve the Navier-Stokes equations, hence one never knows the consequences except by comparison to a code that does. Better to continue using the CFD code. Knowing the errors arising from the assumption, it was possible to continue in conduction-only mode to speed up the process of sensitivity analysis;

- How CST solves the internal radiation transfer is unclear, and subject to doubt; and

- On the issue of importing CAD files: the author is not in favor of using brute force when trying to get insight in thermal problems. While modern tools make it easy to import CAD files, the not-so-easy next step is to get rid of all mechanical and electrical details that are useless for thermal modeling. While the speed of modern computers may allow millions of cells, the consequences are twofold: the layout becomes very complex, hindering insight in what is going on, and the CPU times go through the roof, hindering fast optimization.

Comparison with Experiments

A number of experiments were available for an existing prototype. While the author does not recommend to use general results for checking the accuracy of the numerical model, in this case, because the results are already available, a comparison gave some idea of trends, and could be used to extract some average boundary conditions in the lab. After calibration of the boundary conditions, the model and the experiments matched to within 2°C.

Under normal operating conditions the SOT solder temperature was above the recommended 100°C, the rest of the components appeared to be acceptable. The importance of radiation was tested, and found to be making a significant contribution to the cooling. Fixing a strip of gap pad material between the LEDs, bracket, housing and carrier had limited effect, however introducing a gap pad below between the bottom and main PCBs reduced the temperature by up to 6°C and hence is considered effective. The results, particularly the SOT temperature, was found to be sensitive to the assumed PCB thermal conductivity. Due to uncertainties in the model data, a gap pad was introduced.

As in many other cases encountered, we were faced with a specified maximum "ambient" for a module or component. This is impossible to design to, as the temperature within the
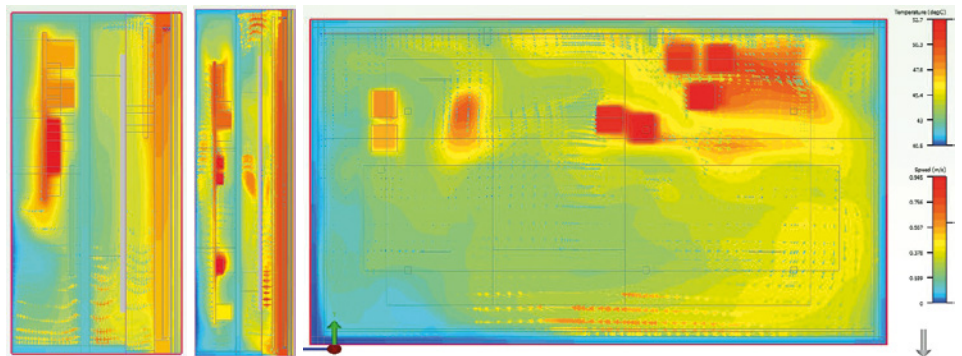

Figure 2. Typical results with flow, total dissipation 18.5W

system varies throughout the system so there is no one temperature a component sees as its own ambient. Another challenge is that the customer cannot control the design of the environment, in this case a car dashboard, into which this product fits, so defining the boundary conditions for Innolux's system is the responsibility of their customer, not Innolux.

It would be much better for the supplier to define a unique point at the outside of their component or module where a given temperature should not be exceeded. Such a spec is independent of the application and so avoids this issue.

Tests with a Dummy System

Tests with a dummy system should ideally focus on just a few issues, the most important being the real-life external boundary conditions for the complex display. Because of the complexity of the layout it does not make sense to model every detail, because it makes the fitting considerably more difficult. Unfortunately, this principle is often forgotten. Determining the boundary conditions that govern real-life applications is always a challenge, because to get sufficient accuracy one should simulate a very big part of the environment wherein the device is operational, including the radiators, the windows, the people etc. noted above. To avoid these problems, it is highly recommended to impose a heat transfer coefficient, including radiation, to be calibrated with real-life measurements.

Gap Pads

It is clear from the analyses that using gap pads or gap fillers improves the thermal performance. Be aware that the thermal data supplied by the manufacturers should be treated with caution, and gap pad data are not an exception unfortunately. The test method usually applies far too high pressure, resulting in too optimistic values. So, if critical, perform a dedicated test, ideally using Mentor Graphics' DynTIM system within which the pressure can be accurately controlled.

Recommendations

How to retrieve the right thermal data for all critical components, including the maximum junction temperature, how this is to be determined, and exactly now useful thermal data such as Rjc and Rjb are generated, requires investigation and discussion. It is highly recommended to ask the vendors of all critical components for more accurate models. For many components even basic but useful thermal resistances such as Rjb and/or Rjc are not available. As a customer, and especially if you build high-end or high reliability systems, you are entitled to get the right data, and especially when you will be held responsible for system failures!

Conclusions

The main conclusion is that, provided some measures are taken, the estimated temperature specs (as far as they are known), could be met, given the current dissipations and assumed boundary conditions. However, it could be foreseen that under certain circumstances these conditions would be worse, to such an extent that natural convection only cannot prevent overheating of the display at maximum ambient temperatures, and hence a forced convection solution should be explored. However, with the available numerical models of the system, it should be easy to check the consequences of such design changes.

In the opinion of the author, there is no other way to reach these conclusions within a realistic timeframe except by using a CFD-code combined with dedicated tests to confirm uncertain parameters required for the modeling. The biggest hurdle to improving the speed and accuracy of the design process is the lack of accurate data for the boundary conditions for the system, coupled with the widely-spread but incorrect habit of prescribing maximum ambient temperatures for the components.

Predicting Water Treatment Plant Performance with FloMASTER

By Jurgen Sprengel, Principal, JS Pump and Fluid System Consultants

Water treatment systems are designed to deal with feed water quality. They comprise mechanical sub-systems made up of pumps, filters and tanks which are connected by valves and pipework generally installed in a series arrangement. Chemical treatment forms an essential part of a water treatment process. However, the fundamental driver is the hydraulic process in producing the required water conditions to enable successful chemical treatment.

This particular Water Treatment Plant (WTP) design is one that treats saline water produced from the coal seam methane gas extraction process. It receives raw water from the gas field's water gathering system which typically contains between 4000 - 8000 mg of salt per litre. The raw water is collected in a storage dam adjacent to the WTP. The treated water and brine that result from the treatment process are temporarily stored in local storage dams. The treated water is then dispatched for beneficial use on an as-need basis, while the brine can be further treated in a brine concentrator.

The WTP is a 20 ML per day WTP comprising four duty Reverse Osmosis (RO) Trains and one standby RO Train, designed to achieve a treated water recovery rate of 85%. The hydraulic envelope of this study comprises the following sub-systems: pre-treatment, filtration, hardness removal (ion exchange), reverse osmosis, post-treatment and storage.

The RO Train Hydraulic Sub-Model

Initially, a single RO Train Hydraulic Sub-Model (figure 2) including pumps, membranes and reject control valve was developed. The membrane feed pressure required to achieve the target recovery rate for the selected raw water composition was obtained from the manufacturer. Variable speed controlled radial flow pumps were selected to produce the required pressures. A modulating Reject Control Valve was installed at the RO Stage 3 brine outlet to enable realistic modeling of a RO Train start/stop event, it being controlled by a PID type controller set at the target reject flow rate.

The RO Train Hydraulic Sub-Model was then tested and optimized in isolation to ensure

Figure 1. WTP Block Diagram
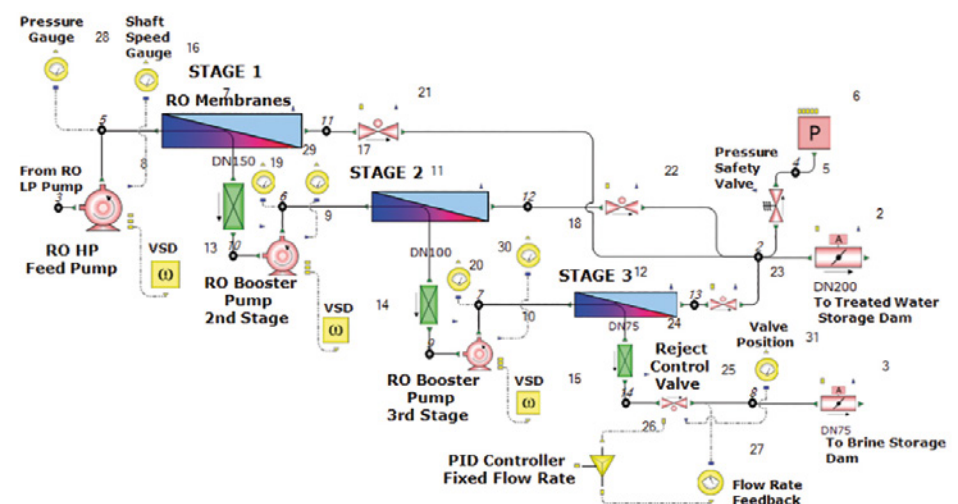
Figure 2. RO Train Hydraulic Sub-Model

its functionality would meet all operational requirements, both in steady state and transient operation.

The Submerged Membrane Filters Hydraulic Sub-Model

Submerged Membrane Filters are located inside flooded cells with cell water level and filtration flow rate being controlled independently.

Raw water supplied by the upstream Inlet Pumps passes through the Disk Filters and enters the Submerged Membrane Filter Cells. The cell inflow rate is controlled by the Cell Inlet Valve via feedback controller in order to maintain individual cell water level set point. The downstream Filtrate Pump extracts water through the internals of the Submerged Membranes, its shaft speed controlled by the water level set point in the IX Feed Tanks. The water volume in the cells allows for some buffer to even out any short-term upstream and downstream pump flow imbalances.

Backwashing of Submerged Membranes is achieved by stopping the Filtrate Pump, closing Membrane Outlet Valve and Cell Inlet Valve and then starting the Backwash Pump. As the Backwash Pump ramps up, drawing water from the IX Feed Tanks, the Membrane Backwash Inlet Valve and Backwash Outlet Valve start opening, both valves controlled by Backwash Pump speed. Backwash waste water from the submerged Membranes is directed to the Site Pump Station for further processing, its clean water content being discharged to the Raw Water Storage Dam.

The WTP Integrated Hydraulic Model

The WTP Integrated Hydraulic Model shown in figure 6 is essentially made up of a multiple of sub-models. Auxiliary sub-systems and control loops were added to create a complete hydraulic model, now consisting of almost 370 hydraulically active components and including a total of 51 centrifugal pumps.

Pumps and valves were modeled based on their actual performance characteristics. Where not available from manufacturers, performance information was utilized as detailed in "Fluid Flow Systems – Second Edition" by D.S. Miller, BHRA 1990.

This model captures all essential elements comprising the complete water treatment system. FloMASTER allows the designer/operator to identify any control deficiencies
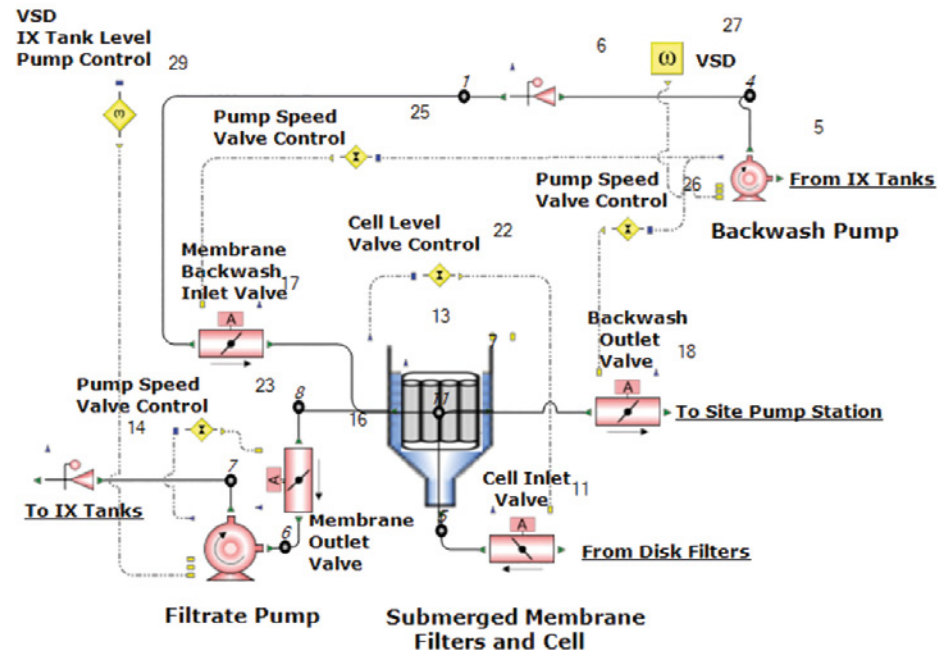
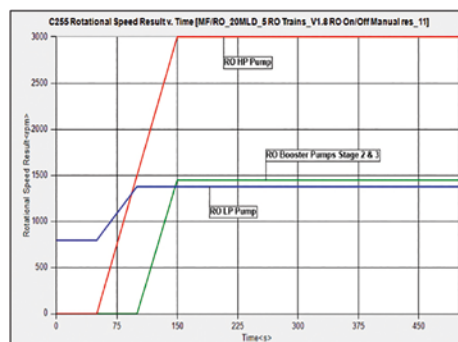Figure 3. Submerged Membrane Filters Hydraulic Sub-Model
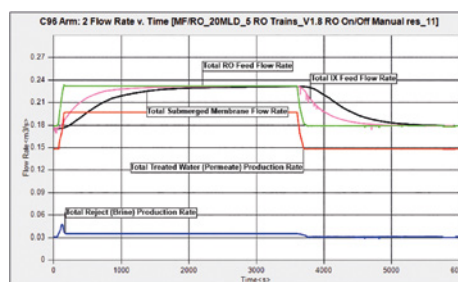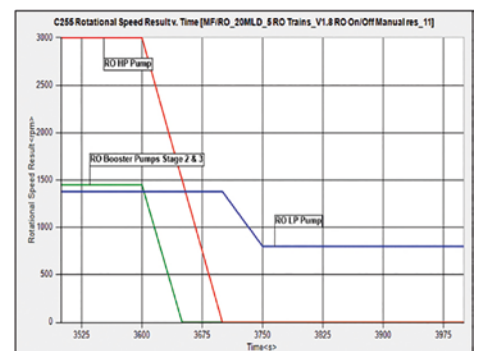

Figure 4. Pump Set Ramp Speeds
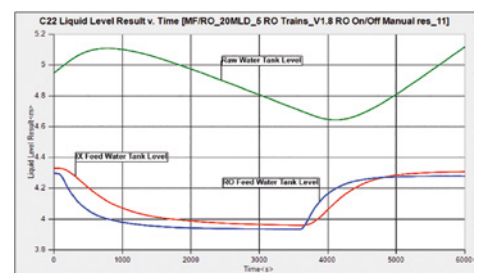

Figure 5. Sub-system flow rates
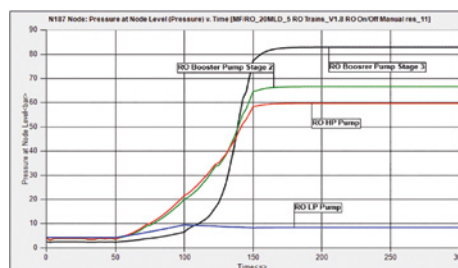

Figure 6. Tank water levels

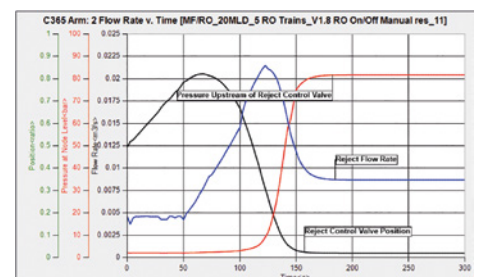Figure 7. RO Pump Discharge Pressure

Figure 8. Reject Control Valve: Reject Flow Rate, Valve Position and Upstream Pressure

or potential bottle necks in the overall process. What-if scenarios can be quickly analyzed and optimized such as the system response to certain equipment failure scenarios.

The Operational Simulations

Two common transient operating scenarios have been selected for further analysis: RO Train start/stop and Submerged Membrane Filter and Disk Filter backwash cycle.

RO Trains are started and stopped in response to the volume of raw water being available at the time. This is considered to be a day-by-day operating scenario in the life of a modern WTP.

Regular Submerged Membrane Filter backwash cycles are an ongoing requirement to keep the membranes at a sufficient level of cleanliness not to impact on overall plant production capacity.

The RO Train Start/Stop Simulation

The RO Train start/stop sequence was manually initiated by setting fixed pump start-up and shutdown time lines.

The main purpose of this RO Train Start/ Stop simulation was to:

- Identify any excessive RO membrane ramp pressure issues,
- Understand the impact on storage volume variation and tank capacity,
- Identify any pressure surge issues,
- Establish the overall dynamic system settling period, and
- Identify potential control system improvements.

For this simulation of a total duration of 6,000s, it was assumed that all components in the hydraulic model would be in service except for stand-by units such as RO Train 5. A time step of 0.5s was selected, sufficient to capture transient events such as pump speed ramp and Reject Control Valve position response to PID controller input

The start-up simulation was initiated with RO Trains 1 to 3 in service, each train operating at 5MLD of raw water inflow. RO Train 4 LP Pump was operating at a shaft speed of 800rpm to provide membrane flushing water with the Reject Control Valve fully open. RO pumps were then ramped up as shown in figure 4, reaching their duty speed after 150s. This

sequence was reversed after 3,600s of operation, resulting in the shutdown of RO Train 4 and ongoing system dynamic settling, eventually achieving stable system operation with three RO Trains in service. Figure 5 shows the upstream sub-systems gradually adjust to rapid downstream flow rate changes. Tank water levels (figure 6) vary by a maximum of about 10% during the RO Train Start/Stop cycle. The system dynamic settling period is about one hour on RO Train start-up.

While pressure ramp rates for the RO HP Pump and RO Stage 2 Booster Pump are acceptable, the ramp rate for RO Stage 3 Booster Pump is in excess of the acceptable membrane pressure loading rate and hence does require further adjustment.

The Reject flow rate, valve position and upstream pressure in figure 8 all indicate a smooth Reject Control Valve response to an increasing upstream pressure.

The Submerged Membrane and Disk Filters Backwash Simulation

A Submerged Membrane Filter backwash

followed by a Disk Filter backwash was simulated with four RO Trains in service. This resulted in a temporary system flow imbalance as the Filtration System capacity was reduced from 100% to about 75%. Normally automated plant operation of the Submerged Membrane Filtration System would initiate a rotating backwash cycle for all active filtration units. However, in this case the backwash cycle for one filtration unit was manually initiated by setting Filtrate and Backwash Pumps start-up and shutdown times as wells as the opening and closing times for the Disk Filter Backwash Valves.

The main purpose of the Submerged Membrane and Disk Filters backwash simulation was to:

- Establish acceptable water level variations in membrane cells,
- Understand the impact on storage volume variation and tank capacity,
- Determine the system recovery time and maximum backwash cycle length, and
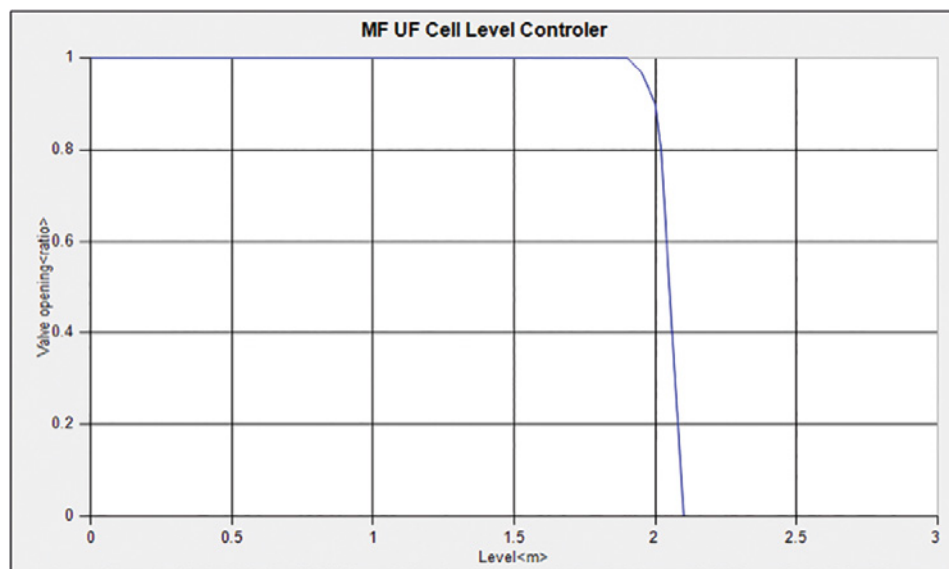- Identify potential control system improvements.

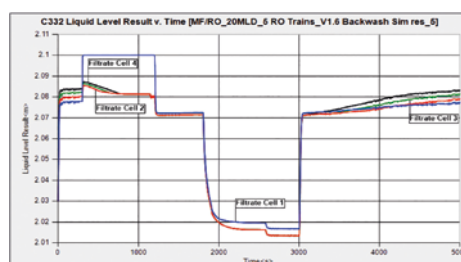**Figure 9.** Cell Inlet Valve Position vs. Cell Water Level

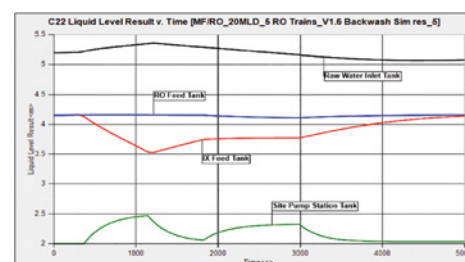
Figure 10. Submerged membrane cell water levels

Figure 11. Tank water levels

For this simulation a total duration of 5,000s was selected at a time step of 1s, sufficient to capture transient events such as pump speed ramps and valve position adjustments.

Cell Inlet Valve position control is shown in figure 9.

Before the Filtration System backwash sequence was started, all four RO Train were operating continuously at rated capacity of a total raw water inflow rate of 20ML per day. After 300s of steady state operation a Filtrate Pump shutdown was initiated followed by a Backwash Pump start 60s later. This backwash operating was reversed after 1,140s resulting in a submerged membrane backwash cycle duration of about 15 minutes. At 1,800s a Disk Filter backwash was initiated and completed at 3,000s, a total duration of about 20 minutes, this action concluding the backwash simulation.

Cell water levels vary by less than 2% during the submerged membrane backwash cycle. However, the variance is 5% during disk filter backwash, both within acceptable limits.

Tank water levels vary by a maximum of about 25% during the backwash cycle. A period of about 2,000s is required for the IX Feed Tank level to recover while the RO Feed Tank level is almost unaffected.

Conclusions

Simulations showed that the modeled system design backwash cycle does have a greater impact on tank level variations than a RO Train start-up. Also confirmed was the conservative selection of tank sizes as the maximum water level variation was less than 25%. However, further tank size reduction would be feasible and cost effective from a hydraulic perspective.

Figure 7 indicated the pressure ramp rate provided by RO Stage 3 Booster Pump being in excess of the maximum acceptable membrane pressure ramp rate of 0.7Bar per second. If left uncorrected this situation may lead to premature membrane wear,

especially in the event of frequent RO Train start-ups. All other RO pump ramp rates have been confirmed acceptable.

Figure 5, 6 and 11 track the sub-system flow rates and tank water levels throughout the modeled transient events. Because of a linear relationship applied between water tank level and upstream pump speed, a relatively slow dynamic settling period has resulted.

In order to manage complexity, the hydraulic model incorporated only relatively basic system controls. A control system looking further upstream and forward feeding flow and level signals would result in more responsive sub-systems within the water treatment plant.
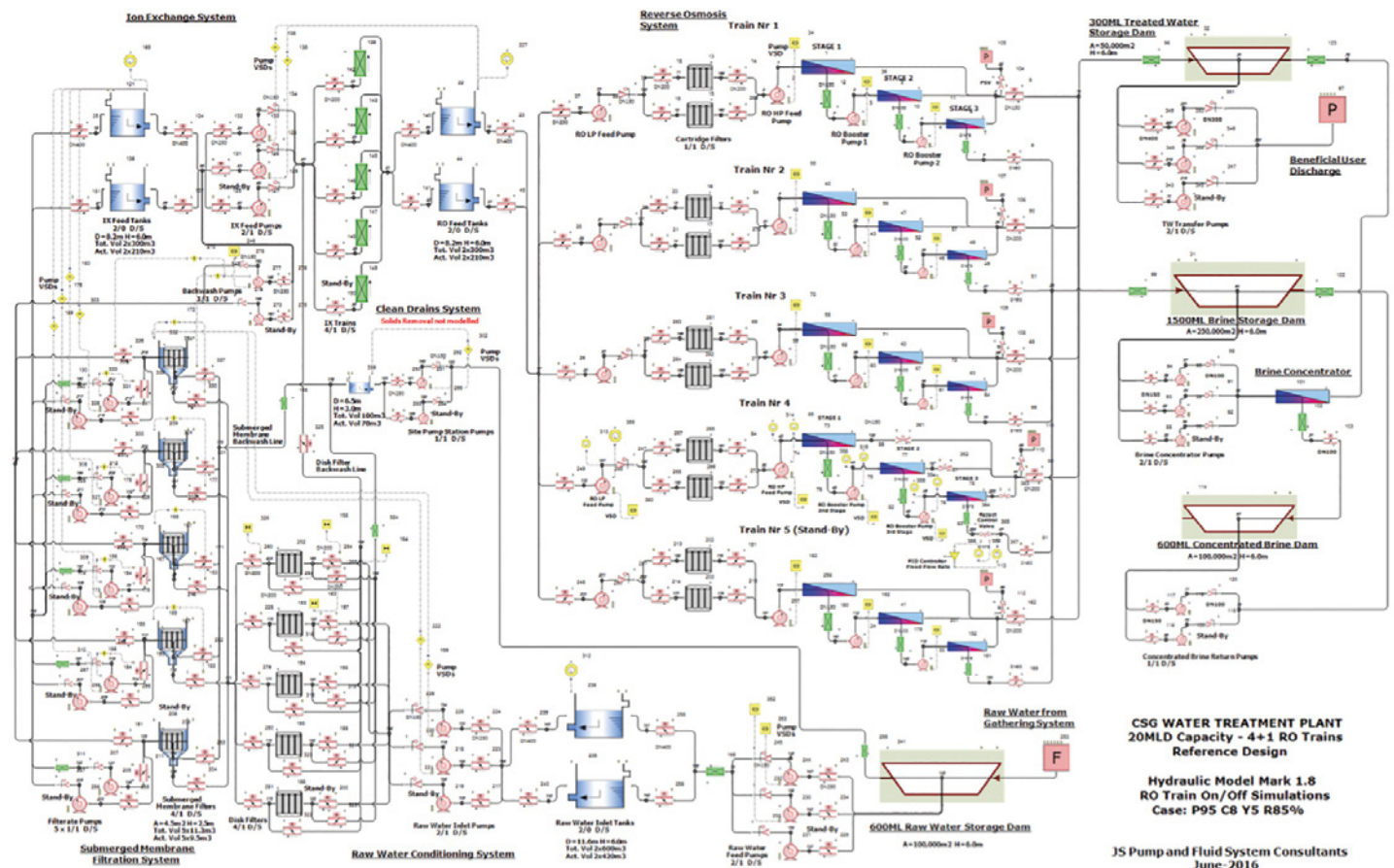

Figure 12. WTP Integrated Hydraulic Model

Geek Hub

Figure 1. Industrial example of two stacks

Spiralled Skyline

By Mike Gruetzmacher,
Technical Marketing
Engineer, Mentor Graphics

Ever wondered why some industrial stacks have spiral structures snaking skyward? Well, since these are industrial plants, designer or artistic reasons can be eliminated. So it must be scientific.

The spirally arranged extensions are called Scruton strakes, named after the British engineer, Christopher Scruton. Working together with D. E. J. Walshe at the National Physics Laboratory in Great Britain, he invented the helical strake and first published the results in 1957[1]. These helical strakes are used to prevent vibrations caused by alternating vortices caused by the wind.

Vortex-induced vibrations (VIV), are caused by vortex shedding and can occur when long slender structures such as chimneys or car antennas are exposed to a flowing fluid. The repeated pattern of wind causes alternating eddies or vortices, also known as a Kármán vortex street. But what do those helical strakes actually do and why are they needed?

For the purposes of this investigation, I used Mentor Graphics' FloEFD 3D CFD Analysis Software, to better understand these structures.

For low Re numbers the vortices downstream the cylinder are steady (figure 2), for higher Re numbers >100, the vortices begin to oscillate (figure 3). The Strouhal number describes the frequency of the vortex shedding:

$$St = \frac{fd}{U}$$

f=frequency of vortex shedding
d=hydraulic diameter
U=flow velocity

These alternating shedding of vortices produce periodic forces across to the flow direction. Each elastic component, including industrial stacks, has a natural frequency. If the excitation frequency generated by the vortex shedding approaches the natural frequency of the stack, resonance and vibrations can occur. This can, at worst, cause damage to the structure.

According to Scruton, another dimensionless quantity was named, the Scruton number:

$$Sc = \frac{2\delta_s m_e}{pb_{ref}^2}$$

δ_s=structural damping by the logarithmic decrement
m_e=effective mass per unit length
p =density of the fluid
b_{ref}=characteristic width of the structure

The Scruton number is an indicator for the design engineer to assess whether further measures must be taken to avoid the effects of vibration damage. Constructive measures may include, for example, damping or other structural engineering measures. Massive, stable stacks seem to be more resistant against these effects, as seen in figure 1. The stack with the larger diameter on the left side is not equipped with the Scruton spirals.

Focusing on the fluid dynamics, the aim of the helical strakes is to interrupt the alternating shedding of the vortices and thus a suppression of the oscillating lateral forces. I was able to quickly set up a simple FloEFD model with the following boundary conditions: Stack diameter: 1.5m, ambient air velocity: 2 m/s (wind velocity 7.2 km/h), as seen in figure 4.

Figure 5 shows a cut plot for velocity and at the top left a curve of the lateral forces depending on the time. We can see the oscillating force in y-direction caused by the alternating vortices.

In comparison, a further variant, which is equipped with exemplary helical strakes. This is demonstrated in figure 6. As we can see in the velocity plot, the alternating vortices don't occur anymore and the curve does not show the oscillating course.

The example in figure 6, has three helices, each 120 degrees apart around the cylinder with a pitch of 7m and 1.2 revolutions each. The helices are not constructed all the way to the top, since in the upper region the vortices are already interrupted by the flow above the stack.

Comparison of the lateral force, time dependent can be seen in figure 7.

As we can see in the graph in figure 7, the stack that is equipped with the helical strakes shows much lower lateral forces and does not oscillate around the x-axis. These are, of course, exemplary results for a slice of the stack, but the qualitative difference is clearly visible.

Thus, the Scruton strakes seem to present an economical solution as opposed to a structural reinforcement of the stack, while at the same time minimizing additional load. Increasing mass often provides remedies, but clever solutions are often the most efficient and here we could explain and present the clever solution using FloEFD with its SmartCells technology.

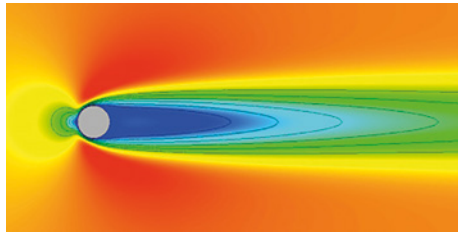Additional applications of the described Scruton strakes can be found in measurement technology to avoid the damage of protection tubes, in oil rigs, car antennas and electrical transmission towers.
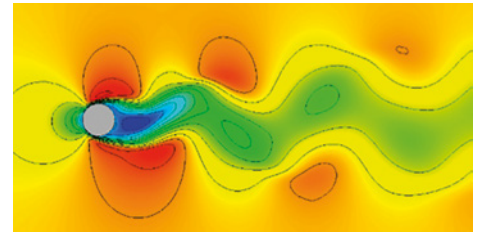

Figure 2. Steady flow at low Re number
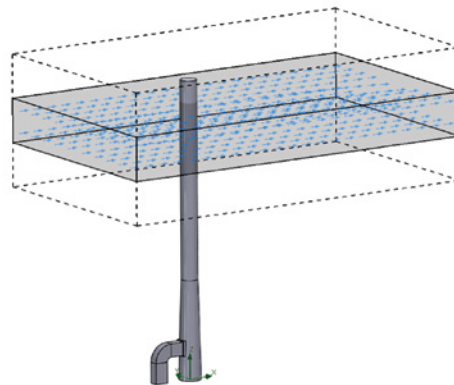

Figure 3. Oscillating at Re>100

Figure 4. FloEFD simulation for one slice
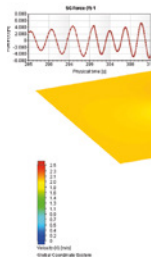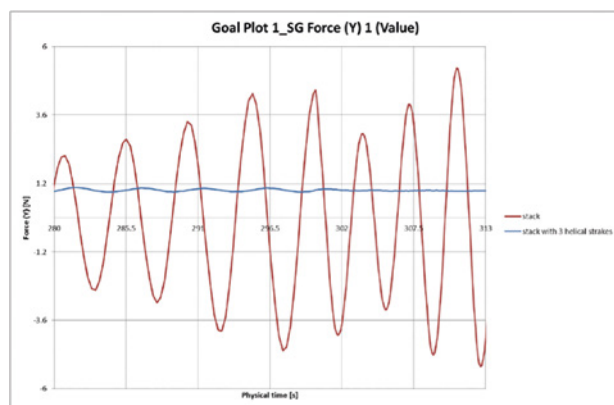

Figure 5. Stack without strakes
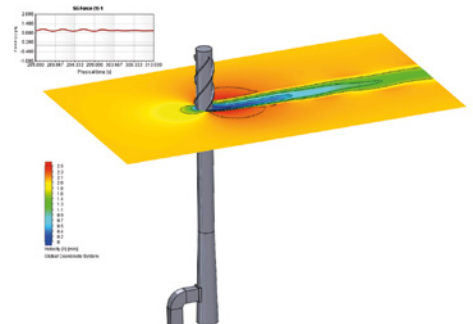
Figure 6. Stack equipped with helical strakes

Figure 7. Time dependent lateral forces

References

[1] C. Scruton and D.E.J. Walshe, A Means for Avoiding Wind-excited Oscillations of Structures with Circular Or Nearly Circular Cross-section, National Physics Laboratory (Great Britain), 1957.

https://www.youtube.com/watch?v=rlpUhgfEZPU

http://www.helicalstrakes.com/

https://en.wikipedia.org/wiki/Scruton_number

https://en.wikipedia.org/wiki/Strouhal_number

Brownian Motion...
The random musings of a Fluid Dynamicist

Brownian Motion or **Pedesis** (from Greek: πήδησις Ρεqε:sιs 'leaping') is the presumably random moving of particles suspended in a fluid (a liquid or a gas) resulting from their bombardment by the fast-moving atoms or molecules in the gas or liquid. The term 'Brownian Motion' can also refer to the mathematical model used to describe such random movements, which is often called a particle theory.
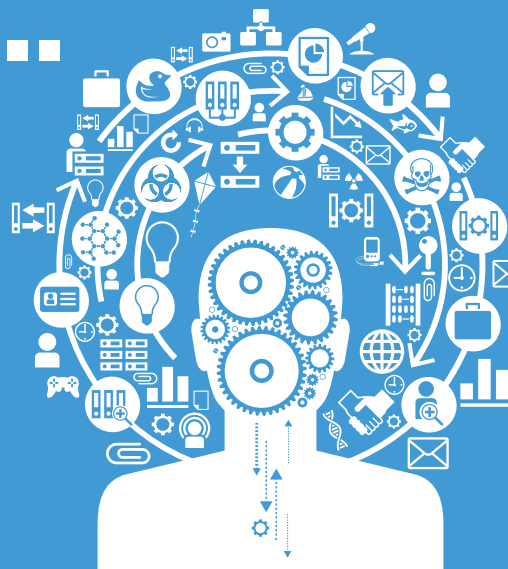
Do you Require a Receipt?

Recently I managed a very brave thing, I left the gas / petrol station without a single piece of paper. I expected to walk across the forecourt back to my car and have someone demand that I prove I had paid for my fuel. And of course without that piece of paper I wouldn't be able to…

Is this a generational thing or is the paper comfort blanket important for any age? In this digital age with pocket scanners and storage on every connected mobile device, paper surely isn't necessary? Most of us travel for work and have endless receipts for hotels, meals, taxis and other subsistence items and I am willing to bet we all have electronic expense systems. We return to the office and scan all those pieces of paper back into digital systems not long after they were output onto paper from digital systems. Yet we still stand at a hotel reception have them print out our details to sign and check out and wait for the often malfunctioning printer to deliver a receipt to prove we stayed and paid. Or diligently take that little piece of paper at every checkout … kudos to the gas station that offered me the ability to walk away without that piece of paper.

I Googled paper receipts, so I accept the source is questionable, but in the US along with 250 million gallons of oil, 10 million trees and one billion gallons of water are consumed just to make those thermal receipt rolls. That is without the receipts printed on regular paper. Staggering, so based on this alone perhaps the days of paper are numbered, or maybe we will always feel like we stole it if we don't tuck a piece of paper into our wallets.
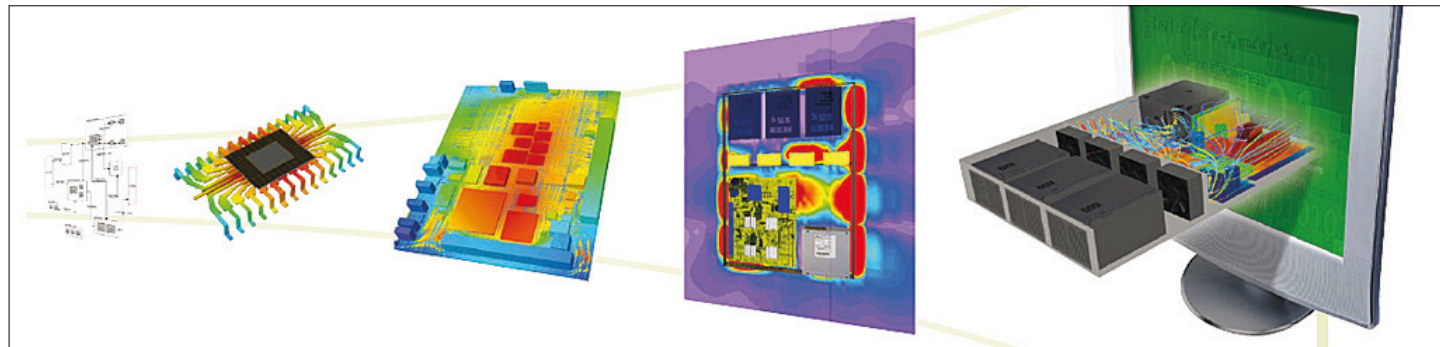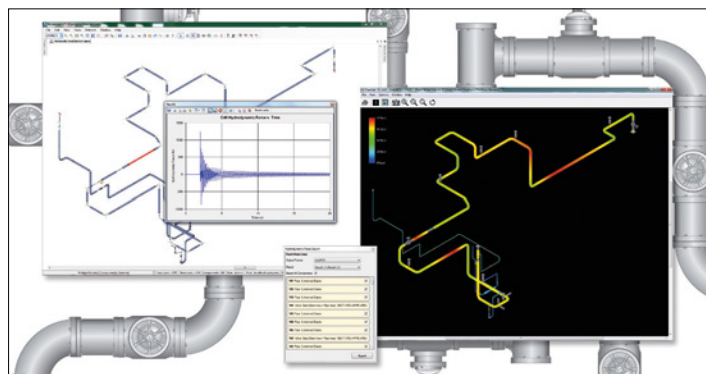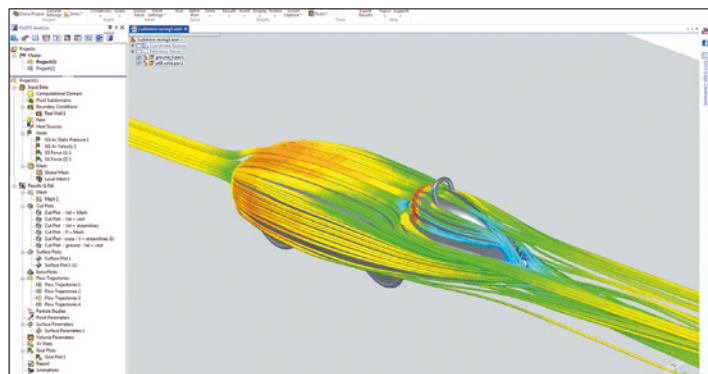
1D Systems CFD Simulation

3D CFD Simulation

Testing Thermal Characterization

Design Optimization

Integrated Solutions
from Mentor

www.mentor.com/mechanical

Mentor®
A Siemens Business